Forensic Science, Medicine, and Pathology

Editors:

Guy N. Rutty, MD, FRCPath
Roger W. Byard, MBBS, MD, FRCPC
Ashraf Mozayani, PharmD, PhD, D-ABFT
Michael Tsokos, MD

Increasing body mass and the mortuary

Roger W. Byard

There is mounting evidence that Western nations are in the grip of an obesity 'epidemic'. Average body mass index (BMI) is increasing, with related diseases such as hypertension, atherosclerosis and diabetes mellitus showing concurrent rises [1]. Estimates by the World Health Organization are that the world's population of one billion overweight individuals will increase by another 50% by 2015 [2]. In the United States alone there has been an increase in morbid obesity in the general population from 0.78 to 2.2% between 1990 and 2000 [3]. In a forensic context, studies from South Australia have shown an increase in morbidly obese bodies subjected to forensic autopsy from 1.3% in 1986 to 4.8% in 2006, with one-third of cases in early 2007 being classified as obese (BMI ≥ 30), and 6% morbidly obese (Class III, BMI ≥ 40) [4, 5]. All of this significantly affects morgue work practices and even burial techniques are having to be modified, with the need for larger coffins and increased width of cemetery excavations. Thus the situation during life is having a critical impact after death.

This concerning development represents more than just a theoretical issue, as it means that mortuary staff who are often already hard pressed by sheer numbers of cases, are now being confronted with bodies that are often extremely difficult to manoeuver and position. Increasing numbers of obese and morbidly obese victims will result in a number of ongoing problems.

Basic forensic mortuary practice requires the transport of corpses from the place of death or storage to the nearest forensic facility. In cases of morbidly obese individuals, who may weigh in excess of 300 kg, this may require assistance from emergency services personnel, with special weight lifting hoists and larger transport vehicles. Once such a body has arrived at a mortuary, however, the difficulties may just be starting. In smaller facilities where bodies are routinely manually lifted onto trolleys and then to dissection tables, there is a distinct risk of back injury for staff. An additional problem encountered in obese individuals is a slower rate of cooling than in individuals with BMIs in the normal range. This results in accelerated decomposition making the bodies even more difficult to move, as skin slippage and blistering renders limbs difficult to grip for lifting. Floors can become dangerously slippery with the excessive amounts of decomposed fluid fat that may exude from these bodies. In cases of infections with hepatitis C or human inmmunodeficiency virus, maintaining safe barrier protection and minimizing exposure will be more difficult given the technical problems of dissecting through many centimeters of subcutaneous adipose tissue with the increased risk of fluid splash. Storage of bodies in standard refrigeration bays may also not be possible due to excessive girth.

Even in morgues where there are hoists and docking systems that use storage trolleys as autopsy tables, there are issues. Standard hoists may not be capable of lifting particularly large bodies, and standard sized tables are not designed to cope with large amounts of excess skin and subcutaneous adipose tissue that may not fit onto table surfaces. Performing adequate external examinations on bodies that are difficult to move or roll, and that may have considerable amounts of body surface concealed within skin folds, may also be taxing for both staff and pathologists.

It is clear that obesity is an increasing problem in all areas of medicine, complicating procedures ranging from

R. W. Byard (✉)
Discipline of Pathology, The University of Adelaide, Level 3
Medical School North Building, Frome Road, Adelaide,
SA 5005, Australia
e-mail: roger.byard@sa.gov.au

the finding of subcutaneous veins for simple blood taking, to fitting obese patients into sophisticated imaging machines for magnetic resonance imaging. It should be no surprise, therefore, that autopsy practice has also been adversely affected.

The question arises as to how to best deal with this situation? The optimal solution would be to have purpose built sections of forensic morgues specifically designed to handle individuals with high BMI's. This could be in the form of a special dissection room adjacent to an external wall with a separate door so that bodies could be loaded directly from transport vehicles onto autopsy tables. The room could be refrigerated to remove the need to transport bodies any further before or after autopsy. Hoists designed to lift loads of up to 800 kg could be installed to enable lifting of bodies to facilitate external inspections. This would not be without cost, however, it would appear that money will have to be spent if autopsy standards are to be maintained in the grossly overweight and if staff health is to be protected. Failure to address these issues in a timely manner may result in difficulties in retaining morgue staff, and in increased claims for work injuries associated with attempts to handle such bodies in suboptimal circumstances. The current trend in increasing body size represents one of the more difficult occupational health and safety issues encountered in forensic facilities in recent years.

References

1. Hunsaker DM, Hunsaker JC III. Obesity epidemic in the United States: A cause of morbidity and premature death. Ch. 4. In: Tsokos M, editor. Forensic Pathology Reviews, vol. 2. Totowa, NY: Humana Press, Inc; 2004. p. 59–98.
2. Behn A, Ur E. The obesity epidemic and its cardiovascular consequences. Curr Opin Cardiol. 2006;21:353–60.
3. Arterburn DE, Maciejewski ML, Tsefvat J. Impact of morbid obesity on medical expenditure in adults. Int J Obes. 2005;29:334–9.
4. Byard RW, Bellis M. Significant increases in body mass index (BMI) in an adult forensic autopsy population from 1986 to 2006—implications for modern forensic practice. J Forensic Legal Med. 2008;15:356–8.
5. Byard RW, Bellis M. Increase in adult body weights in coronial autopsies? An impending crisis. Med J Aust. 2007;187:195–6.

ORIGINAL ARTICLE

A morphometric analysis of the infant calvarium and dura

Eric Breisch · Elisabeth A. Haas ·
Homeyra Masoumi · Amy E. Chadwick ·
Henry F. Krous

Abstract Literature addressing the anatomic development of the dura and calvarium during childhood is limited. Nevertheless, histological features of a subdural neomembrane (NM), including its thickness and vascularity, developing in response to an acute subdural hematoma (SDH) have been compared to the dura of adults to estimate when an injury occurred. Therefore, we measured the morphometric growth of the calvarium and dura and the vascular density within the dura during infancy. The mean thicknesses of the calvarium and dura as a function of occipitofrontal circumference (OFC), as well as the mean number of vessels per $25\times$ field, were determined from the right parasagittal midparietal bone lateral to the sagittal suture of 128 infants without a history of head trauma. Our results showed that as OFC increased, the mean thicknesses of the calvarium and dura increased while the vascular density within the dura decreased. Our morphometric data may assist in the interpretation of subdural NM occurring during infancy. We recommend future investigations to confirm and extend our present data, especially by evaluating cases during later infancy and beyond as well as by sampling other anatomic sites from the calvarium. We also recommend morphometric evaluation of subdural NM associated with SDH in infancy and childhood.

E. Breisch · E. A. Haas · H. Masoumi · A. E. Chadwick ·
H. F. Krous (✉)
Department of Pathology, Rady Children's Hospital and Health Center, 3020 Children's Way, MC5007, San Diego, CA 92123, USA
e-mail: hkrous@rchsd.org

E. Breisch
Department of Surgery/Division of Anatomy, UCSD School of Medicine, La Jolla, CA, USA

H. F. Krous
Departments of Pathology & Pediatrics, UCSD School of Medicine, La Jolla, CA, USA

Introduction

A subdural hematoma (SDH) is an important complication of abusive or accidental head trauma in infants and children. The organization of a SDH involves formation of a neomembrane (NM), the histological features of which include fibroblastic and vascular proliferation, collagen formation, and hemosiderin deposition. The appearance and thickness of a NM have been compared to the underlying normal dura in an attempt to estimate its histological age, thereby determining when an injury was sustained. The aging of NMs in infants and children has been based on observations of NMs occurring in adults that were reported in 1936 by Munro and Merritt [1] and tabulated in both editions of *Forensic Neuropathology* authored by Leetsma [2, 3]. It is unclear whether the observations of Munro and Merritt [1] are valid in early childhood, given that no similar studies have been undertaken in this age period. Even the literature regarding the developmental anatomy of the calvarium and dura in early childhood is limited. One study of grossly normal dura from 11 children found it was "relatively vascular", occasionally revealed hemosiderin, and nearly always contained intradural blood [4]. Other investigators reported that 31% of SIDS cases and 13% of control infants had organizing subdural neomembranes, a difference that was not statistically significant [5]. In all but two cases, birth trauma was excluded. Recent studies have provided elegant qualitative

descriptions of the meningeal embryology and anatomy of the dura, but morphometric data were not included [6–8]. Therefore, the aim of this study is to report the morphometric development of the calvarium and dura in infants.

Methods

This study was approved by the Rady Children's Hospital-San Diego (RCHSD) Institutional Review Board.

Cases without evidence of head trauma were selected from the San Diego SIDS Research Project database. Standardized perpendicular microscopic sections of the sagittal suture and adjacent right parasagittal mid-parietal bone with attached dura were obtained prospectively from 132 infants who died suddenly and underwent autopsy at either the San Diego Medical Examiner's Office or RCHSD. Four cases were excluded: two cases without documented OFC at death, and two because of excessive tangential orientation. In 11 cases, the calvarium had been stripped from the dura; these cases are included only in the calvarium measurements, but excluded from the dural and vessel calculations. After rapid decalcification of the paraffin block with 5% hydrochloric acid, microscopic sections were cut at 4 μm and stained with hematoxylin and eosin. This method allows excellent histological preservation of the tissues (and is routinely used for the interpretation of pediatric bone marrow biopsies in our department). Immunohistochemical staining was not undertaken to identify endothelium.

A diagnosis of SIDS was assigned according to the criteria for the general definition recently proposed in 2004 in San Diego [9]. Diagnoses of non-SIDS cases were based upon analysis of information obtained from the medical history, circumstances of death, and postmortem findings.

All measurements were made directly through the microscope using a micrometer. Mean thicknesses of the parietal bone of the calvarium and the attached dura were determined for each case from measurements of three contiguous $25\times$ power fields ($10\times$pf) 2.5 cm lateral to the sagittal suture. One measurement was obtained in each contiguous field. Measurements were not taken from sites showing mild, microfocal acute hemorrhage that occurred in a small percentage of the specimens. The mean vascular density for each case was calculated after counting all of the blood vessels in five random $25\times$ power fields of dura beginning approximately 1 cm and extending laterally from the superior sagittal suture. The mean number of blood vessels per $25\times$ power field rather than per square millimeter was chosen since the thin membranous nature of the specimens being measured often did not fill the entire microscopic field. Calculation of vascular density within the dura using square millimeters as the denominator

would have resulted in misleading data, given that some of the microscopic fields were not completely filled by tissue. Capillaries were the predominate vessels in each of the sections. Mean vascular densities were not calculated specifically for the periosteal and subdural sides of the dura. Each of the calculated means was plotted as a function of OFC.

Statistical analyses

The difference in distribution of measurements by quartile groups of age at death was calculated by Analysis of Variance; these statistics were performed using SPSS version 11.5. A Simple Interactive Statistical Analysis (SISA) procedure was used to test statistical significance of a difference between two correlation coefficients from a single sample.

Results

The 128 infants were classified as follows: SIDS, 61 (48%); other natural deaths, 36 (28%); unclassified sudden infant death (USID) [9], 22 (17%); and accidents not involving head trauma, 9 (7%). The mean ± standard deviation (SD) for age was 84.5 ± 72 days, and the range was 0–345 days. Among the 128 infants, 49% were white, 31% were Hispanic, 9% were African American, 7% were Asian/American Indian/Pacific Islander, 2% were other, and 2% were unknown. Analysis of ethnicity data revealed the two infants with mixed race heritage had the thickest calvarium; there were no other significant results. Males comprised 63% of the sample. Among 107 cases with available information, 60% were born at term gestation. The OFC was within the normal range for postconceptual age for all of the cases. None of the cases had evidence of microcephaly, macrocephaly or hydrocephalus.

The thicknesses of the calvarium ($P < 0.01$) and dura ($P < 0.01$) increase with increasing OFC (Figs. 1, 2). The difference between slopes of the growth of the calvarium and the dura is statistically significant at the 0.05 level. Conversely, vascular density within the dura decreases with increasing OFC ($P < 0.05$) (Fig. 3).

Tables 1, 2, 3 show the medians and percentiles of the measured variables by age quartile during infancy at the time of death. The median thickness of the calvarium during the first quartile was 1037 μm compared to 1689 μm during the third quartile. The median thickness of the dura during the first quartile was 485 μm compared to 607 μm during the third quartile. The differences of the thickness of the calvarium and dura were statistically significant between groups ($P < 0.01$). The median number of vessels per
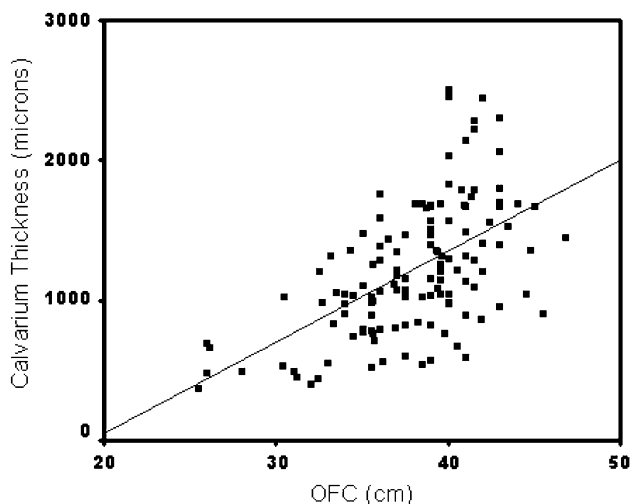
Fig. 1 The thickness of the calvarium increases with increasing OFC. Pearson correlation coefficient = .569, r^2 = .324, $P < 0.01$. (n = 128)

Fig. 2 The dura increases in thickness with increasing OFC in infancy. Pearson correlation coefficient = .370, r^2 = .137, $P < 0.01$. (n = 128)
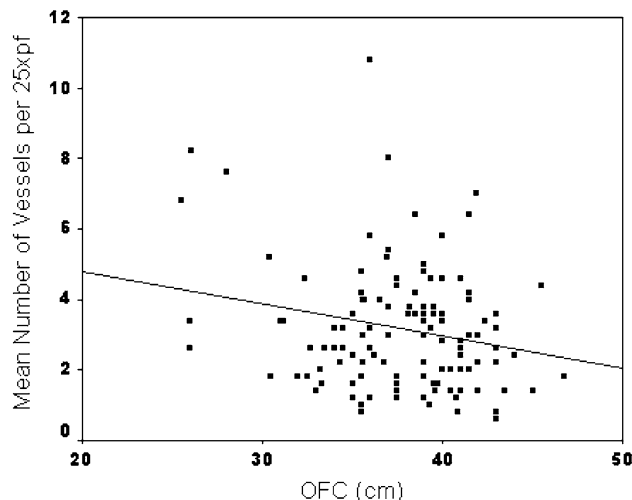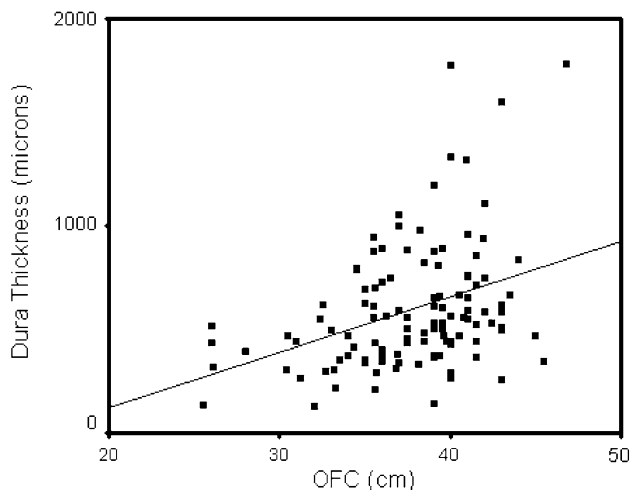

Fig. 3 The density of vessels in the dura gradually decreases with increasing OFC during infancy. Pearson correlation coefficient is −.218, r^2 = .0474, $P < 0.05$. (n = 117)

Table 1 Calvarium thickness in microns by age and percentile

Age (days)	Number	25th percentile	Median	75th percentile	P value
0–90	81	771	1037	1320	<.01
91–180	32	1104	1455	1779	
181–270	11	1397	1689	1799	
271–365	4	1018	1463	1640	

Table 2 Dural thickness in microns by age and percentile

Age (days)	Number	25th percentile	Median	75th percentile	P value
0–90	77	354	485	652	<.01
91–180	27	530	663	858	
181–270	10	467	607	1029	
271–365	3	347	469	530	

Table 3 Number of dural vessels per 25× power field by age and percentile

Age (days)	Number	25th percentile	Median	75th percentile	P value
0–90	77	1.9	3.2	4.2	NS*
91–180	27	1.4	2.6	3.6	
181–270	10	2.1	2.6	3.45	
271–365	3	1.4	3.4	4.4	

* Not significant

25× power field ranged between 3.2 and 4.2 during the four quartiles of infancy, but the differences were not statistically significant. Figure 4a through c illustrate the histology of the calvarium and dura at OFCs of 26, 33, and 40 cm, respectively.

Discussion

Our data, obtained from prospectively collected autopsy specimens from infants between the ages of 0–345 days, provide baseline measurements of bone and dura thickness as a function of OFC. We observed a progressive increase in the thickness of the calvarium with increasing OFC (Figs. 1, 4a–c). The postnatal growth of the calvarium proceeds very rapidly during the first year and is followed
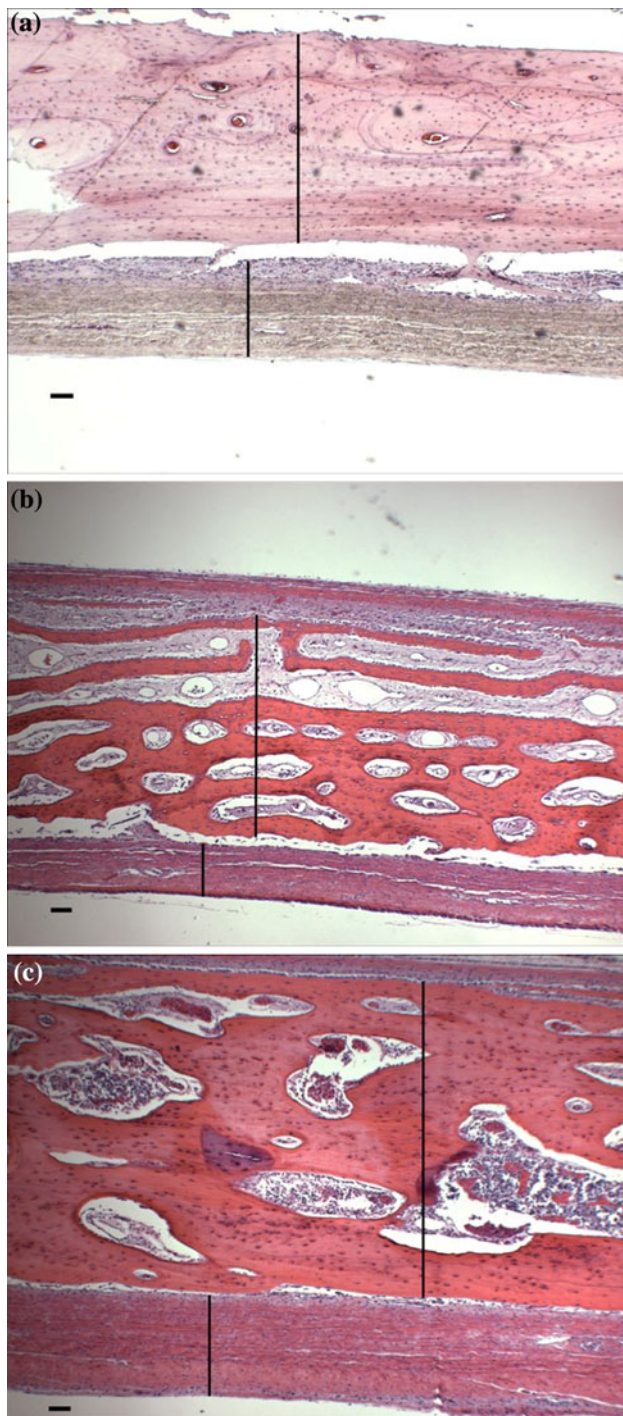
Fig. 4 a The calvarium surfaces the dura of an infant with an OFC of 26 cm. The *vertical bars* indicate dimensions selected for measuring the thickness of the calvarium and dura. The horizontal marker equals 100 μm. Hematoxylin and eosin, 40×. **b** The calvarium surfaces the dura of an infant with an OFC of 33 cm. The *vertical bars* indicate dimensions selected for measuring the thickness of the calvarium and dura. The horizontal marker equals 100 μm. Hematoxylin and eosin, 40×. **c** The calvarium surfaces the dura of an infant with an OFC of 40 cm. The *vertical bars* indicate dimensions selected for measuring the thickness of the calvarium and dura. The horizontal marker equals 100 μm. Hematoxylin and eosin, 40×

by a much slower growth rate until approximately the seventh year when the skull approaches adult size [10]. Since our cases were limited to infants, we are unable to address growth during the second year of life.

Expansional growth of the calvarium during the first two years of life is achieved by membranous ossification at the sutures and along the outer and inner surfaces in a process characterized by concomitant accretion and absorption of the deep and superficial surfaces, thus permitting growth accommodation for changes in the curvature of the calvarium [11]. Previous reports indicate that the calvarium is unilaminar until the diploe appear in approximately the fourth year of life, forming a trilaminar calvarium [10] In an adult, the inner table of the calvarium is thinner than the outer table, which accounts for the increased incidence of inner table fracture compared to the outer table in head trauma [10, 12]. In our analysis, we were unable to establish when that disparity in thickness develops, since the calvarium remained unilaminar throughout the study interval.

The normal dura consists of outer and inner layers [13]. The outer layer is a very dense fibrous membrane that is tightly attached to the inner table of the calvarium and serves as its periosteum. The inner layer is comprised of less dense fibrous connective tissue lined on its inner aspect by a layer of mesothelial cells that are in direct contact with the arachnoid layer of the leptomeninges [10]. Our study restricted the measurement of thickness of the dura to the dense components of the inner and outer layers since mechanical forces required for removal of the calvarium routinely disrupted the mesothelial layer. We found that the thickness of dura increased with increasing OFC (Figs. 2, 4a–c), but at a slower rate when compared with the rate of increase of the thickness of the calvarium (Pearson correlation coefficients are .370 and .569, respectively; the difference between the slopes of the growth of the calvarium and the dura is significant at the 0.05 level).

The blood supply to the dura is derived from the meningeal vessels. The vascular pattern of the inner and outer dura have been described in adults [6, 14], but not in early childhood to our knowledge. In our specimens, the small arterioles and venules were located primarily in the dense collagenous part of the dura while the capillaries were in the periosteum. We are unaware of previous studies in which the density of blood vessels in the dura was measured. Our data show that there is a slight decrease in the vascular density with increasing head circumference (Fig. 3). The significance of this finding is unknown, but it suggests a possible decrease in metabolic demand despite increasing thickness. The mere presence of blood vessels in the dura in the absence of other histological features of NMs must be viewed from a forensic viewpoint as normal

in that it provides nourishment to this developing structure. Depending on their age, NMs following SDH require the presence of other histological findings such as fibrin, siderophages, fibroblastic proliferation, and/or collagen deposition.

In practice and as expert witnesses in cases of pediatric abusive head injury, pathologists commonly use data reported by Munro and Merritt in 1936 [1] to "age" neomembranes evolving from acute subdural hematomas. The Munro and Merritt data were derived from adults found to have subdural neomembranes at autopsy. To our knowledge, it has not been established that their data (which have been tabulated by Leestma [2]) are valid in infants and toddlers; nor did they take into account the morphometric development of the calvarium and dura. The recent study examining microscopic features of grossly normal dura from one third trimester intrauterine death and 10 infants between 2 weeks and 10 months of age provided data on the frequency of intradural blood and intra- and extracellular hemosiderin, but not on quantitative changes in dural thickness and vascularity or changes in the appearance of the calvarium, as undertaken in our study [4]. These investigators did emphasize, however, the importance of being familiar with the pediatric dura in order to properly interpret true pathologic findings when they are present.

Our study is limited by restricting measurements to the right mid-parietal bone and dura taken approximately 2.5 cm lateral to the sagittal suture. The calvarium gets progressively thicker as the lateral distance from the sagittal suture increases until a rather uniform thickness is achieved as the base of the skull is approached. Thus, our data can not be generalized to all sites within the cranium. In this regard, fractures (and NMs) have been observed in all regions of the cranium. The susceptibility of the calvarium to fracture is influenced by not only the direction and force of the impact, but also by the unique anatomic characteristics and biomechanical properties at each site. Secondly, our sample contains relatively few cases from the last three months (quartile) of infancy and none after the first birthday.

However, our study is strengthened by the large number of cases that were collected prospectively, use of standardized microscopic sections, and basing the results on OFC rather than gestational or postnatal age, body length, or body weight. When our measurements were analyzed with respect to the latter variables, the results produced a scattergram lacking any developmental interpretation. Finally, our results provide morphometric data for future reference and comparison.

In conclusion, we have provided morphometric data on the growth of the calvarium, dura, and density of dural vessels during infancy which can serve as a baseline for further investigation of NMs after subdural hemorrhage in infancy. These data may also be useful in the morphometric evaluation of other disorders, including bone responses of the infant calvarium to biomechanical stresses and craniofacial anomalies. We recommend future investigations to confirm our findings and to extend our present data by not only evaluating cases during later infancy and beyond but also by sampling other anatomic sites from the calvarium. Finally, an analysis of NMs as a function of the developmental status of the calvarium and dura is indicated.

Key points

1. The histological features of neomembranes, a reparative response to acute subdural hematomas, have been used to age their duration from the time of an injury in early childhood.
2. Efforts to age neomembranes have been based on data derived from characteristics of the dura in adults, but not early childhood.
3. Although qualitative descriptions exist, quantitative morphometric analyses of the calvarium and dura in early childhood are lacking.
4. Our data show that as OFC increased in infancy, the mean thicknesses of the calvarium and dura increased while the vascular density within the dura decreased.

References

1. Munro D, Merritt HH. Surgical pathology of subdural hematoma. Based on a study of one hundred and five cases. Arch Neurol Psychiatry. 1936;35:64–78.
2. Leestma JE. Forensic neuropathology. New York: Raven Press; 1988.
3. Leestma JE. Forensic neuropathology. 2nd ed. Boca Raton, FL: CRC Press; 2009.
4. Croft PR, Reichard RR. Microscopic examination of grossly unremarkable pediatric dura mater. Am J Forensic Med Pathol. 2009;30:10–3.
5. Rogers CB, Itabashi HH, Tomiyasu U, Heuser ET. Subdural neomembranes and sudden infant death syndrome. J Forensic Sci. 1998;43:375–6.
6. Kerber CW, Newton TH. The macro and microvasculature of the dura mater. Neuroradiology. 1973;6:175–9.
7. Mack J, Squier W, Eastman JT. Anatomy and development of the meninges: implications for subdural collections and CSF circulation. Pediatr Radiol. 2009;39:200–10.

8. Squier W, Mack J. The neuropathology of infant subdural haemorrhage. Forensic Sci Int. 2009;187:6–13.

9. Krous HF, Beckwith JB, Byard RW, et al. Sudden infant death syndrome and unclassified sudden infant deaths: a definitional and diagnostic approach. Pediatrics. 2004;114:234–8.

10. Williams PL, Warwick R. Gray's anatomy. 36th British Edition. Philadelphia: W.B. Saunders Co/Churchill Livingstone; 1980.

11. Ford EHR. The growth of the foetal skull. J Anat. 1956;90:63–72.

12. Hollinshead WH. Anatomy for Surgeons. Head and Neck. vol 1. 3rd ed. Harper & Row; 1982. p. 4–5.

13. Carpenter MB. Human neuroanatomy. 7th ed. Baltimore: Williams and Wilkins Co; 1981.

14. Lang J. Zur vascularisation der Dura mater cerebr. I. Z Anat Entwickl-Gesch. 1971;135:20–34.

Index and ring finger ratio- a morphologic sex determinant in South-Indian children

Tanuj Kanchan · G. Pradeep Kumar

Abstract To investigate the sexual dimorphism of index and ring finger ratio in South Indian children. The index finger length (IFL) and the ring finger length (RFL) were measured in 350 subjects aged between 2 and 12 years using a steel measuring tape. The index and ring finger ratio was computed by dividing index finger length by ring finger length. The data obtained were analyzed statistically using SPSS, version 11.0. Mean RFL was greater than mean IFL in both males and females. The mean ring finger length was longer in males than females and mean index finger length longer in females than males. However, these sex differences observed for index and ring finger length were not significant in both hands. Statistically significant sex differences were observed from the derived index and ring finger ratio. The mean index and ring finger ratio was found to be higher in females than males. Significant correlation was found between age and index and ring finger lengths. Index and ring finger ratio however, did not show any significant correlation with age. This study suggests that among South-Indian children, the index and ring finger ratio of 0.97 and less is indicative of male, and a ratio of more than 0.97 is indicative of female sex. The ratio can be a useful sex indicator irrespective of the age of the individual.

Introduction

Identification of human remains is an essential element of any medicolegal investigation. It is not uncommon to find the peripheral parts of the body such as hand and foot in mass disasters, and assault cases where the body is dismembered to conceal the identity of the victim. When an individual hand is recovered and brought for examination, somatometry of the hand, osteological and radiological examination can help in the determination of primary indicators of identification such as sex, age and stature [1–17]. Accurate sexing of the human remains primarily narrows down the pool of possible victim matches and thus helps the investigation. Studies have been conducted on sex determination from morphometric parameters of hand in adult Indian populations [16, 17].

Sexing of prepubertal human remains is a challenge for forensic experts and physical anthropologists worldwide. The Index and ring finger ratio is a sexually dimorphic biometric marker, related to prenatal estrogen and testosterone levels in utero, and determined genetically by the HOX genes [18] Various studies in the past have studied the index and ring finger ratio in males and females. Men have been reported to have lower ratio than women. Voracek and Loibl published a much detailed scientometric analysis and bibliography of research on digit ratio during

T. Kanchan (✉)
Department of Forensic Medicine and Toxicology, Kasturba Medical College (Affiliated to Manipal University), Mangalore, India
e-mail: tanujkanchan@yahoo.co.in

G. Pradeep Kumar
Department of Forensic Medicine and Toxicology, Kasturba Medical College (Affiliated to Manipal University), Manipal, India

Fig. 1 Manipal, the study area is a coastal township in Karnataka state in South India

the last decade [19]. McIntyre et al. [20] based on a study of hand radiographs indicate that relative digit lengths are sex-dimorphic in children. Index and ring finger ratio has been found to be a useful sex determinant in South-Indian adult and adolescent population [21, 22]. The present research investigates the sexual dimorphism of index and ring finger ratio in South Indian children.
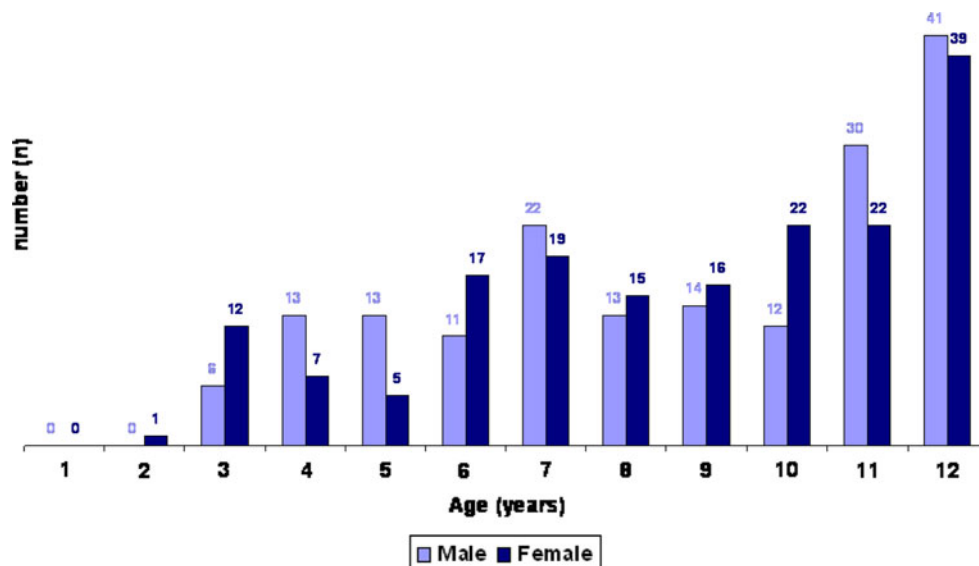
Materials and methods

The study was conducted in Manipal, a coastal township in Karnataka state in South India (Fig. 1). The data were collected on a sample of 350 children (175 males and 175 females) of South Indian origin inhabiting in Manipal. Prior to the research, an informed consent for the study was taken from the Principal/Head of the Primary schools included in the study. The subjects included in the study were children aged between 2 and 12 years. Mean age of males and females was 8.7 years. Age distribution of the study subjects is shown in Fig. 2. The subjects were asked to place their forearm and hand on a flat surface with palm facing upwards and the fingers extended and close to each other. Care was taken to see that the forearm was directly in line with the middle finger and that there was no abduction or adduction at the wrist joint. The index finger length (IFL) and the ring finger length (RFL) were measured in each hand using a steel measuring tape. The distance between the mid point of the proximal most flexion crease at the base, and the most forward placed point (tip) of index and ring finger in the midline on the ventral (palmer) surface were recorded for each hand to the nearest millimeter [21]. The landmarks and measurements for index and ring finger length measurements are shown in Figs. 3 and 4. Effect of hand dominance on measurements has been suggested [23] and hence, only right handed subjects were included in the present study. The measurements were taken by one observer (TK) in order to avoid inter-observer error. The subjects with any disease, deformity, or trauma of the index or ring fingers of either hand were excluded from the study. The index and ring finger ratio was computed by dividing index finger length by ring finger length.
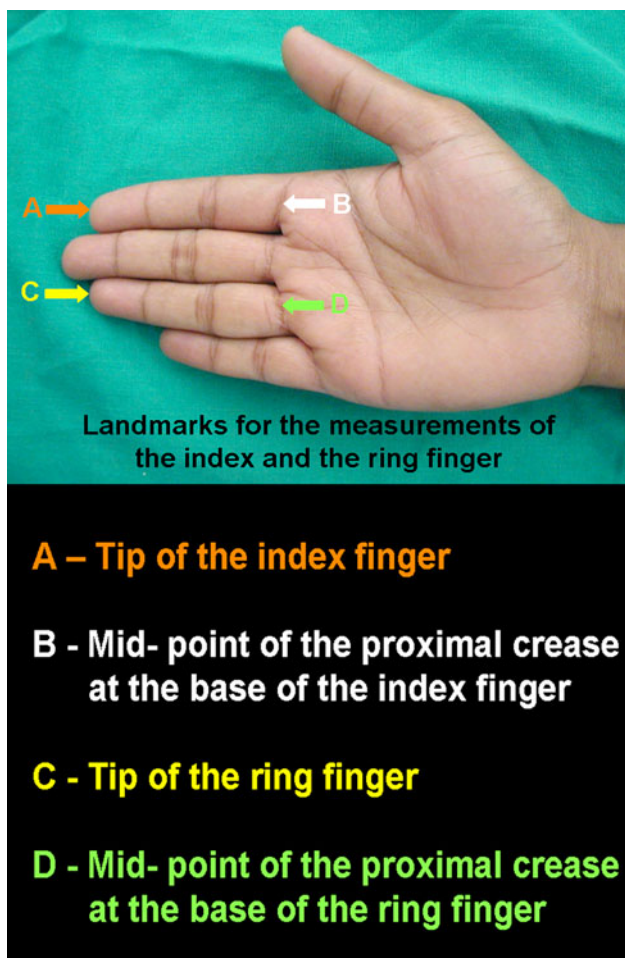
Fig. 2 Age distribution of the study group

Fig. 3 Landmarks on the hand for the measurement of index and ring finger length

The data obtained were analyzed statistically using SPSS (Statistical Package for Social Sciences, version 11.0) computer software. Pearson correlation was applied to test the relationship between age and length of index and ring finger and index and ring finger ratio. Student's *t*-test was performed to compare the index and the ring finger lengths and the ratio in the right and left hands, and between males and females. Statistical significance was set at the standard 0.05 level. Sex differentiation from index and ring finger ratio was based on Sectioning point analysis.

$$\text{Sectioning point} = \frac{\text{Mean male value} \pm \text{Mean female value}}{2}$$

Results

Descriptive statistics for index and ring finger lengths for both hands in males and females are shown in Tables 1 and 2, respectively. No significant differences were observed in
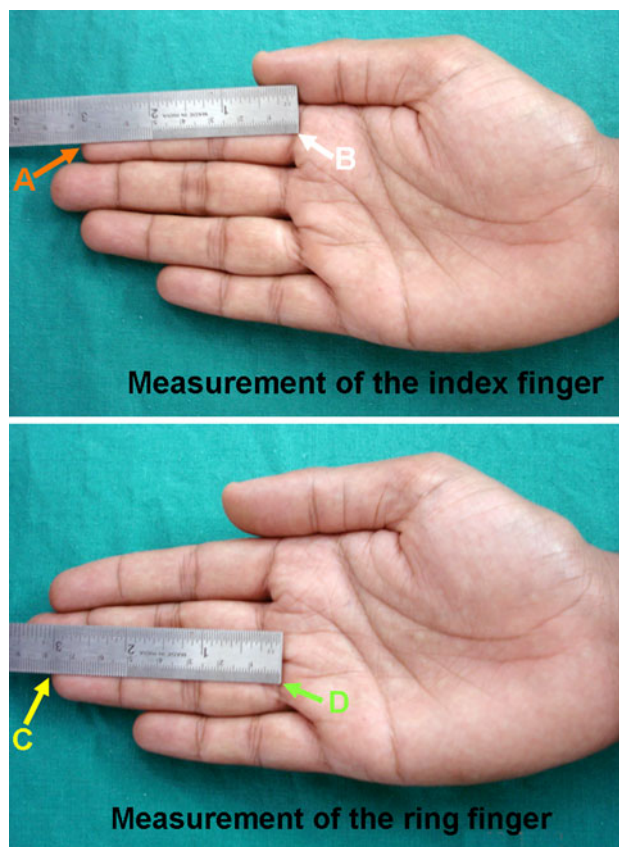
Fig. 4 Measurement of index and ring finger lengths

the length of index and ring finger between right and left hands. The ring finger was longer than the index finger in both males and females. Difference between the mean RFL and the IFL was 2.9 mm in the right hand and 3.0 mm for the left hand in males, and 0.6 mm for the right and 0.7 mm for the left hand in females. When the finger lengths are compared between males and females, the ring fingers were longer in males than females and index finger longer in females than males in both hands. However, the sex differences in index and ring finger lengths between males and females was not found to be statistically significant ($P > 0.05$). Male–female differences in index and ring finger lengths are shown in Table 3.

Table 1 Descriptive statistics: Index and ring finger length (mm) in males

	Right hand		Left hand	
	IFL	RFL	IFL	RFL
Minimum	41.0	44.0	41.0	44.0
Maximum	74.0	74.0	73.0	73.0
Mean	54.2	57.1	53.9	56.9
SD	6.3	6.5	6.4	6.6

SD standard deviation, *IFL* index finger length, *RFL* ring finger length

Table 2 Descriptive statistics: index and ring finger length (mm) in females

| | Right hand | | Left hand | |
	IFL	RFL	IFL	RFL
Minimum	40.0	41.0	40.0	41.0
Maximum	75.0	76.0	75.0	74.0
Mean	55.7	56.3	55.4	56.1
SD	7.7	7.8	7.7	7.7

SD standard deviation, *IFL* index finger length, *RFL* ring finger length

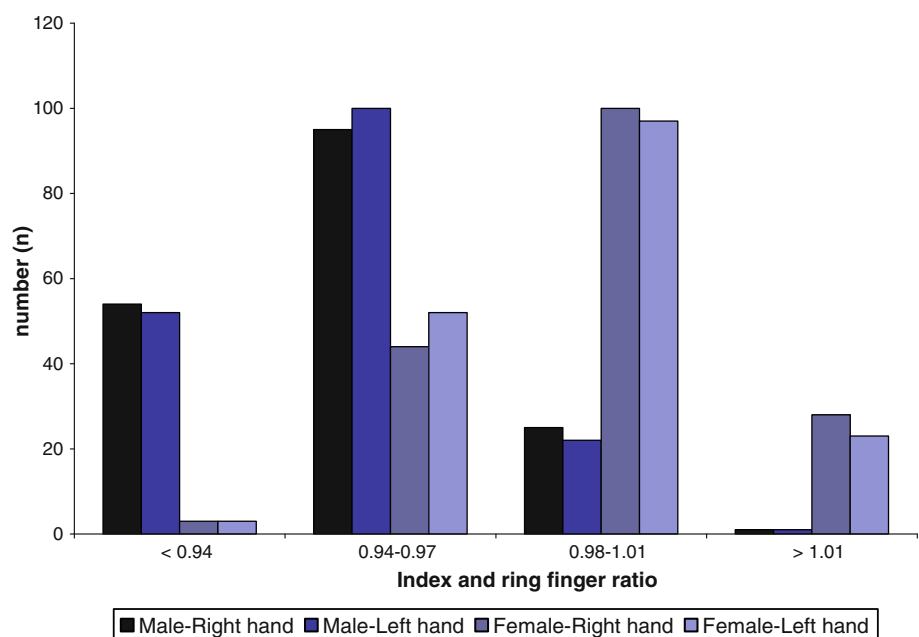**Table 3** Index and ring finger length (mm): Male–female differences

	Male	Female	*t*-value	*P*-value
Right IFL	54.2	55.7	–1.932	0.054
Left IFL	53.9	55.4	0.989	0.324
Right RFL	57.1	56.3	–1.840	0.670
Left RFL	56.9	56.1	0.994	0.321

IFL index finger length, *RFL* ring finger length

Table 4 Descriptive statistics: index and ring finger ratio in males and females

| Sex | Right hand | | Left hand | |
	Male	Female	Male	Female
Minimum	0.89	0.90	0.89	0.90
Maximum	1.02	1.06	1.02	1.06
Mean	0.95*	0.99*	0.95*	0.99*
SD	0.03	0.03	0.02	0.02

SD standard deviation, * P value ≤ 0.001

Table 5 Correlation coefficients (Pearson) of finger lengths and Index and ring finger ratio with age

	Male	Female
Age		
Right IFL	0.794*	0.804*
Left IFL	0.792*	0.805*
Right RFL	0.826*	0.831*
Left RFL	0.820*	0.830*
Right IR Ratio	–0.106	–0.137
Left IR Ratio	–0.061	–0.113

IFL index finger length, *RFL* ring finger length, *IR* index−ring, * P value ≤ 0.001

Index and ring finger ratio ranged from 0.89 to 1.02 in males, and from 0.90 to 1.06 with in females (Table 4). The derived ratio showed a statistically significant difference ($P \leq 0.001$) between males (Mean ratio = 0.95) and females (Mean ratio = 0.99). A 'sectioning point' of 0.97 was derived to discriminate male and female hands from the index and ring finger ratio. Distribution of index and ring finger ratio among male and female children is depicted in Fig. 5. Significant correlation was found between age and index and ring finger lengths. Index and ring finger ratio however, did not show any significant correlation with age (Table 5).

Discussion

In the mid-1950s, Rösler collected a massive sample of hand outline drawings. With regard to the distal finger-

Fig. 5 Distribution of index and ring finger ratio among male and female children in right and left hands

extent pattern, Rösler differentiated radial (longer index than ring finger), ulnar (reversed pattern), and intermediate hand types, which reflect higher (more female-typical), lower (more male-typical), and intermediate digit ratio respectively [24]. Sexual dimorphism of index and ring finger ratio is reported to be established in utero between the 13th and 14th week of gestation [25, 26], under the influence of prenatal androgens and estrogens [27–29].

Morphological sex differences in the absolute length of fingers have been demonstrated in various studies, male fingers being longer than females [30]. Sex difference in the length of the ring finger found in our study is similar to that reported by Lippa [31]. In females, the index and ring fingers tend to be almost equal in length, whereas in males the ring finger tends to be much longer. Thus, the index and ring finger ratio becomes a significant parameter for determining sex [21]. Men have been reported to have lower index and ring finger ratio than women. Lower index and ring finger ratio have thus been considered "masculine" and higher ratios as "feminine". Besides sexual dimorphism, index and ring finger ratio shows significant ethnic and population differences [32–34]. Manning reported that the Asians tend to have a low index to ring finger ratios [27]. In our study, the mean index and ring finger ratio in male children is significantly lower than females in both hands similar to the observations in the earlier studies [21, 22, 27, 31, 35–37] where on an average, males demonstrated lower digit ratios than females. Findings of our study with regard to sexual dimorphism of index and ring finger ratio in South Indian children are similar to those observed in the South Indian adult and adolescent population [21, 22]. The index and ring finger ratio, a putative biomarker for the organizational (permanent) effects of prenatal androgens on the human brain, body, and behavior, has received extensive research attention in psychology in the past decade [24] but not much is written about in forensic literature, in particular relating its importance in medicolegal investigations. Voracek has suggested that the sexual dimorphism exhibited by the index and ring finger ratio is not large and hence its application in medicolegal investigations is limited [38].

The index and ring finger ratio as a sexually dimorphic trait is established early in life and remains fairly stable postnatal; it does not change with age and growth in a population group [27, 39]. A positive correlation was found between age and index and ring finger lengths corroborating the fact that there is an increase in finger lengths with age among children. However, index and ring finger ratio does not show any significant correlation with age confirming the fact that this sexually dimorphic ratio is independent of age similar to observations of Manning [27] and Lippa [31]. Sectioning point derived for sex differentiation was similar to that observed in South Indian adult

and adolescent population [21, 22]. Our study further confirms the observations of other researchers that the sex differences in the index and ring finger ratio that appears early do not show appreciable change with growth [33] and thus it can be a useful sex indicator irrespective of the age of the individual especially when DNA analyses cannot be performed.

Conclusions

DNA technology has simplified the issue of sex determination to a great extent, but technology has its limitations with regard to skilled man power, time and financial issues involved, especially in developing countries and in cases when DNA analyses cannot be performed. Various techniques in forensic anthropology are still most commonly employed for identification of human remains.

The study confirms the sexually dimorphic nature of index and ring finger ratio in South Indian children. The study suggests that the index and ring finger ratio of 0.97 and less is indicative of male, and a ratio of more than 0.97 is indicative of female sex and confirms that the sexual dimorphism of index and ring finger ratio is a constant feature among different age-groups in South Indian population.

Key points

1. The ring finger is longer than the index finger in males and females. The difference between the mean ring finger and the index finger length is larger in males than females.
2. The ring fingers are longer in males than females while the index fingers are longer in females than males in both hands. The sex differences in index and ring finger lengths however are not statistically significant ($P > 0.05$).
3. Index and ring finger ratio shows a statistically significant difference ($P \leq 0.001$) between males and females. A 'sectioning point' of 0.97 is derived to discriminate sex from the index and ring finger ratio.
4. The index and ring finger ratio does not show appreciable change with growth and thus it can be a useful sex indicator irrespective of the age of the individual.

Junior College and Madhava Kripa School in Manipal where the study was conducted. Informed consent was taken from the Principal/ Head of the Primary schools included in the study. The authors are indebted to the subjects who willingly participated in the study. We also wish to thank the anonymous reviewers for their thoughtful suggestions.

References

1. Abdel-Malek AK, Ahmed AM, el-Sharkawi SA, el-Hamid NA. Prediction of stature from hand measurements. Forensic Sci Int. 1990;46:181–7.

2. Bhatnagar DP, Thapar SP, Batish MK. Identification of personal height from the somatometry of the hand in Punjabi males. Forensic Sci Int. 1984;24:137–41.

3. Krishan K, Sharma A. Estimation of stature from dimensions of hands and feet in a North Indian population. J Forensic Leg Med. 2007;14:327–32.

4. Sanli SG, Kizilkanat ED, Boyan N, Ozsahin ET, Bozkir MG, Soames R, et al. Stature estimation based on hand length and foot length. Clin Anat. 2005;18:589–96.

5. Rastogi P, Nagesh KR, Yoganarasimha K. Estimation of stature from hand dimensions of north and south Indians. Leg Med (Tokyo). 2008;10:266–8.

6. Shintaku K, Furuya Y. Estimation of stature based on the proximal phalangeal length of Japanese women hand. J UOEH. 1990; 12:215–9.

7. Meadows L, Jantz RL. Estimation of stature from metacarpal lengths. J Forensic Sci. 1992;37:147–54.

8. Rastogi P, Kanchan T, Menezes RG, Yoganarasimha K. Middle finger length- a predictor of stature in Indian population. Med Sci Law. 2009;49:123–6.

9. Smith SL. Attribution of hand bones to sex and population groups. J Forensic Sci. 1996;41:469–77.

10. Scheuer JL, Elkington NM. Sex determination from metacarpals and the first proximal phalanx. J Forensic Sci. 1993;38:769–78.

11. Lazenby RA. Identification of sex from metacarpals: effect of side asymmetry. J Forensic Sci. 1994;39:1188–94.

12. Falsetti AB. Sex assessment from metacarpals of the human hand. J Forensic Sci. 1995;40:774–6.

13. Case DT, Ross AH. Sex determination from hand and foot bone lengths. J Forensic Sci. 2007;52:264–70.

14. Scheuer JL, Elkington NM. Sex determination from metacarpals and the first proximal phalanx. J Forensic Sci. 1993;38:769–78.

15. Agnihotri AK, Purwar B, Jeebun N, Agnihotri S. Determination of sex by hand dimensions. The Internet Journal of Forensic Science 2006; 1. Available at: http://www.ispub.com/ostia/index. php?xmlFilePath=journals/ijfs/vol1n2/hand.xml (Accessed February 10, 2008).

16. Kanchan T, Rastogi P. Sex determination from hand dimensions of North and South Indians. J Forensic Sci. 2009;54:546–50.

17. Krishan K, Kanchan T, Sharma A. Sex determination from hand and foot dimensions in a North Indian population. J Forensic Sci 2010; (in press).

18. Kyriakidis I, Papaioannidou P. Epidemiologic study of the sexually dimorphic second to fourth digit ratio (2D:4D) and other finger ratios in Greek population. Coll Antropol. 2008;32:1093–8.

19. Voracek M, Loibl LM. Scientometric analysis and bibliography of digit ratio (2D:4D) research, 1998–2008. Psychol Rep. 2009;104: 922–56.

20. McIntyre MH, Cohn BA, Ellison PT. Sex dimorphism in digital formulae of children. Am J Phys Anthropol. 2006;129:143–50.

21. Kanchan T, Kumar GP, Menezes RG. Index and ring finger ratio- a new sex determinant in South-Indian population. Forensic Sci Int. 2008;181:53.e1–4.

22. Kanchan T, Kumar GP, Menezes RG, Rastogi P, Rao PPJ, Menon A, Shetty BSK, Babu YP, Monteiro FNP, Bhagavath P, Nayak VC. Sexual dimorphism of index to ring finger ratio in south Indian adolescents. J Forensic Leg Med. 2010; doi:10.1016/j.jflm. 2010.02.009.

23. Means LW, Walters RE. Sex handedness and asymmetry of hand and foot length. Neuropsychologia. 1982;20:715–9.

24. Voracek M, Dressler SG, Loibl LM. The contributions of Hans-Dieter Rösler: pioneer of digit ratio (2D:4D) research. Psychol Rep. 2008;103:899–916.

25. Van Anders SM, Hampson E. Testing the prenatal androgen hypothesis: measuring digit ratios, sexual orientation, and spatial abilities in adults. Horm Behav. 2005;47:92–8.

26. Garn SM, Burdi AR, Babler WJ, Stinson S. Early prenatal attainment of adult metacarpal- phalangeal rankings and proportions. Am J Phys Anthropol. 1975;43:327–32.

27. Manning JT. Digit ratio: a pointer to fertility, behaviour, and health. New Brunswick: Rutgers University Press; 2002.

28. Lutchmaya S, Baron-Cohen S, Raggatt P, Knicmeyer R, Manning JT. 2nd to 4th digit ratios, fetal testosterone and estradiol. Early Hum Dev. 2004;77:23–8.

29. Putz DA, Gaulin SJC, Sporter RJ, McBurney DH. Sex hormones and finger length: what does 2D:4D indicate? Evol Hum Behav. 2004;25:182–99.

30. Williams TJ, Pepitone ME, Christensen SE, Cooke BM, Huberman AD, Breedlove NJ, et al. Finger-length ratios and sexual orientation. Nature. 2000;404:455–6.

31. Lippa RA. Are 2D: 4D finger-length ratios related to sexual orientation? yes for men, no for women. J Pers Soc Psychol. 2003; 85:179–88.

32. Manning JT, Stewart A, Bundred PE, Trivers RL. Sex and ethnic differences in 2nd to 4th digit ratio of children. Early Hum Dev. 2004;80:161–8.

33. Manning JT, Henzi P, Venkatramana P, Martin S, Singh D. Second to fourth digit ratio: ethnic differences and family size in English, Indian and South African population. Ann Hum Biol. 2003;30:579–88.

34. Manning JT, Barley L, Walton J, Lewis-Jones D, Trivers RL, Singh D, et al. The 2nd to 4th digit ratio, sexual dimorphism, population differences, and reproductive success, evidence for sexually antagonistic genes? Evol Hum Behav. 2000;21:163–83.

35. McFadden D, Shubel E. Relative lengths of fingers and toes in human males and females. Horm Behav. 2002;42:492–500.

36. Manning JT, Callow M, Bundred PE. Finger and toe ratios in humans and mice: implications for the aetiology of diseases influenced by HOX genes. Med Hypotheses. 2003;60:340–3.

37. Manning JT, Scutt D, Wilson J, Lewis-Jones DI. The ratio of 2nd to 4th digit length: a predictor of sperm numbers and concentrations of testosterone, luteinizing hormone and oestrogen. Hum Reprod. 1998;13:3000–4.

38. Voracek M. Why digit ratio (2D:4D) is inappropriate for sex determination in medicolegal investigations. Forensic Sci Int. 2009;185:e29–30.

39. Voracek M. Comparative study of digit ratios (2D:4D and other) and novel measures of relative finger length: testing magnitude and consistency of sex differences across samples. Percept Mot Skills. 2009;108:83–93.

ORIGINAL ARTICLE

Virological investigations in sudden unexpected deaths in infancy (SUDI)

M. A. Weber · J. C. Hartley · M. T. Ashworth ·
M. Malone · N. J. Sebire

Abstract Previous studies have implicated viral infections in the pathogenesis of sudden unexpected death in infancy (SUDI), and routine virological investigations are recommended by current SUDI autopsy protocols. The aim of this study is to determine the role of post-mortem virology in establishing a cause of death. A retrospective review of 546 SUDI autopsies was carried out as part of a larger series of >1,500 consecutive paediatric autopsies performed over a 10-year period, 1996–2005, in a single specialist centre. Virological tests were performed as part of the post-mortem examination in 490 (90%) of the 546 SUDI autopsies, comprising 4,639 individual virological tests, of which 79% were performed on lung tissue samples. Diagnostic methods included immunofluorescence assays (using a routine respiratory virus panel; 98% of cases), cell culture (61%), rapid culture techniques such as the DEAFF test for CMV (55%), PCR (13%), electron microscopy (10%), and others. Virus was identified in only 18 cases (4%), viz. five cases of enterovirus, four of RSV, three of HSV and CMV, and one each of adenovirus, influenza virus and HIV. In seven of the 18 cases the death was classified as due to viral infection, whilst of the remaining 11 cases, death was due to bacterial infection in five, a non-infective cause in one and unexplained in five. Virus was identified in 33% of deaths due to probable viral infections, but also in 6% of SUDI due to bacterial infections, and in 2% of SUDI due to known non-infective causes and unexplained SUDI. When predominantly using immunofluorescence, virus is identified in only a small proportion of SUDI autopsies, resulting in a contribution to the final cause of death in <2% of SUDI post-mortem examinations. Routine post-mortem virological analysis by means of an immunofluorescence respiratory virus panel appears to be of limited benefit in SUDI for the purposes of determining cause of death. Application of a broader panel using more sensitive detection techniques may reveal more viruses, although their contribution to the final cause of death requires further exploration.

Keywords SUDI · SIDS · Sudden death · Infancy · Autopsy · Infection · Virology

M. A. Weber (✉) · M. T. Ashworth · M. Malone · N. J. Sebire
Department of Paediatric Histopathology, Great Ormond Street
Hospital for Children and UCL Institute of Child Health,
Great Ormond Street, London WC1N 3JH, UK
e-mail: WeberM1@gosh.nhs.uk

J. C. Hartley
Department of Microbiology, Great Ormond Street Hospital
for Children and UCL Institute of Child Health,
Great Ormond Street, London WC1N 3JH, UK

Introduction

Sudden unexpected death in infancy (SUDI) encompasses all infant deaths (aged 1 week–1 year of age) that occur relatively suddenly and unexpected by history; in around a third of cases, the post-mortem examination and/or review of the clinical history and death scene will reveal a cause of death (explained SUDI), whilst the remainder will remain unexplained using current investigative autopsy protocols [1]. The latter group ('unexplained SUDI') is broadly equivalent to 'sudden infant death syndrome' (SIDS) if death occurred during sleep [2] and for the purposes of this study, the terms 'unexplained SUDI' and 'SIDS' will be used synonymously. Many risk factors have been identified for unexplained SUDI/SIDS, including prone sleeping, co-sleeping and maternal smoking, as well as high ambient room temperatures, excessive clothing and/or bedding,

head covering, preterm birth and/or intrauterine growth restriction, multiple pregnancy, high parity, young maternal age and low socioeconomic class [3–22]. As a way of explaining the association of apparently diverse risk factors with unexplained SUDI/SIDS, the 'triple risk hypothesis' suggests that in these cases death occurs as a consequence of the concurrent interaction of three factors: an intrinsically vulnerable infant, a critical developmental period, and exposure to exogenous stressors [23]. This model therefore suggests that death may be the result of different aetiologies that share a final common pathway, rather there being a single common cause for SIDS [23–25].

Infection has been previously identified as a cause of death in explained SUDI, usually based on a combination of histopathological and microbiological findings [1, 7, 26–29]. Several studies have suggested that many currently unexplained SUDI/SIDS deaths may likewise be related to infection, possibly mediated by abnormal systemic immune responses to otherwise transient or subclinical bacterial infections [30]; for example, the so-called 'common bacterial toxin hypothesis' postulates that some SIDS may be caused by bacterial toxins, most likely produced by upper respiratory tract organisms such as Staphylococcus aureus [31–33].

Similarly, previous studies have implicated viral infections in the pathogenesis of unexplained SUDI/SIDS, usually by acting as 'environmental stressors' as part of the triple risk hypothesis; alternatively, sudden death may also occasionally be caused by an overwhelming, disseminated viral infection (explained SUDI) [1]. The current SUDI autopsy protocol in the UK [34] recommends that routine virological investigations are carried out, either using a nasopharyngeal aspirate obtained in the Accident and Emergency (A&E) department, or by collecting a postnasal swab or nasopharyngeal aspirate, lung sample, cerebrospinal fluid (CSF) or faeces at post-mortem 'if indicated' and not already taken in the A&E department. However, these recommendations give little guidance as to what viruses should be routinely tested for, or about preferred virus detection methods that should be used in the post-mortem setting (other than making reference to 'viral cultures, immunofluorescence and DNA amplification techniques'). Furthermore, similar to the interpretation of a positive bacterial pathogenic isolate, the interpretation of a positive virological result may be difficult in the absence of histological evidence of inflammation.

The aim of this study is therefore to establish the frequency of virus detection in SUDI autopsies and, specifically, to determine the contribution of post-mortem virology in establishing a cause of death.

Methods

A retrospective review of 546 SUDI autopsies was performed as part of a larger series of >1,500 consecutive paediatric autopsies performed over a 10-year period, 1996–2005, in a single specialist centre. SUDI was defined as the sudden and unexpected death of an infant aged 7–365 days. Local research ethics committee approval was obtained prior to the start of this project.

All autopsies were entered into a purposefully designed Microsoft Access database by a single paediatric pathologist (MAW). The information was extracted from paper copies of the post-mortem reports, and was entered using strictly defined criteria. For each organ system, all macroscopic and microscopic findings were separately entered. All microbiological data, including all bacteriological and virological tests, were extracted from a central computerised pathology database and imported into the database. Entries were manually checked for accuracy.

For the purposes of this study, only those specimens that were collected at the time of the post-mortem examination were included in the analysis, and the investigations were restricted to immunofluorescence, molecular tests (such as the polymerase chain reaction or PCR), electron microscopy (EM) and cell culture results only. Specimens that had been taken after death but prior to the post-mortem examination (e.g. in the A&E department at the referring hospital) were excluded from the analysis, as were all serological investigations, although the results of these would have been included in the assessment of the final cause of death.

Following a review of the post-mortem findings (which included the macroscopic and histological findings, and the results of all ancillary investigations), and of the clinical history available to the pathologist at the time of the autopsy (including any given details of the death scene investigation), the final cause of death was classified into two broad categories: unexplained SUDI and explained SUDI. The latter was further categorised into deaths due to viral infections (e.g. myocarditis or gastroenteritis, or other histological (with or without immunohistochemical) evidence of disseminated viral infection), deaths caused by non-viral infections (bacterial infections and three cases of Pneumocystis jirovecii (carinii) pneumonitis), and deaths due to non-infective causes (e.g. those due to accidents, inflicted injury or previously undiagnosed structural congenital heart disease). Modified chi-squared (comparison of proportion) test was used to assess the significance of differences in frequencies between these groups.

Results

Of the 546 SUDI, post-mortem virological investigations were performed in 490 (90%) cases. Of the 56 patients in whom no post-mortem virological analyses were performed, 27 died of a clear non-infective cause of death, 11 of bacterial infection, and 18 deaths were unexplained.

Of the 490 cases in which virological investigations were performed at autopsy, there were 21 SUDI due to presumed viral infections, 86 SUDI due to non-viral infections (comprising 83 bacterial infections and three cases of Pneumocystis jirovecii (carinii) pneumonitis), 57 SUDI who died from known non-infective causes of death, and 326 otherwise unexplained deaths (unexplained SUDI). Overall, there were 4,639 different virological tests for the 490 SUDI cases, and 79% of these were performed on lung samples.

In 89% of cases in whom a lung sample was taken for virology, a panel of viruses was tested for by immunofluorescence (adenovirus, influenza virus types A and B, parainfluenza virus types 1 and 3, and respiratory syncytial virus or RSV) (Fig. 1). Overall, diagnostic methods included immunofluorescence assays (98% of cases), cell culture (61%), rapid culture techniques such as the DEAFF (detection of early antigen fluorescent foci) test for cytomegalovirus (CMV; 55%), PCR (13%), EM (10%), and others. Of the 4,639 virological tests overall, only 25 (<1%) were positive for virus.

Of the 490 SUDI, virus was detected in 18 (4%) infants overall, including in seven (33%) of the 21 deaths classified as due to viral infections, in five (6%) of the 86 deaths due to non-viral infections, in one (2%) of the 57 SUDI who died from known non-infective causes, and in five (2%) of the 326 unexplained SUDI (Table 1). There was a significantly higher prevalence of virus detection in the non-viral infection group compared to unexplained SUDI (difference 4.3%, 95% CI 0.5% to 11.5%, $P = 0.02$), but there was no difference in virus detection between unexplained SUDI and the non-infective cause-of-death group (difference 0.2%, 95% CI -2.3% to 7.8%, $P > 0.99$).

Overall, the 18 cases with viral isolates comprised five cases of enterovirus, four cases of RSV, three of herpes simplex virus (HSV) and CMV, and one each of adenovirus, influenza virus and HIV (Fig. 2; Table 2). Whilst virus detection was significantly higher in the viral infection group, it is noteworthy that a virus was not detected in two-thirds ($n = 14$) of these deaths, including eight cases of myocarditis, five cases of gastroenteritis, and one case of disseminated CMV infection (diagnosed on histology of the kidneys).

Discussion

The results of this study have shown that, firstly, when predominantly using immunofluorescence on post-mortem lung tissue, virus is identified in only a small proportion of SUDI. Furthermore, whilst at least two-thirds of the 18 cases in which virus was detected showed significant pathology, virus detection was essential to the diagnosis of the final cause of death in <2%. Virus was identified in significantly more cases that died from a viral infection than in infants who died from a non-viral infection or an unexplained cause. Conversely, virus was detected in up to

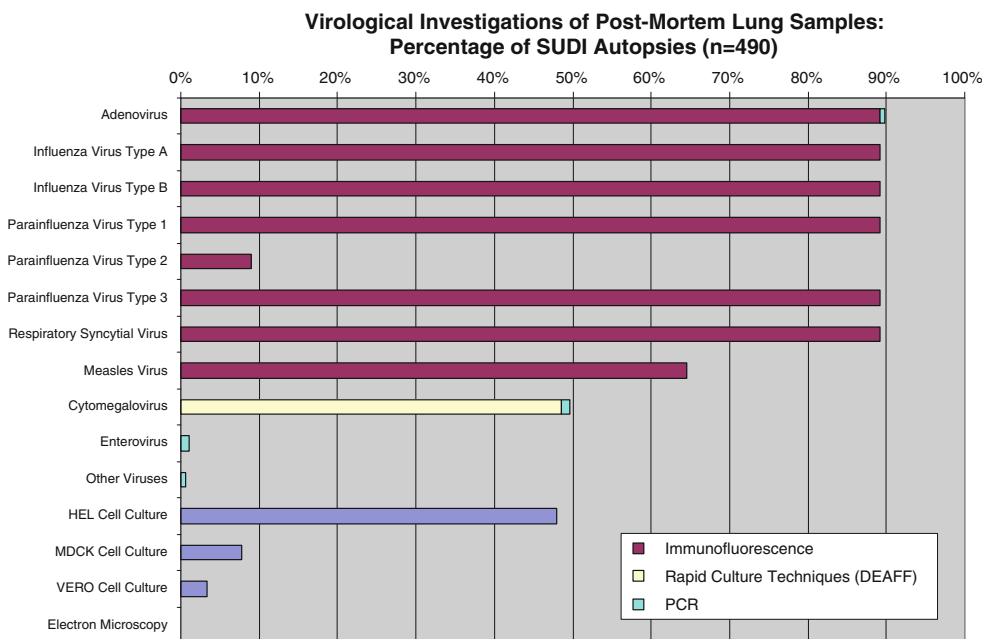**Fig. 1** Virological investigations of post-mortem lung samples

Table 1 Virus detection in SUDI: overall, virus was identified in only 4% of all SUDI in which virological investigations were performed as part of the post-mortem examination ($n = 490$)

SUDI category	Virus detected N (%)	Total number of cases	Statistics[a]
A. Explained SUDI: viral infections	7 (33)	21	N/A
B. Explained SUDI: non-viral infections	5 (6)	86	A vs. B $P = 0.001$
C. Explained SUDI: non-infective causes of death	1 (2)	57	A vs. C $P = 0.0002$
D. Unexplained SUDI	5 (2)	326	A vs. D $P < 0.0001$
E. All SUDI	18 (4)	490	N/A

No virus was detected in two-thirds of cases in which death was classified as due to viral infection. On the other hand, virus was identified in up to 2% of sudden deaths due to non-infective causes, presumably either reflecting normal/asymptomatic carriage or an incidental viral infection with no bearing on the final cause of death

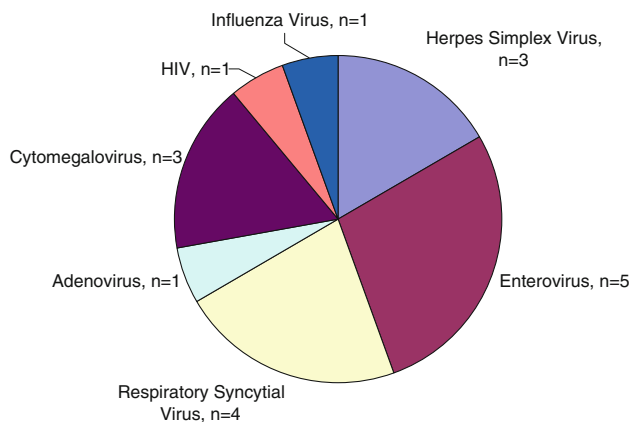[a] Comparison of proportion test; *N/A* not applicable

Fig. 2 Specific viruses detected in SUDI. Almost half (44%) of these were detected by PCR

2% of sudden deaths due to non-infective causes, presumably either reflecting normal/asymptomatic carriage or an incidental viral infection with no bearing on the cause of death.

Secondly, although the interpretation of positive findings in the absence of histological evidence of active infection remains difficult, there was no difference in the frequency of virus detection in this series between unexplained deaths and sudden deaths due to non-infective causes, suggesting that virus identified in the former, with no other clinical history or morphological evidence of viral infection, may likewise merely represent normal/asymptomatic carriage or an incidental viral infection with no bearing on the cause of death. The observed small, but statistically significant, difference in viral detection between the non-viral infection group and unexplained SUDI group suggests that in a small proportion of cases overwhelming bacterial infections may complicate an antecedent viral infection.

Several studies have shown a higher prevalence of virus detection in SIDS cases (on average 22%) compared to controls (on average 8%) [35]; similar results were obtained in a recent German study, with virus isolated in 23 of 93 (25%) SIDS compared to 2 of 25 (8%) non-SIDS [36]. The low viral yield in this series (including all SUDI from 1996 to 2005 inclusive) may be partly explained by the predominant use of immunofluorescence, PCR being considered the more sensitive technique for virus detection [37], although long post-mortem intervals, with resultant degradation of viral particles, may also have played a role. Furthermore, unlike most bacteriological investigations, virus isolation/identification is usually determined by targeted virological analyses that can only detect those viruses against which the analysis has been specifically designed for, e.g. immunofluorescence or PCR against CMV will not detect RSV or vice versa. This does not apply to all virological techniques, and exceptions include the use of EM or cell cultures for virus isolation, but even the latter require a degree of anticipatory judgement as the different cell lines (such as VERO, HEL or MDCK) are sensitive to only a limited range of different viruses. Thus, whilst most centres will test for a panel of different viruses, and may occasionally employ EM or cell cultures, there remains a high likelihood that unless a specific virus is specifically tested for, it will remain undetected. Which viruses to test for, however, remains controversial; although many (predominantly respiratory) viruses have been implicated in SIDS, including RSV, influenza virus, rhinovirus, adenovirus and CMV), none has been consistently associated with SIDS [35]. Moreover, the optimum post-mortem sample sites for virological investigations in this setting remain currently undetermined.

As these data indicate, the mere detection of a virus does not necessarily indicate infection or even imply a contributory role leading to the patient's demise, as the viral

Table 2 Table of all 18 cases in whom virus was detected at post-mortem

Virus isolated	Virus detection method(s)	Specimen(s) tested	Cause of death and associated pathological findings
Enterovirus	PCR	Lung tissue	Myocarditis, pneumonitis
Enterovirus	PCR	Heart and lung tissue	Pericarditis/myocarditis
Enterovirus	PCR, tissue culture	Bowel contents	Infarction of atrioventricular node of uncertain aetiology; focal chronic inflammatory infiltrates in lungs and larynx; Coxsackie B5 virus isolated from bowel contents
Enterovirus	Not specified	Bowel contents	Unexplained SUDI; evidence of previous inflicted injury (healing/healed rib fractures with pulmonary haemosiderin-laden macrophages)
Enterovirus	Not specified	Bowel contents	Unexplained SUDI; echovirus type 7 isolated from bowel contents
RSV	IF	Lung tissue	Prominent lymphocytic infiltrate in bronchi
RSV	IF	Lung tissue	Diffuse alveolar damage and pneumonia but no viral inclusions; large secundum-type atrial septal defect with pulmonary hypertension; Down syndrome
RSV	IF	Lung tissue	Pneumonia, no viral inclusions
RSV	IF	Tissue NOS	Pneumonia and acute tracheobronchitis, no viral inclusions
CMV	DEAFF	Lung tissue	Disseminated CMV infection with inflammatory infiltrates and viral inclusions in lungs, liver, kidneys, spleen and lymph nodes
CMV	DEAFF	Tissue NOS	Diffuse lymphocytic infiltrate in portal tracts, sparse lymphocytic infiltrate in lungs, no viral inclusions, negative immunohistochemical staining for CMV
CMV	DEAFF, PCR, tissue culture	Lung tissue	Unexplained SUDI, no significant pathological findings, normal lung histology
HSV	PCR	Liver tissue	Disseminated HSV infection with widespread liver necrosis and viral inclusions; pneumonia
HSV	Tissue culture	Lung tissue	Disseminated HSV type 1 infection with widespread liver necrosis and viral inclusions in lungs
HSV	PCR	Spleen tissue	Unexplained SUDI, no significant pathological findings, normal spleen histology
Adenovirus	PCR	Lung tissue	Unexplained SUDI, no significant pathological findings, normal lung histology
Influenza virus	IF	Lung tissue	Pneumonia, A/Fujian/411/2002-like influenza A H3 virus isolated from lung tissue
HIV	PCR	Liver tissue	Pneumocystis jirovecii (carinii) pneumonitis/pneumonia; marked lymphoid depletion thymus, spleen and lymph nodes

Virus was detected in 18 SUDI (4%), and of these, two-thirds of cases showed significant pathology that may have been associated with the virus detected. (*PCR* polymerase chain reaction, *IF* immunofluorescence, *DEAFF* detection of early antigen fluorescent foci for CMV, *NOS* not otherwise specified)

isolate may (1) represent a contaminant (the contamination presumably having occurred during the sampling or laboratory process); (2) represent 'established/asymptomatic carriage' (e.g. HSV, varicella-zoster virus and adenovirus); (3) represent a current incidental infection with no bearing on the final cause of death; (4) indicate a contributory viral infection (e.g. a preceding viral infection that subsequently lead to an overwhelming secondary bacterial infection and death); or (5) indicate a fatal viral infection (e.g. disseminated HSV infection in a neonate). Most pathologists would agree that a significant viral isolate would be one that is associated with significant inflammatory changes, but even then the distinction between an 'incidental or

contributory viral infection' and one that has directly led to the patient's demise can be a difficult one.

Whilst there are conflicting epidemiological data on the role of viral (upper respiratory tract) infections in the pathogenesis of SIDS, the temporal association between SIDS and viral epidemics [38], and the winter peaks of SIDS in many countries, at least in earlier years [39–41], suggest an association between viral infection and SIDS. Furthermore, a higher proportion of SIDS infants display symptoms of infection prior to death compared to age-matched controls [42, 43] and, as outlined above, several (though not all) studies have shown a higher prevalence of virus detection in SIDS cases (on average 20–25%)

compared to controls (around 8%) [35, 36, 44]. Moreover, the presence of mild inflammatory changes in the (particularly upper) respiratory tract is a common histopathological feature in SIDS and considered additional evidence of a preceding viral infection [44], although it has been shown that the extent of respiratory tract and pulmonary inflammation is similar in SIDS and control infants that died of non-infective causes, suggesting that the microscopic inflammatory changes in themselves are not lethal [45]. However, it has been shown that the presence of a viral infection may further increase the risk of sudden death if combined with other factors associated with SIDS, such as prone sleeping, head covering or smoking [35]. Potential mechanisms whereby viral infections may cause or predispose to sudden death in SIDS are likely to include either direct induction of a 'cytokine storm', similar to bacterial toxins, or, more likely, by indirect, synergistic means, for example, by increasing nasopharyngeal colonisation of toxigenic bacteria and/or promoting the induction of pyrogenic toxins [30].

In summary, the findings of this study have shown that virus is detected in <5% of SUDI autopsies when predominantly using immunofluorescence of post-mortem lung tissue, testing for the routine respiratory virus panel available during the study period. Immunofluorescence of post-mortem lung tissue was positive for virus in a very small proportion of SUDI autopsies (<1%), with almost half of all viruses in this series being detected by PCR. There was no difference in the frequency of virus detection in this series between unexplained SUDI and SUDI due to non-infective causes, suggesting that virus identified in the former, with no other clinical history or morphological evidence of viral infection, may likewise merely represent normal/asymptomatic carriage or an incidental viral infection with no bearing on the final cause of death. Overall, virus detection was essential to the diagnosis of the final cause of death in <2% of SUDI. Routine respiratory virus panel immunofluorescence thus appears to be of limited benefit in determining a cause of death at autopsy. Further research is required to determine the most effective virus detection method(s) in a post-mortem setting, and to establish which virus(es) to routinely test for and which tissue or fluid sample(s) to take for virological analysis in SUDI autopsies.

Key points

1. Virus is detected in <5% of SUDI when predominantly using immunofluorescence of post-mortem lung tissue.
2. Routine respiratory virus panel immunofluorescence of post-mortem lung tissue is positive for virus in a very

small proportion of SUDI (<1%); almost half of all viruses in this series were detected using PCR.
3. There was no difference in the frequency of virus detection in this series between unexplained SUDI and SUDI due to non-infective causes, suggesting that virus identified in the former, with no other clinical history or morphological evidence of viral infection, may likewise merely represent asymptomatic carriage or an incidental viral infection with no bearing on the final cause of death.
4. Overall, virus detection was essential to the diagnosis of the final cause of death in <2% of SUDI. Routine respiratory virus panel immunofluorescence in particular appears to be of limited benefit in determining a cause of death at autopsy.
5. Further research is required to determine the most effective virus detection method(s) in a post-mortem setting, and to establish which virus(es) to routinely test for and which tissue or fluid sample(s) to take for virological analysis in SUDI.

References

1. Weber MA, Ashworth MT, Risdon RA, Hartley J, Malone M, Sebire NJ. The role of post-mortem investigations in determining the cause of sudden unexpected death in infancy (SUDI). Arch Dis Child. 2008;93:1048–53.
2. Krous HF, Beckwith JB, Byard RW, Rognum TO, Bajanowski T, Corey T, Cutz E, Hanzlick R, Keens TG, Mitchell EA. Sudden infant death syndrome and unclassified sudden infant deaths: a definitional and diagnostic approach. Pediatrics. 2004;114:234–8.
3. Fleming PJ, Gilbert R, Azaz Y, Berry PJ, Rudd PT, Stewart A, et al. Interaction between bedding and sleeping position in the sudden infant death syndrome: a population based case-control study. BMJ. 1990;301:85–9.
4. Mitchell EA, Scragg R, Stewart AW, Becroft DM, Taylor BJ, Ford RP, et al. Results from the first year of the New Zealand cot death study. N Z Med J. 1991;104:71–6.
5. Dwyer T, Ponsonby AL, Newman NM, Gibbons LE. Prospective cohort study of prone sleeping position and sudden infant death syndrome. Lancet. 1991;337:1244–7.
6. Scragg RK, Mitchell EA. Side sleeping position and bed sharing in the sudden infant death syndrome. Ann Med. 1998;30:345–9.
7. Fleming P, Blair P, Bacon C, Berry J, editors. Sudden unexpected deaths in infancy. The CESDI SUDI studies 1993–1996. London: The Stationary Office; 2000.
8. Hauck FR, Herman SM, Donovan M, et al. Sleep environment and the risk of sudden infant death syndrome in an urban population: the Chicago Infant Mortality Study. Pediatrics. 2003;111: 1207–14.
9. Fleming PJ, Blair PS, Ward PM, Tripp J, Smith IJ. Sudden infant death syndrome and social deprivation: assessing epidemiological

factors after post-matching for deprivation. Paediatr Perinat Epidemiol. 2003;17:272–80.

10. Malloy MH. Sudden infant death syndrome among extremely preterm infants: United States 1997–1999. J Perinatol. 2004;24:181–7.

11. Gilbert R, Salanti G, Harden M, See S. Infant sleeping position and the sudden infant death syndrome: systematic review of observational studies and historical review of recommendations from 1940 to 2002. Int J Epidemiol. 2005;34:874–87.

12. Vennemann MM, Findeisen M, Butterfass-Bahloul T, Jorch G, Brinkmann B, Kopcke W, et al. Modifiable risk factors for SIDS in Germany: results of GeSID. Acta Paediatr. 2005;94:655–60.

13. Tappin D, Ecob R, Brooke H. Bedsharing, roomsharing, and sudden infant death syndrome in Scotland: a case-control study. J Pediatr. 2005;147:32–7.

14. Anderson ME, Johnson DC, Batal HA. Sudden infant death syndrome and prenatal maternal smoking: rising attributed risk in the Back to Sleep era. BMC Med. 2005;3:4.

15. Shah T, Sullivan K, Carter J. Sudden infant death syndrome and reported maternal smoking during pregnancy. Am J Public Health. 2006;96:1757–9.

16. Blair PS, Sidebotham P, Berry PJ, Evans M, Fleming PJ. Major epidemiological changes in sudden infant death syndrome: a 20-year population-based study in the UK. Lancet. 2006;367:314–9.

17. McGarvey C, McDonnell M, Hamilton K, O'Regan M, Matthews T. An 8 year study of risk factors for SIDS: bed-sharing versus non-bed-sharing. Arch Dis Child. 2006;91:318–23.

18. Horsley T, Clifford T, Barrowman N, Bennett S, Yazdi F, Sampson M, Moher D, Dingwall O, Schachter H, Côté A. Benefits and harms associated with the practice of bed sharing: a systematic review. Arch Pediatr Adolesc Med. 2007;161:237–45.

19. Ruys JH, de Jonge GA, Brand R, Engelberts AC, Semmekrot BA. Bed-sharing in the first four months of life: a risk factor for sudden infant death. Acta Paediatr. 2007;96:1399–403.

20. Fleming P, Blair PS. Sudden infant death syndrome and parental smoking. Early Hum Dev. 2007;83:721–5.

21. Moon RY, Horne RS, Hauck FR. Sudden infant death syndrome. Lancet. 2007;370:1578–87.

22. Blair PS, Mitchell EA, Heckstall-Smith EM, Fleming PJ. Head covering—a major modifiable risk factor for sudden infant death syndrome: a systematic review. Arch Dis Child. 2008;93:778–83.

23. Byard RW, Krous HF, editors. Sudden infant death syndrome. Problems, progress & possibilities. London: Arnold, Hodder Headline Group; 2001.

24. Filiano JJ, Kinney HC. A perspective on neuropathologic findings in victims of the sudden infant death syndrome: the triple-risk model. Biol Neonate. 1994;65:194–7.

25. Fleming P, Tsogt B, Blair PS. Modifiable risk factors, sleep environment, developmental physiology and common polymorphisms: understanding and preventing sudden infant deaths. Early Hum Dev. 2006;82:761–6.

26. Sadler DW. The value of a thorough protocol in the investigation of sudden infant deaths. J Clin Pathol. 1998;51:689–94.

27. Mitchell E, Krous HF, Donald T, Byard RW. An analysis of the usefulness of specific stages in the pathologic investigation of sudden infant death. Am J Forensic Med Pathol. 2000;21:395–400.

28. Arnestad M, Vege A, Rognum TO. Evaluation of diagnostic tools applied in the examination of sudden unexpected deaths in infancy and early childhood. Forensic Sci Int. 2002;125:262–8.

29. Morris JA, Harrison LM, Partridge SM. Postmortem bacteriology: a re-evaluation. J Clin Pathol. 2006;59:1–9.

30. Highet AR. An infectious aetiology of sudden infant death syndrome. J Appl Microbiol. 2008;105:625–35.

31. Morris JA, Haran D, Smith A. Hypothesis: common bacterial toxins are a possible cause of the sudden infant death syndrome. Med Hypotheses. 1987;22:211–22.

32. Morris JA. The common bacterial toxins hypothesis of sudden infant death syndrome. FEMS Immunol Med Microbiol. 1999;25:11–7.

33. Blackwell CC, Gordon AE, James VS, MacKenzie DA, Mogensen-Buchanan M, El Ahmer OR, et al. The role of bacterial toxins in sudden infant death syndrome (SIDS). Int J Med Microbiol. 2002;291:561–70.

34. Kennedy H. Sudden unexpected death in infancy. A multi-agency protocol for care and investigation. The report of a working group convened by The Royal College of Pathologists and The Royal College of Paediatrics and Child Health. London: The Royal College of Pathologists/The Royal College of Paediatrics and Child Health; 2004.

35. Samuels M. Viruses and sudden infant death. Paediatr Respir Rev. 2003;4:178–83.

36. Bajanowski T, Rolf B, Jorch G, Brinkmann B. Detection of RNA viruses in sudden infant death (SID). Int J Legal Med. 2003;117:237–40.

37. Freymuth F, Vabret A, Cuvillon-Nimal D, Simon S, Dina J, Legrand L, Gouarin S, Petitjean J, Eckart P, Brouard J. Comparison of multiplex PCR assays and conventional techniques for the diagnostic of respiratory virus infections in children admitted to hospital with an acute respiratory illness. J Med Virol. 2006;78:1498–504.

38. Uren EC, Williams AL, Jack I, Rees JW. Association of respiratory virus infections with sudden infant death syndrome. Med J Aust. 1980;1:417–9.

39. Carpenter RG, Gardner A. Environmental findings and sudden infant death syndrome. Lung. 1990;168(Suppl):358–67.

40. Beal S, Porter C. Sudden infant death syndrome related to climate. Acta Paediatr Scand. 1991;80:278–87.

41. Douglas AS, Allan TM, Helms PJ. Seasonality and the sudden infant death syndrome during 1987–9 and 1991–3 in Australia and Britain. BMJ. 1996;312:1381–3.

42. Cameron MH, Williams AL. Development and testing of scoring systems for predicting infants with high-risk of sudden infant death syndrome in Melbourne. Aust Paediatr J. 1986;22(Suppl 1):37–45.

43. Platt MW, Blair PS, Fleming PJ, Smith IJ, Cole TJ, Leach CE, et al. A clinical comparison of SIDS and explained sudden infant deaths: how healthy and how normal? CESDI SUDI Research Group. Confidential Inquiry into Stillbirths and Deaths in Infancy study. Arch Dis Child. 2000;82:98–106.

44. Fleming KA. Viral respiratory infection and SIDS. J Clin Pathol. 1992;45(Suppl):29–32.

45. Krous HF, Nadeau JM, Silva PD, Blackbourne BD. A comparison of respiratory symptoms and inflammation in sudden infant death syndrome and in accidental or inflicted infant death. Am J Forensic Med Pathol. 2003;24:1–8.

ORIGINAL ARTICLE

The cardiovascular, respiratory, and metabolic effects of a long duration electronic control device exposure in human volunteers

Donald M. Dawes · Jeffrey D. Ho · Robert F. Reardon · James R. Miner

Abstract Electronic control devices (ECD) have become popular in law enforcement because they have filled a gap left by other law enforcement devices, tactics, or tools and have been shown to reduce officer and suspect injuries. Civilians are using the same technology for defensive purposes. TASER C2 is the latest generation civilian-marketed device from the manufacturer. Unlike the law enforcement devices, the device discharges for 30 s continuously. This study is the first to look at the cardiovascular, respiratory, and metabolic effects of this device on human subjects. This was a prospective, observational study of human subjects involved in a training course. Subjects were exposed for 30 s on the anterior thorax. Vital signs, ECG, troponin I, pH, lactate, and creatine kinase (CK) were measured before and immediately after the exposure. Troponin I, pH, lactate, and CK were measured again 24 h after the exposure. Continuous spirometry was used to evaluate the respiratory effects. Echocardiography was also performed before, during, and immediately after the exposure to determine heart rate and rhythm. Eleven subjects completed the study. There were no clinically important electrocardiogram changes and no positive troponins. Spirometry showed an increase in minute ventilation during the exposure. There was no important change in CK at 24 h. Lactate was slightly higher and pH was slightly lower after the exposure, but similar to the effects of physical exertion. Echocardiography was performed in 6 subjects. In half of these subjects, the rhythm was determined to be "sinus" and in the other half the rhythm was indeterminant. In our study, the civilian device caused a mild lactic acidosis. No other important physiologic effects were found.

Keywords TASER · Electronic control device · Echocardiography · ECG · Troponin · pH · Acidosis · Spirometry

Introduction

Electronic control devices (ECD) have become popular in law enforcement because they have filled a gap left by other law enforcement devices, tactics, or tools and have been shown to reduce officer and suspect injuries [1–3]. Lee et al. [4] did not find this benefit in their paper, but their results were based on reporting from only 4 departments out of the 126 they sent surveys to, and they only reported on "serious officer injuries requiring emergency room visits". The devices deliver electrical charge from a capacitor in discrete pulses at fast rates leading to the depolarization of peripheral motor neurons within a "zone of capture" and subsequent involuntary, sub-tetanic muscle contraction. The devices also depolarize afferent sensory neurons leading to pain. There is likely to also be a smaller mechanistic effect from the direct depolarization of skeletal muscle in the immediate area of the charge delivery, and it has been theorized that more distant muscle effects may be the result of reflex arc involvement [5–7]. There may also be a pain-related behavioral effect.

Civilians are using the same technology being used by law enforcement for defensive purposes. TASER C2 is the latest generation civilian-marketed device from the manufacturer. Unlike the law enforcement devices, the device

D. M. Dawes
Lompoc Valley Medical Center, Lompoc, CA, USA

J. D. Ho (✉) · R. F. Reardon · J. R. Miner
Department of Emergency Medicine, Hennepin County Medical Center, 701 Park Avenue South, Minneapolis, MN 55415, USA
e-mail: jeffrey.ho@hcmed.org

discharges for 30 s continuously. The device was designed for the purpose of affording the user a "window of escape." This is different from the law enforcement use that is to assist in control and restraint. Jauchem, et al previously studied the device in an animal model [8]. This study is the first to look at the cardiovascular, respiratory, and metabolic effects of this device in human subjects, and the first study of durations longer than 15 s in human subjects.

Methods

This was a prospective, observational study of the effects of the TASER C2 device on human subjects approved by the institutional review board at Hennepin County Medical Center (Minneapolis, MN)and conducted at the manufacturer headquarters in Scottsdale, AZ. The subjects were a convenience sample of law enforcement or correctional officers participating in a training course at the headquarters and receiving an electronic control device exposure as part of the course. The training objective was to demonstrate the long incapacitation time of the civilian device to make officers aware of the potential safety concern to them when encountering suspects armed with such a device.

Subjects provided informed consent and completed a medical-screening questionnaire that was reviewed by a study physician. There were no specific exclusion criteria except that subjects had to be at full duty status with their department, be approved by their department for a TASER training course, and not be pregnant. Potential subjects were asked beforehand not to engage in physical activity within 48 h of the course. Subjects who did not comply with this or would not be able to avoid physical activity before the 24-hour blood draw were not eligible for the study. Subjects were given a TASER X26 or C2 as compensation for their participation.

A commercial skin resistance analyzer (Omron Fat Loss Monitor HBF-306, Omron Healthcare, Inc., Bannockburn, Illinois) was used to determine body fat percentage. The subjects were laid supine on a training mat for testing. Baseline vital signs (blood pressure and heart rate) were taken (Nonin 2120, Plymouth, MN) and baseline venous CK, troponin I, pH, and lactate were drawn (this baseline was taken approximately 5 min before the actual exposure, mostly due to the several minutes of quiet breathing before the exposure to obtain baseline respiratory data). All blood was immediately analyzed after the draw using the Abbott Point-of-Care i-STAT (East Windsor, NJ) and CG4+ and troponin I cartridges. CK, not available from Abbott, was collected and sent by courier to LabCorp (Phoenix, AZ) for analysis. A "positive" troponin was any troponin outside

of the reporting range for normal for the i-STAT cartridge (0.08 ng/mL).

The subjects were fitted with a neoprene mask. The probes were removed from the firing cartridge and clipped off and the wires were taped to the skin in conductive gel. All exposures were chest to abdomen in the mid-line. Continuous respiratory data were collected by a breath-by-breath gas exchange system (Medical Graphics CPX Ultima, St. Paul, MN). The CPX Ultima measures the oxygen and carbon dioxide concentrations of breathed air, the respiratory rate, and the tidal volume on a breath-by-breath basis. Subjects had surface electrocardiography (Welch Allyn Cardio-perfect, Skaneateles Falls, NY) performed. A subset of subjects had echocardiography (Sonosite M-Turbo, Bothell, WA) performed by a non-blinded attending physician expert in ultrasonography. This subset was determined by the availability of the ultrasonographer during the testing period. The echocardiography was performed using a 1–5 MHz phased-array transducer. Parasternal long-axis views including the anterior leaflet of the mitral valve were obtained pre-exposure, during the exposure, and post-exposure. The two-dimensional view of the heart was assessed in real time by the ultrasonographer prior to changing to the M-mode for measurement of the heart rate and determination of the rhythm. Heart rate was determined by measuring the time between contractions. Heart rhythm was determined by imaging the anterior leaflet of the mitral. The presence of both E and A waves was used as evidence for sinus rhythm (Fig. 1a). The E wave corresponds to the mitral valve opening with passive filling of the left ventricle. The A wave corresponds to the mitral valve opening with atrial contraction.

After allowing several minutes to collect baseline spirometry, to perform the surface electrocardiography, and echocardiography, the firing cartridge was loaded into an "off the shelf" TASER C2, and subjects had a 30-second continuous exposure from the device. The subjects were visually monitored at all times by study physicians for evidence of physiologic compromise such as syncope, vomiting, and hypoxia.

The ultrasonographer repeated his test during the exposure (an attempt was made for continuous visualization of the heart during the exposure) and immediately after the exposure. Vital signs, blood draw for CK, troponin I, pH, and lactate, and surface ECG were repeated immediately (within 30 s to 1 min generally, and not more than 2 min) after the exposure. Spirometry was continued for several minutes after the exposure until a rest breathing pattern was achieved. Troponin I, pH, lactate, and CK were drawn again at 24 h, at which time the subject was reassessed by a study physician. A blinded cardiologist read the surface electrocardiograms.
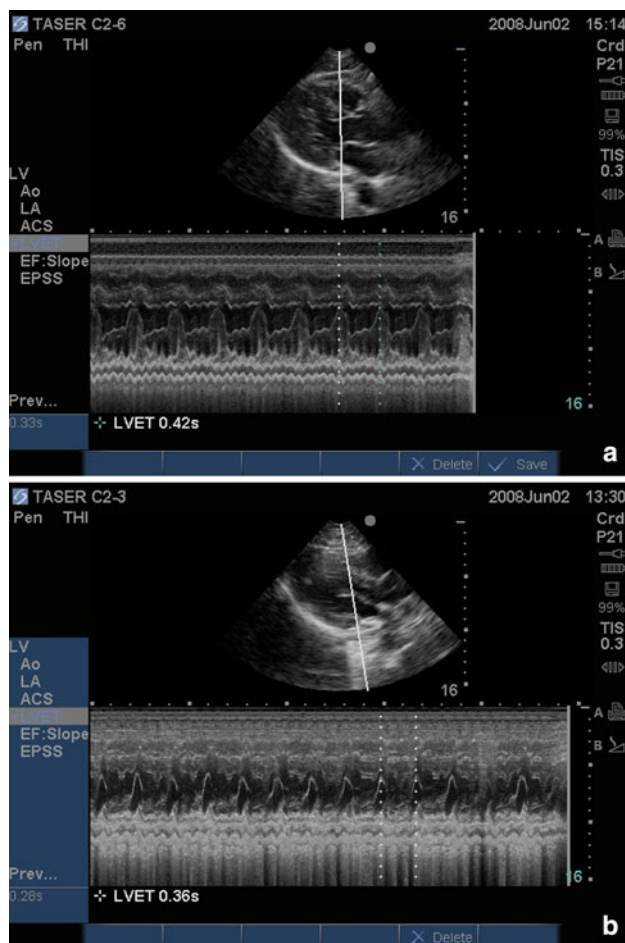
Fig. 1 a Intraexposure in a sinus subject. b Intra-exposure echocardiogram on an indeterminant subject

Data were entered into an Excel spreadsheet (Microsoft Corp, Redmond, WA) and exported into STATA 10.0 (Stata Corp, College Station, TX). Data were analyzed with descriptive statistics.

Results

12 subjects were enrolled. One subject voluntarily withdrew from the study just prior to the exposure. The subject appeared overly nervous to the study physicians and was hyperventilating and when asked if he was sure he wanted to proceed (asked of all subjects), he withdrew. Eleven subjects completed the study. Subject characteristics are presented in Table 1. The median age was 25 years (range 21–40). Ten of eleven were male (89.9%). The median body mass index was 30.7 kg/m^2 (range 24.1–41.7). The median body fat was 24.2% (range 8.3–41.0). Most of our subjects reported no significant past medical history, although one subject had rheumatoid arthritis, and one subject had several medical problems including hypertension, obstructive sleep apnea, GERD, and depression. Six of the 11 subjects had echocardiography. The vital signs are presented in Table 2. The echocardiography results are presented in Table 3. The median heart rate during exposure was 152.5 beats per minute (range 100–176). The electrocardiography results, as read by the blinded cardiologist, are presented in Table 4. The cardiologist only noted a change based on rate if the rate increased or decreased more than 10 beats per minute. Subject 11 had non-specific ST segment depression in the post-exposure electrocardiogram. The subject had no subjective complaints, had no cardiac risk factors, had no evidence of capture during the exposure, and had a negative troponin at 24 h. There were no "positive" troponins at 24 h in any subject. There were no episodes of syncope, vomiting, or hypoxia (skin color) during the exposures. There were no reported adverse outcomes after the exposures or at 24 h. The pH, lactate, and CK are presented in Table 5. There was no clinically important change in CK. The pH dropped immediately post-exposure and lactate increased. The respiratory data are presented in Table 6. Minute ventilation increased during the exposure compared to baseline.

Table 1 Subject characteristics

	Sex	Age	PMH	Medications	BMI	% Body fat	Spread (inches)
1	M	24	Appendectomy	None	31.9	28.5	16
2	M	25	None	INH	30.7	27.7	13
3	M	33	Rheumatoid arthritis	Prednisone, Humira, Methotrexate	24.4	16.7	14
4	M	29	Kerotoplasty	Predforte	41.7	34.4	16
5	M	40	Hypertension, GERD, OSA, depression	Prevacid, Cymbalta, Zyrtec, "Blood pressure medications"	33.0	32.8	14
6	M	25	None	None	24.1	8.3	14
7	M	30	None	None	28.7	22.9	17
8	M	21	None	None	24.4	14.1	17
9	M	22	None	None	35.3	24.2	17.5
10	F	23	Cholecystectomy	None	38.4	41	17.5
11	M	24	None	None	28.3	18.2	17

Table 2 Vital signs

	Pre-exposure blood pressure	Pre-exposure heart rate	Post-exposure blood pressure	Post-exposure heart rate
1	144/97	89	131/85	89
2	152/78	95	147/76	86
3	121/67	85	128/70	67
4	158/89	117	190/82	114
5	127/81	87	128/81	87
6	142/74	90	107/51	90
7	143/93	91	165/83	90
8	137/91	80	148/77	105
9	137/75	105	154/80	115
10	139/62	73	132/63	83
11	154/93	72	142/88	92

All blood pressures are in mmHG and heart rates in beats per second

Table 3 Echocardiography results

	Exposure heart rate	Sinus/indeterminant/other
1	X	X
2	X	X
3	X	X
4	X	X
5	X	X
6	136	Indeterminant
7	162	Sinus
8	166	Indeterminant
9	176	Indeterminant
10	100	Sinus
11	143	Sinus

X—not performed on this subject

There were episodes of non-compliance with the no-exertion requirements before and after the exposure. One subject had a very high baseline CK value (1,956 U/L). This subject was a weightlifter who had lifted weights and used Hydroxycut® (a weight-loss product that contains caffeine and other stimulants) within 48 h of the testing. One subject reported mountain biking in the 24 h after the exposure and before the second CK draw, and another reported jogging between the draws. Unfortunately, none of these activities were reported in the initial screening.

Discussion

We did not find any clinically important cardiac, respiratory, or metabolic effects with the exposure to the TASER C2 except a mild lactic acidosis. Our results were consistent with prior studies with other electronic control devices. Vilke et al. subjected volunteers to a 5-second TASER X26 discharge. In this study there were no positive troponins at 6 h and no ischemic changes or arrhythmias on surface electrocardiogram. There was a change in pH from 7.45 to 7.42 at 1-minute after the 5-second discharge in this study, and lactate increased from 1.4 to 2.8 [9]. Other studies have shown no evidence of cardiac injury or arrhythmias based on troponin and surface electrocardiogram [10–15]. In a study by Ho et al. a 15-second TASER X26 exposure led to a pH change from a baseline of 7.37–7.35 immediately after the exposure, having a trough of 7.33 at 2 min. The lactate was 2.1 immediately after the exposure and peaked at 4.5 at 6 min. As a comparison, the exertion regimen in that study, which consisted of 30 s of push-ups followed by a sprint on a treadmill of less than 2 min, led to a pH of 7.13 immediately after the exposure with a trough of 7.07

Table 4 Electrocardiography results

	Pre-exposure	Post-exposure	Change
1	NSR at 92, sinus arrhythmia	NSR at 92, sinus arrhythmia	None
2	NSR at 98, incomplete RBBB	NSR at 77, incomplete RBBB	Rate decrease by 21
3	NSR at 82, incomplete RBBB	NSR at 72, incomplete RBBB	None
4	NSR at 98	Sinus tachycardia at 103	None
5	NSR at 78	NSR at 83, sinus arrhythmia	Sinus arrhythmia
6	NSR at 88, RAD	Sinus tachycardia at 107	Rate increased by 19
7	NSR at 91	NSR at 86, artifact	None
8	NSR at 90, possible LAE	NSR at 97, possible LAE	None
9	Sinus tachycardia at 120	Sinus tachycardia at 113	None
10	NSR at 90	NSR at 75	Rate decreased by 15
11	NSR at 90, u waves present	NSR at 94, u waves present, <1 mm St depression inferior/lateral leads	Nonspecific minimal ST depression

NSR Normal sinus rhythm, RBBB Right bundle branch block, LAE Left atrial enlargement

Table 5 Blood results

	pH	Lactate	CK
Pre-exposure (median, range)	7.358, 7.307–7.595	1.46, 0.56–5.51	140, 95–502
Post-exposure (median, range)	7.273, 7.196–7.393	5.63, 1.47–17.29	127, 92–476
24 h post-exposure (median, range)	7.340, 7.242–7.388	2.25, 1.1–2.77	187, 124–461

Table 6 Breathing results

	PETCO$_2$	PETO$_2$	Respiratory rate	Tidal volume	Minute ventilation
Pre-exposure (median, range)	36, 31–40	107, 100–112	17, 12–23	0.93, 0.59–1.37	15.1, 11.5–19.1
During exposure (median, range)	27, 23–40	113, 91–124	35, 6–68	0.72, 0.39–2.41	20, 13.7–60.3
Post-exposure (median, range)	38, 31–44	112, 109–120	19, 12–26	1.47, 0.98–2.72	25.7, 19.2–38.4

at 2 min and a lactate of 13.2 immediately after the exposure, with a peak of 14.7 6 min [16]. Allsop et al. [17] found that venous pH decreased from 7.39 to 7.04 after a 30-second maximal sprint. In our study, there were no positive troponins at 24 h and no important changes on surface electrocardiogram. There was one subject with non-specific ST segment changes, but this subject had no complaints, no risk factors, no evidence of capture on echocardiography, and had a negative troponin at 24 h. Our pH and lactate results were more pronounced than the Vilke et al. and Ho, et al. studies, but not inconsistent with the six times duration of the Vilke et al. study and the 2 times duration of the Ho et al. study. Our results were not as pronounced as the 30-second exertion regimen in the Ho et al. study. Another Ho et al. [12] study examined CK after a 5-second exposure to the back with an X26 and found a change of 57 U/L at 24 h. Van Meenen et al. [15] also found a small change in CK at 24 h (174.1–181.4) with 2–5 s exposures (92% had 5 s exposures). Our CK results were similar to Ho et al. with a change of 47 U/L at 24 h. This suggests at least that duration, within this timeframe, may be an unimportant contributor to CK rise. In a study by Ho et al. [18] there was no evidence of respiratory impairment in 15-second exposures. Vilke et al. [9] also had no evidence of respiratory impairment. In our study, we also had no evidence of respiratory impairment. Minute ventilation increased during the exposure.

Previous human studies with chest exposures have not demonstrated direct cardiac capture including discharges up to 15 s and up to three simultaneous discharges, although only one study included probes imbedded in the chest ($n = 92$) [19–22]. In our study, we were only able to determine the rhythm in 3 of 6 subjects during the exposure, but the rates of the indeterminant subjects were 136, 166, and 176, so if captured occurred, it was at a relatively low rate compared to the device pulse rate.

In a Bozeman letter to the editor, he reports on 4,058 field cases in which there is no suggestion of sudden collapse due to an electronic control device exposure [23]. With the studies by Hall et al. and McManus et al. [24, 25] this gives a total of 4,387. The number of chest exposures is not clear given the information in the papers or abstracts. However, in the Bozeman et al. [26] study (incorporating 1,201 subjects), 15% of all exposures, and 22% of all probe exposures were "trans-cardiac". A study of arrest-related deaths temporal to electronic control device use has reported a low incidence of ventricular fibrillation [27]. In Lee et al. there was an increase in arrest-related deaths in the first year after deployment of electronic control devices, but this study was a survey with limited return and there was no attempt to determine if the devices were used in the arrest-related death cases. In addition, the rate of arrest-related deaths returned to baseline in the following years [4].

The risk of harm associated with this device needs to be considered in terms of its intended use. The intended use is for self-defense in a situation in which the user is at reasonable risk of bodily harm. This device offers an alternative to persons either not inclined to carry a firearm or specifically prevented from doing so by law. In police scenarios, the mortality from firearms is 50% [28]. While this number may not translate directly into civilian use, the mortality is likely significant. In addition, the risk of accidental self-harm or other unintentional injury or mortality in personally carrying a gun or keeping a gun at home needs to be considered. The safety profile is reasonable given the intended use of the device.

Limitations

The primary limitation of our study was the small number of subjects. Rare events cannot be reliably detected in such a small study. We could not obtain surface ECG data during the exposures (a limitation no researcher has been

able to overcome to date) and we did not get determinable rhythms in 50% of our subjects. This limits the conclusions that can be made about the intra-exposure cardiac rhythms. In addition, our connection was by wire taped into conductive gel on the skin. While the conductive gel should lower the skin resistance, this may not exactly replicate the conditions of an imbedded probe and our data need to be interpreted with this in mind.

Most of our subjects were "healthy" volunteers. This limitation is likely less important as the intended target in most cases will be physiologically normal since it will be an attacker targeting a victim, although there may be circumstances in which the attacker is under the influence of drugs or has other physiologic variables not replicated in this study.

Conclusions

In our study, the civilian device caused a mild lactic acidosis. No other important physiologic effects were found.

Key points

1. Thirty-second exposures to the anterior thorax from the TASER C2 electronic control device did not cause myocardial damage as determined by serum troponin I.
2. Thirty-second exposures to the anterior thorax from the TASER C2 electronic control device did not cause clinically important electrocardiogram (ECG) changes.
3. There was no evidence of rapid cardiac capture during thirty-second exposures to the anterior thorax from the TASER C2 electronic control device.
4. Thirty-second exposures to the anterior thorax from the TASER C2 electronic control device did not cause respiratory impairment.
5. Thirty-second exposures to the anterior thorax from the TASER C2 electronic control device did cause moderate changes in pH and lactate.

References

1. MacDonald JM, Kaminski RJ, Smith, M. The effect of less-lethal weapons on injures in police use-of-force events. Am J Public Health. 2009; 10.2105/AJPH.2009.159616.

2. Smith M, Kaminski R, Rojek J, Alpert G, Mathis J. The impact of conducted energy devices and other types of force and resistance on officer and suspect injuries. PIJPSM. 2007;30(2):423–46.
3. Jenkinson E, Neeson C, Bleetman A. The relative risk of police use-of-force options: evaluating the potential for deployment of electronic weaponry. J Clin Forensic Med. 2006;13:229–41.
4. Lee B, Vittinghoff E, Whiteman D, Park M, Lau L, Tseng Z. Relation of TASER (electrical stun gun) deployment to increase in in-custody sudden deaths. Am J Cardiol. 2009;103(6):877–80.
5. Despa F, Basati S, Zhang Z, D'Andrea J, Reilly J, Bodnar E, Lee R. Electromuscular incapacitation results from stimulation of spinal reflexes. Bioelectromagnetics. 2009;30:411–21.
6. Reilly J, Diamant A, Comeaux J. Dosimetry considerations for electrical stun devices. Phys Med Biol. 2009;54:1319–35.
7. Sun H, Webster J. Estimating neuromuscular stimulation within the human torso with TASER stimulus. Phys Med Biol. 2007;52:6401–11.
8. Jauchem J, Seaman R, Klages C. Physiological effects of the TASER C2 electronic control device. Forensic Sci Med Pathol. 2009;5:189–98.
9. Vilke G, Sloane C, Bouton K, et al. Physiological effects of a conducted electrical weapon on human subjects. Ann Emerg Med. 2007;50(5):569–75.
10. Sloane C, Chan T, Levine S, Dunford J, Neuman T, Vilke G. Serum troponin I measurement of subjects exposed to the TASER X26. J Emerg Med. 2008;35(1):29–32.
11. Vilke GM, Sloane C, Levine S, Neuman T, Castillo E, Chan T. Twelve-lead electrocardiogram monitoring of subjects before and after voluntary exposure to the TASER X26. Am J Emerg Med. 2008;26:1–4.
12. Ho JD, Miner JR, Lakireddy DR, et al. Cardiovascular and physiologic effects of conducted electrical weapon discharge in resting adults. Acad Emerg Med. 2006;13:589–95.
13. Bozeman W, Barnes D, Winslow J, Johnson J, Phillips C, Alson R. Immediate cardiovascular effects of the TASER X26 conducted electrical weapon. J Emerg Med. 2009;26:567–70.
14. Levine S, Sloane C, Chan T, Dunford J, Vilke G. Cardiac monitoring of human subjects exposed to the TASER. J Emerg Med. 2007;33:113–7.
15. VanMeenen K, Cherniack N, Bergen M, Gleason L, Teichman R, Servatius R. Cardiovascular evaluation of electronic control device exposure in law enforcement trainees: a multisite study. JOEM 2010; (in press).
16. Ho J, Dawes D, Cole J, Hottinger J, Overton K, Miner J. Lactate and pH evaluation in exhausted humans with prolonged TASER X26 exposure or continued exertion. Forensic Sci Int. 2009; (in press).
17. Allsop P, Cheetham M, Brooks S, Hall GM, Williams C. Continuous intramuscular pH measurement during the recovery from brief, maximal exercise in man. Eur J Appl Physiol. 1990;59:465–70.
18. Ho J, Dawes D, Bultman L, Thacker J, Skinner L, Bahr J, Johnson M, Miner J. Respiratory effect of prolonged electrical weapon application on human volunteers. Acad Emerg Med. 2007;14:197–201.
19. Ho JD, Dawes DM, Reardon RF, Lapine AL, Dolan BJ, Lundin EJ, Miner JR. Echocardiographic evaluation of a TASER-X26 application in the ideal human cardiac axis. Acad Emerg Med. 2008;15(9):838–44.
20. Dawes DM, Ho JD, Reardon RF, Miner JR. Echocardiographic evaluation of TASER X26 probe deployment into the chests of human volunteers. Am J Emerg Med. 2010;28(1):49–55.
21. Ho J, Dawes D, et al. Ultrasound measurement of cardiac activity during conducted electrical weapon application in exercising adults. Ann Emerg Med. 2007;50(3):S108.
22. Dawes D, Ho J, Reardon R, Sweeney J, Miner J. The physiologic effects of multiple simultaneous electronic control device discharges. West J Emerg Med. 2010;11:49–56.

23. Bozeman W. Additional information on TASER safety. Ann Emerg Med. 2009;54(5):758–9.
24. Hall C, Butler C, Kadar A, Palmer S. Police use of force, injuries and death: prospective evaluation of outcomes for all police use of force/restraint including conducted energy weapons in a large Canadian city. Acad Emerg Med. 2009;16:S198–9.
25. McManus J, Forsyth T, Hawks R, Jui J. A retrospective case series describing the injury pattern of the advanced M26 TASER in Multnomah County, Oregon. Acad Emerg Med. 2004;11:587.
26. Bozeman W, Teacher E, Winslow J. Incidence and outcomes of transcardiac TASER probe deployments. Acad Emerg Med. 2009;16:S196.
27. Swerdlow C, Fishbein M, Chaman L, Lakkireddy D, Tchou P. Presenting rhythm in sudden death temporally proximate to discharge of TASER conducted electrical weapons. Acad Emerg Med. 2009;16:1–13.
28. Ordog GL, Wasserberger J, Schlater T, Balasubramanium S. Electronic gun (TASER) injuries. Ann Emerg Med. 1987;16(1): 73–8.

Use of reflectance spectrophotometry and colorimetry in a general linear model for the determination of the age of bruises

Vanessa K. Hughes · Neil E. I. Langlois

Abstract Bruises can have medicolegal significance such that the age of a bruise may be an important issue. This study sought to determine if colorimetry or reflectance spectrophotometry could be employed to objectively estimate the age of bruises. Based on a previously described method, reflectance spectrophotometric scans were obtained from bruises using a Cary 100 Bio spectrophotometer fitted with a fibre-optic reflectance probe. Measurements were taken from the bruise and a control area. Software was used to calculate the first derivative at 490 and 480 nm; the proportion of oxygenated hemoglobin was calculated using an isobestic point method and a software application converted the scan data into colorimetry data. In addition, data on factors that might be associated with the determination of the age of a bruise: subject age, subject sex, degree of trauma, bruise size, skin color, body build, and depth of bruise were recorded. From 147 subjects, 233 reflectance spectrophotometry scans were obtained for analysis. The age of the bruises ranged from 0.5 to 231.5 h. A General Linear Model analysis method was used. This revealed that colorimetric measurement of the yellowness of a bruise accounted for 13% of the bruise age. By incorporation of the other recorded data (as above), yellowness could predict up to 32% of the age of a bruise—implying that 68% of the variation was dependent on other factors. However, critical appraisal of the model revealed that the colorimetry method of determining the age of a bruise was affected by skin tone and required a measure of the proportion of oxygenated hemoglobin, which is obtained by spectrophotometric methods. Using spectrophotometry, the first derivative at 490 nm alone accounted for 18% of the bruise age estimate. When additional factors (subject sex, bruise depth and oxygenation of hemoglobin) were included in the General Linear Model this increased to 31%—implying that 69% of the variation was dependent on other factors. This indicates that spectrophotometry would be of more use that colorimetry for assessing the age of bruises, but the spectrophotometric method used needs to be refined to provide useful data regarding the estimated age of a bruise. Such refinements might include the use of multiple readings or utilizing a comprehensive mathematical model of the optics of skin.

Introduction

The bruise is a significant injury in the eyes of the law in Australia. A bruise results from blunt force injury to the skin when the force is sufficient to rupture blood vessels within the skin, resulting in extravasation of blood and the formation of a bruise or skin hematoma [1, 2]. Although the color of blood is red, due to the hemoglobin molecule, the appearance of extravasated blood within the skin varies according its oxygenation and the depth of its location below the skin's surface [3–6]. When blood is released into the skin as a result of trauma, there is an ensuing inflammatory reaction: hemoglobin is catabolized into the yellow pigment bilirubin [7, 8] and the golden-brown pigment hemosiderin. Eventually, bilirubin and hemosiderin are

V. K. Hughes
School of Arts and Sciences (NSW) ACU National,
North Sydney, Australia

N. E. I. Langlois (✉)
Forensic Science South Australia, University of Adelaide,
21 Divett Place, Adelaide, SA 5000, Australia
e-mail: Neil.Langlois@sa.gov.au

removed by the macrophages and a healing reaction follows with a gradual fading of color.

An estimation of the age of a bruise may be attempted by direct visual examination or by the inspection of photographs taken of the injured area [1, 9, 10], but these methods are subjective in nature [11, 12] and may not be reliable. Forensic investigators would benefit from a non-invasive, objective, scientifically validated method for determining the age of bruises. Previous authors have suggested that either colorimetry or reflectance spectrophotometry might provide a solution [13–15].

Colorimetry can be used to measure the color of a surface. Many different systems have been developed to numerically express the visual perception of color. The Commission Internationale de l'Éclairage (CIE) proposed a method of standardized color measurement, the CIE-$L*a*b*$ system, which takes into account the non-linear color perception of the human eye [16, 17]. In the CIE-$L*a*b*$ system, the $L*$ value defines the relative brightness (or luminosity) of the sample ranging from total black ($L* = 0$) to total white ($L* = 100$). The $a*$ value is the red-green coordinate. A positive $a*$ value defines the color quality "red" and a negative $a*$ value defines the color quality "green". The $b*$ value is the blue-yellow coordinate. A positive $b*$ value defines the color quality "yellow" and a negative $b*$ defines the color quality "blue" [17]. A colorimeter can be used to calculate the relative luminosity and hues of a surface, such as skin, thus allowing a more accurate, non-subjective assessment of color than by visual assessment [18, 19]. Colorimetry has been used to evaluate skin color and postmortem hypostasis [15, 20–23]. For the purpose of this study, yellowness was measured using the calculated $b*$ value and by using two specific measures of yellow: the American Society for Testing Materials (ASTM) E313 and D1925 values [24].

Reflectance spectrophotometry measures the change in light intensity relative to its wavelength after it has interacted with a sample. The device comprises a light source, a probe and an analyzer, and the results are recorded on a dedicated computer. The spectrophotometer measures the intensity of light throughout the spectrum and is an accurate and objective device [25]. Over the range 470–510 nm the absorption spectrum of hemoglobin is nearly flat, but the absorption of bilirubin is decreasing from its peak around 460 nm [26, 27] and hemosiderin has a sloping absorption curve [28]. Therefore, the value of the first derivative around 480–490 nm corresponds to the presence of degradation products of hemoglobin [25]. When blood is released into the tissue, it would be expected to be predominantly in the form oxyhemoglobin which would relinquish its oxygen in the tissue to become predominantly deoxyhemoglobin [14]. The ratio of oxyhemoglobin to deoxyhemoglobin can be calculated using differences in the absorption spectra. To date, investigators using spectrophotometry have studied only small groups [29–31].

This study aims to determine if reflectance spectrophotometry or colorimetry can be used to determine the age of a bruise, using a large group of subjects with bruises of known age.

Materials and methods

Reflectance spectra were collected from normal skin and bruises in 149 volunteers using a Cary 100 Bio UV–visible spectrophotometer fitted with a Cary fiber optic couple and Cary fiber optic reflectance probe (Varian Australia Pty Ltd., Frenches Forrest, New South Wales, Australia). The instrument was calibrated before each series of measurement using zero and baseline corrections as previously described [25]. Calibrations and measurements were performed under similar conditions. Subjects were measured in a seated position and were asked to remain still for 5 min before any readings were taken. All measurements were taken from the central region of the bruise. An area of non-bruised skin adjacent to the bruised area was also measured and used as the control. Subjects were instructed to hold the probe gently and completely perpendicular to the skin so as to prevent light from entering the probe or pressure from affecting the measurements obtained. To avoid skin color changes due to excessive contact or friction against the probe heads, only one measurement was made on the test site, as has been recommended [22]. The absorption spectrum of the bruise was obtained over the range 830–360 nm. A data interval of 1 nm was selected, with a signal averaging time of 0.2 s for each data point (resulting in a scan time of 70 s). Double beam mode was used with 2.5 Abs of rear beam attenuation and the slit width was set to 3.0 nm.

The volunteers worked at or had been admitted as patients to Westmead Hospital or the Children's Hospital, NSW, Australia, and the age, sex, skin color and approximate body size of each volunteer were recorded. The extent of trauma, age of the bruise, and the site of the bruise were also recorded for each subject (see below). The age of the bruise at the first and subsequent consultations was also recorded. Some subjects presented with new bruises on multiple occasions, other subjects came for repeat examination of the same bruise. Subjects were not examined more than once in a 24 h period. Ethics permission was obtained from both the Western Sydney Area Human Research Ethics Committee [HS/TG HREC2002/5/4.6(1432)] and ratified by the Human Research Ethics committee at the University of Sydney [3231] before subjects were recruited. To be eligible to participate in this study, subjects were required to know the age and cause of

the bruise that was to be examined, be in good health, have no difficulty conversing in English and able to give written consent. All subjects were aged 18 years or older. Only bruises on legs and arms that were easy to access while the subject remained clothed were used. Subjects with cuts or abrasions on the surface or near the bruise were also excluded, to prevent potential contamination of the wound or probe. Volunteers with excessive hair over the bruised region were also excluded as hair was found to interfere with measurements. All volunteers recruited for the study had bruises that had been acquired from recreational or normal daily activities. No identifying data were collected.

The age and gender of each subject was recorded. The subject's body size and build was visually assessed. Using this assessment subjects were classified into three body size classes: 'Underweight'—very little fat content, prominent bones and muscles, 'Normal weight'—normal fat for body size, and 'Overweight'—increased fat for body size. The bruise size was measured and the subject was asked how it had been acquired. Using this information the bruise was classified as being either (1) a small bruise caused by a minor trauma, (2) a large bruise caused by a minor trauma, (3) a small bruise caused by a major trauma, (4) or a large bruise caused by a large trauma. Minor trauma was be defined as the type of trauma a person would experience if he or she walked into an object, e.g., a coffee table. Major trauma was defined as the type of trauma experienced if hit by a car or by a paintball. The bruise was regarded as 'small' if it was less than 5 cm in diameter and 'large' if was 5 cm or larger. The skin tone of each subject was determined by measuring the CIEL*a*b* "b*" value of an area of adjacent control skin and was classified as: b* +0.10 to 0.5 'Fair', b* −0.51 to −1.50 'Medium', b −1.51 to −3.0 'Olive to Dark'. The location of the bruise was coded into one of four categories: upper limb, hand, lower limb, foot.

All bruises were photographed. These were examined by a forensic pathologist (NL) who classified them as being intradermal, deep (subcutaneous) or mixed using the criteria of Bohnert [3].

The oxygenation of hemoglobin within the bruise was calculated by subtracting the absorption at an isosbestic point (805 nm) and a nonisosbestic point (660 nm). The formula {Bruise 805 nm/Bruise 660} − {Control 805 nm/Control 660} was used to measure the oxygenation of hemoglobin, which is an adaptation of the method proposed by Randenburg et al. [31].

The first derivative was calculated using the mathematical software provided with the Cary Win UV spectrophotometer. The native trace of both the control site and the bruised site were converted to the first derivative using a filter size of 9 and a bandwidth of 3. The values obtained at 480 and 490 nm in the control value was subtracted from the value obtained at 480 and 490 nm in the bruise scan, respectively.

Scans were converted into CIEL*a*b* values using the Cary Win UV color application, 85-101684-00 version 2.00(15) supplied by Star-Tek (Victoria, Australia). The CIEL*a*b* values were calculated based over a scan range of 830–360 nm using a 1 nm data interval. The results were based on a CIE D65 illuminant with an observer angle of two degrees for the CIEL*a*b* color space. After testing the software using a Kodak color card (results not shown) it was found that the software produced a negative b* value to indicate yellowness. Therefore, in order for our results to truly reflect the CIEL*a*b* system and prevent confusion, the signs of all results were changed to the corresponding positive value. The value obtained for the CIEL*a*b* "b*" value from the control scan was also used to determine the color of the subject's skin.

Statistical analysis was performed using SPSS Student Version 11 (SPSS Inc, Prentice Hall, UK). The possible confounding subject-related variables were analysed using Spearman's correlation to determine if there was any correlation between them and the age of a bruise. A general linear model univariate analysis was then conducted using the reflectance spectrophotometry and colorimetry methods that had a moderate correlation with the age of a bruise and the possible confounding variables, so as to determine if it was possible to create a model that could predict the age of a bruise. Using a backward stepwise selection process, variables were removed until only the significant variables remained.

All measurements of the first derivatives at 480 and 490 nm as well as the color measurements b*, E313 and D1925 used in the analyses refer to the bruise minus the control value.

Results

A total of 147 subjects were recruited for this study comprising 28 males and 119 females with ages ranging from 18 to 72 years (mean = 35.88, median = 32.00, SD = ±11.47). A total of 240 scans were obtained, of which 233 were of sufficient quality to allow analysis. The age of the bruise at the first and subsequent consultations was recorded; the ages of the bruises ranged from 0.5 to 231.5 h (mean = 76.39 h, median = 72.00 h, SD = ±48.56 h). The frequency distribution of the scans acquired for bruises of different age groups is shown in Fig. 1; the frequencies of subjects and scans made for categories of body build, bruise size and degree of trauma, bruise site, and depth of bruise is shown in Table 1.

The results of the general linear model analysis indicated that measurement of yellow using the CIE b* value
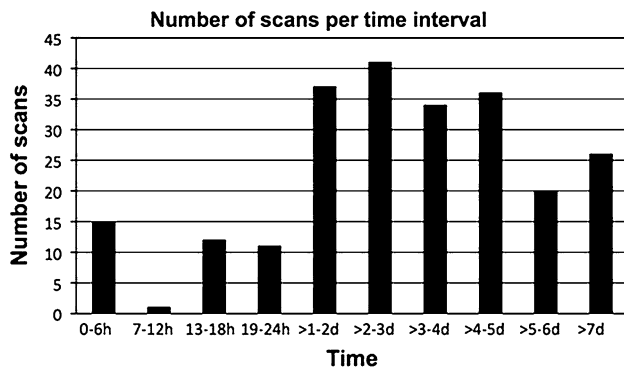
Number of scans per time interval

Fig. 1 Number of scans of bruises in time intervals (note non-linear X-axis)

Table 1 Frequencies of subjects and scans made for categories of body build, bruise size and degree of trauma, bruise site, and depth of bruise

	Number of subjects	Number of scans
Frequency of body build of volunteers		
Build		
Slender	9	16
Average	92	141
Large	46	76
Total	147	233
Frequency of bruise size and trauma sustained		
Bruise size/trauma		
Small bruise/minor trauma	111	177
Large bruise/minor trauma	22	32
Small bruise/major trauma	12	19
Large bruise/major trauma	2	5
Total	147	233
Frequency of site of bruise		
Site		
Arm	60	98
Hand	22	28
Leg	58	97
Foot	7	10
Total	147	233
Frequency of depth of bruise		
Depth		
Deep	114	178
Intra-dermal	5	7
Mixed	28	48
Total	147	233
Number of volunteer in each skin tone catagory		
Skin tone		
Fair	67	121
Medium	60	85
Olive/dark	20	27
Total	147	233

by colorimetry accounted for only around 12% of the predicted age of the bruise. The use of the specific measures of yellowness, E313 and D1925, improved the prediction to 13%. The best estimate of bruise age was obtained using the calculated ASTM E313 value by adding the gender of the subject, an estimate of the depth of the bruise, the spectrophotometric measurement of the proportion of oxygenated hemoglobin, the site of the bruise and skin tone into the analysis. However, the ASTM E313 value in conjunction with these factors only predicted 32% of the age of the bruise, meaning that 68% of the variation between the observed and predicted bruise age was dependent on other factors.

The calculation of the first derivative values showed similar results, with the first derivative at 490 nm being slightly superior to the value at 480 nm (alone estimating 18 and 14% of the bruise age, respectively). The general linear model indicted that only the gender of the subject, the estimated depth of the bruise, and the calculation of the proportion of oxygenated hemoglobin improved the ability of the first derivative method to predict the age of bruises. Using these additional factors first derivative at 490 nm accounted for at best 31% of the predicted age of the bruise, leaving 69% of the prediction of the age of bruise to other factors.

The measurements of yellow (using b^*, E313 and D1925) as well as the values of the first derivative calculations (at 480 and 490 nm) were plotted against the known age of the bruise. These plots were examined to assess the changes at the very early times of 0.5–24 h. There was no clear trend to indicate if accumulation of degradation products of hemoglobin or if the development of yellow color occurred gradually from time zero, or if there was a lag. Overall for all the data, the best curve of fit was a simple parabola, showing an increase to around 7 days and then a decline (Fig. 2). The first derivative at 490 nm measures the amount of bilirubin and hemosiderin while the ASTM E313 color number measures the amount of yellow. The correlation between the two values was strong with a correlation of coefficient squared (r^2) value of 0.789 ($P \geq 0.001$). The yellowness ASTM E313 color number was divided by the first derivative at 490 nm and plotted against the age of the bruise; most of the plotted points lay along a straight, horizontal line as would be expected (Fig. 3). However, there was a degree of scatter indicating that measured yellow color did not always relate to the presence of hemoglobin breakdown products.

Discussion

This study has confirmed that observation of the color yellow in a bruise or the measurement of the presence of
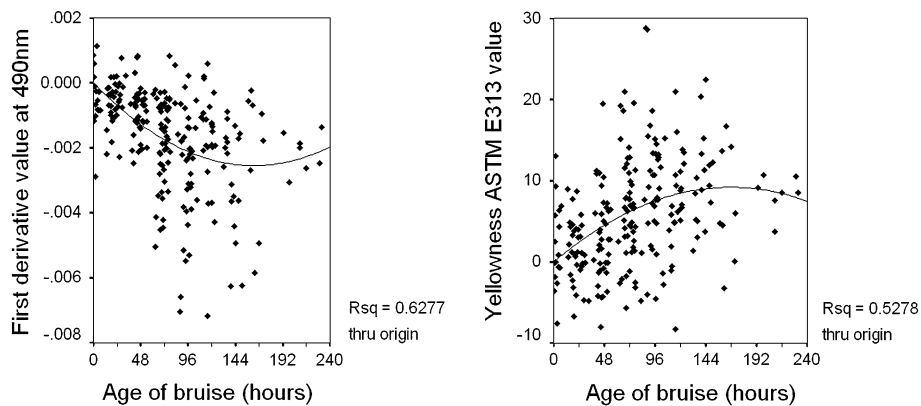
Fig. 2 Time trends of first derivative at 490 nm (*left*) and yellowness ASTM E313 (*right*) with line of best fit

breakdown products of hemoglobin do provide information regarding the age of a bruise. However, by themselves these are of limited use. Using additional factors increases the ability to predict the age of bruises, but the predictive values must be regarded as too low to be useful, providing around only one-third of the age estimation using the general linear model with the methodology of this study.

The factors that improve the accuracy of the bruise age prediction using colorimetry include the proportion of oxygenated hemoglobin, the site of the bruise and skin tone. As the proportion of oxygenated hemoglobin within a bruise is derived using spectrophotometry, it is not applicable to measurements of yellow color made using only a colorimeter which uses a light source and three receptors from which color data is calculated [22, 32]. Skin tone should not have been incorporated into the multivariate general linear model as the yellow measurement of control skin had been subtracted from the bruise color measurement. The result indicated that subtraction of the control was not working adequately. This may also account for some of the lack of correlation between the measurement of yellowness and the first derivative value and the scatter seen in Fig. 3. The finding also accounts for the inclusion of the site into the multivariate general linear model for colorimetric prediction of bruise age. Critical analysis revealed that the hand was the only site that was significantly different (out of hand, arm, leg and foot that were coded) and that it was consistently appearing more yellow at a given time than expected. When a bruise on the hand was recorded, the control site was usually taken proximally, further up the extremity. Observation revealed that a person's hand tends to be more yellow (a finding also recorded by others [33]), presumably due to sun exposure, than the arm. Thus, due to imperfect subtraction by the control, bruises of the hand were appearing more yellow at a given time than bruises on other sites.

Although it appeared that colorimetry provided the best prediction of bruise age when combined with additional factors, critical analysis shows colorimetry to be impaired by the underlying skin color.

Measurement of the first derivative values was not affected by skin tone in the study group. However, there were no deeply pigmented, negroid, subjects. The addition of subject sex as a significant factor was not expected, with females displaying more breakdown of hemoglobin at a given age of bruise than males. However, the small number of male subjects questions the validity of this observation. The depth of the bruise as judged by inspection was also a significant variable. This was not unexpected. However, the fact that mixed depth bruises showed more breakdown of hemoglobin at a given age of bruise than deep intradermal, coupled with the low number of purely intradermal bruises places uncertainty on this finding.

It has been written that a bruise will not appear yellow in under 18 h [1]. This observation has been supported by others. For yellow to be seen in a bruise the local accumulation of yellow pigments of hemoglobin breakdown needs to exceed the background color of skin by a sufficient level to be perceived by the human visual system. The requirement for a period of time before the appearance of yellow color could be due to a true delay resulting from the need to recruit macrophages to the injured area and then for macrophages to induce their heme oxygenase enzymes to allow the degradation of hemoglobin. It was hoped to be able to demonstrate a lag phase in the development of yellow color and the change in the first derivative values, however, this was not clearly present (Fig. 2). A lack of data from early bruises may be partly the reason for this (Fig. 1) and for the colorimetry data: the inability to completely correct for skin tone may have caused obfuscation.

This large spectrophotometry study of bruises has demonstrated that there is a relationship between the
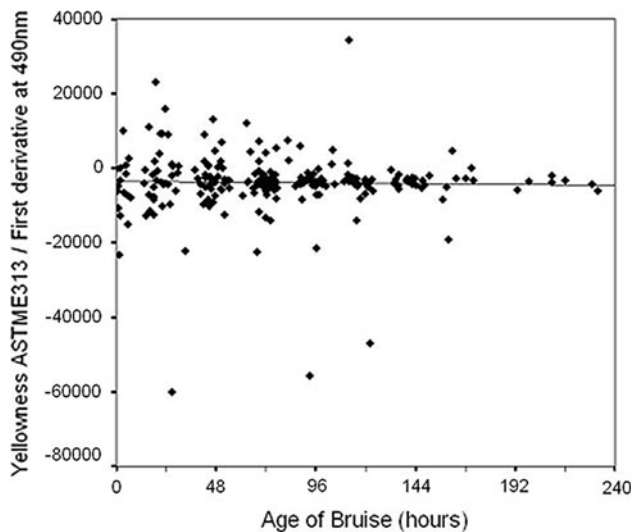
Fig. 3 Yellowness ASTM E313 divided by first derivative at 490 nm against time. Although there is good correlation between the two variables ($r^2 = 0.8$), it can be seen there are a number of outlier points

demonstration of breakdown products of hemoglobin and the age of a bruise. However, the relationship is a weak one and other factors have to be taken into account. Colorimetry measurements can be significantly affected by skin tone. For spectrophotometry, subject dependent factors include gender and bruise depth. The size of the bruise, the degree of trauma, subject build, bruise site and subject age were not factors that influenced being able to determine the age of the bruise.

This study is limited by the small numbers in some subject groups (for example the number of male subjects, the number of purely intradermal bruises and small numbers of early bruises). Also, only a single measurement was taken from each bruise using the probe which has a sampling area around 3 mm in diameter. The results suggest that simple analysis of spectrophotometric data of this type is of limited use in determining the age of bruises. The use of complex mathematical modeling based on the optical properties of skin combined with collection of spectrophotometric data over larger areas has shown promise in bruise age determination [31], however, in the published study the subjects and bruises were similar. It is possible that subject related variables will need to be included into any methodology that is used to determine the age of bruises by spectrophotometry.

Key points

1. Measurement of yellow color using colorimetry provides information regarding the age of a bruise. However, measurements appear affected by skin tone.

2. Measurement of the accumulation of the degradation products of hemoglobin by using reflectance spectrophotometry to obtain the first derivative value at 490 nm provides information regarding the age of a bruise, which is not affected by skin tone.

3. Subject related factors such as gender, depth of the bruise and spectrophotometric measurement of the oxygenation of hemoglobin in the bruise increase the predictive value of the first derivative value at 490 nm.

4. Even when subject related factors are incorporated into the general linear model with first derivative value at 490 nm, using the methodology of this study provides only 31% of the prediction of the age of a bruise.

References

1. Langlois NEI, Gresham GA. The ageing of bruises: a review and study of the color changes with time. Forensic Sci Int. 1991;50:227–38.

2. Langlois NEI. The science behind the quest to determine the age of bruisies—a review of the English language literature. Forensic Sci Med Pathol. 2007;3(4):241–51.

3. Bohnert M, Baumgartner R, Pollak S. Spectrophotometric evaluation of the color of intra- and subcutaneous bruises. Int J Legal Med. 2000;113:343–8.

4. Gibson IM. Measurement of skin color in vivo. J Soc Cosmet Chem. 1971;22:725–40.

5. Kienle A, Lilge L, Vitkin A, Patterson MS, Wilson BC, Hibst R, et al. Why do veins appear blue? A new look at an old question. Appl Optics. 1996;35:1151–60.

6. Kollias N. The physical basis of skin color and its evaluation. Clin Dermatol. 1995;13:361–7.

7. Muir R, Niven JSF. The local formation of blood pigments. J Pathol. 1935;41:183–97.

8. Tenhunen R. The enzymatic degradation of heme. Semin Hematol. 1972;9:19–29.

9. Schwartz AJ, Ricci LR. How accurately can bruises be aged in abused children? Literature review and synthesis. Pediatrics. 1996;97:254–7.

10. Stephenson T, Bialas Y. Estimation of the age of bruising. Arch Dis Child. 1996;74:53–5.

11. Hughes VK, Ellis P, Langlois NEI. The perception of yellow in bruises. J Clin Forensic Med. 2004;11:257–9.

12. Munang LA, Leonard PA, Mok JYQ. Lack of agreement on color description between clinicians examining childhood bruising. J Clin Forensic Med. 2002;9:171–4.

13. Klein A, Rommeiß S, Fischbacher C, Jagemann K-U, Danzer K. Estimating the age of hematomas in living subjects based on spectrometric measurements. In: Oehmichen K, editor. The wound healing process. Lübeck: Schmidt-Römhild; 1995. p. 283–91.

14. Randeberg LL, Winnem A, Blindheim S, Haugen OA, Svaasand LO. Optical classification of bruises. Proc SPIE. 2004;5312:54–64.

15. Yajima Y, Nata M, Funayama M. Spectrophotometric and trismus analysis of the colours of subcutaneous bleeding in living persons. Leg Med. 2003;5:S342–3.
16. Billmeyer FW. Survey of color order systems. Color Res Appl. 1987;12:173–86.
17. Wyszecki G, Stiles WS. Color science. Concepts and methods, quantitative data and formula. 2nd ed. New York: Wiley; 1982.
18. Westerhof W. CIE colorimetry. In: Serup J, Jemec GBE, editors. Handbook of non-invasive methods and the skin. Boca Radon: CRC Press; 1995. p. 385–96.
19. Weatherall IL, Coombs BD. Skin color measurements in terms of CIELAB color space values. J Invest Dermatol. 1992;99:468–73.
20. Bohnert M, Weinman W, Pollak S. Spectroscopic evaluation of postmortem lividity. Forensic Sci Int. 1999;99:149–58.
21. Feather JW, Hajizadeh-Saffar M, Leslie G, Dawson JB. A portable scanning reflectance spectrophotometer using visible wavelengths for the rapid measurement of skin pigments. Phys Med Biol. 1989;34:807–20.
22. Takiwaki H. Measurement of skin color: practical application and theoretical considerations. J Med Invest. 1998;44:121–6.
23. Trujillo O, Vanezis P, Cermignani M. Photometric assessment of skin color and lightness using a tristimulus colorimeter: reliability of inter and intra-investigator observations in healthy adult volunteers. Forensic Sci Int. 1996;81:1–10.
24. Anon. Standard practice for calculating yellowness and whiteness indices from instrumentally measured color coordinates: ASTM international; 2006. Report No.: E313-05.
25. Hughes VK, Ellis P, Burt T, Langlois NEI. The practical application of reflectance spectrophotometry for the demonstration of hemoglobin and its degradation in bruises. J Clin Pathol. 2004;57: 355–9.
26. Amazon K, Soloni F, Rywlin AM. Separation of bilirubin from hemoglobin by recording derivative spectrophotometry. Am J Clin Pathol. 1981;75:519–23.
27. Makarem A. Hemoglobins, myoglobins and haptoglobins. In: Henry RJ, Cannon DC, Winkelman JW, editors. Clinical chemistry principles and techniques. 1st ed. Maryland: Harper and Row; 1974. p. 1111–214.
28. Wells CL, Wolken JJ. Microspectrophotometry of haemosiderin granules. Nature. 1962;193:977–8.
29. Carson DO. The reflectance spectrophotometric analyses of the age of bruising and livor [MSc]. Dundee: University of Dundee; 1998.
30. Klein A, Rommeiß S, Fischbacher C, Jagemann K-U, Danzer K. Estimating the age of hematomas in living subjects based on spectrometric measurements. In: Oehmichen M, Kirchner H, editors. The wound healing process—forensic pathological aspects. Lübeck: Schmidt-Römhild; 1995.
31. Randeberg LL, Haugen OA, Haaverstad R, Svaasand LO. A novel approach to age determination of traumatic injuries by reflectance spectroscopy. Lasers Surg Med. 2005;38:277–89.
32. Vanezis P. Interpreting bruises at necropsy. J Clin Pathol. 2001; 54:348–55.
33. Brunsting LA, Sheard C. The color of the skin as analyzed by spectrophotometric methods. III The rôle of superficial blood. J Clin Invest. 1929;7:593–613.

CASE REPORT

Fatal hemorrhage following trans-sphenoidal resection of a pituitary adenoma: a case report and review of the literature

C. Kepron · M. Cusimano · M. S. Pollanen

Abstract   A 58-year-old woman with acromegaly developed massive epistaxis 7 days following trans-sphenoidal resection of a growth hormone-secreting pituitary adenoma. At autopsy, it was determined that the source of the hemorrhage was a rupture of the intracavernous segment of the internal carotid artery secondary to a bacterial arteritis. We describe the gross dissection and histologic examination undertaken in this unusual case, discuss the possible etiology of the infection and review the potential complications of this surgical approach with a view to improving forensic examination of these patients.

Keywords   Forensic pathology ·
Trans-sphenoidal resection · Pituitary adenoma ·
Pyogenic arteritis · Post-operative complication ·
Iatrogenic

Introduction

The trans-sphenoidal approach to the sella turcica is the simplest and safest approach with published mortality rates of 0.1–0.9% [1–5]. Although rare, potentially fatal complications may result from this surgical procedure, including hemorrhage from the carotid artery or its branches [1, 5–7]. Here we present one such complication in a patient who died of massive epistaxis and hemoaspiration 1 week following resection of a pituitary adenoma. This case is unique in that the fatal hemorrhage occurred secondary to bacterial infection and necrosis of the intracavernous segment of the internal carotid artery.

The case

A 58-year-old woman presented to her primary care physician with symptoms of acromegaly that had been gradually worsening over a period of approximately 30 years. Her past medical history was significant only for hypertension and a 42 pack-year smoking history. Investigations showed an elevation of serum growth hormone (GH), and an MRI scan revealed a two centimeter mass in the pituitary gland associated with a small area of hemorrhage and remodeling of the sella turcica; the mass also appeared to extend around the right internal carotid artery. She was referred to the neurosurgical service at a tertiary care hospital where the decision was made to proceed with a trans-sphenoidal endoscopic resection of the mass. Although the tumour was found to be adherent to the right internal carotid artery the surgery was completed without intraoperative complication. The surgeons felt they had removed all of the visible tumour, although there was acknowledgement in the operative note that a tiny piece may have been left adherent to the right internal carotid artery. There was good hemostasis and a bone graft was used to repair the sellar floor as per routine surgical protocol. The patient was discharged to the ward in good

C. Kepron (✉) · M. S. Pollanen
Department of Laboratory Medicine and Pathobiology,
University of Toronto, Medical Sciences Building, Room 6215,
1 King's College Circle, Toronto, ON M5S 1A8, Canada
e-mail: ckepron@gmail.com

M. Cusimano
Department of Surgery, Division of Neurosurgery, St. Michael's
Hospital, University of Toronto, 1005-2 Queen Street East,
Toronto, ON M5C 3G7, Canada

M. S. Pollanen
Ontario Forensic Pathology Service, 26 Grenville Street,
Toronto, ON M7A 2G9, Canada

condition. On post-operative day (POD) #3 she developed a headache, a cerebrospinal fluid (CSF) leak that presented as serosanguinous rhinorrhea and episodic systemic hypertension. On POD #6 she experienced an episode of epistaxis, but was not found to be actively bleeding when she was examined the following day. A sample of CSF was sent for bacterial culture on POD #7, and was found to be positive for anaerobic Gram positive cocci and diphtheroid bacilli. On POD #8 she developed massive epistaxis that could not be controlled with nasal packing, and she then suffered a cardiac arrest. In spite of intubation via a surgical airway, she could not be resuscitated and died later that day.

Autopsy findings

At autopsy, the patient was acromegalic with coarse facial features and broadening of the distal fingers and toes. There was evidence of both the prior surgical procedure as well as the resuscitation attempt, including a tracheotomy with endotracheal tube and bilateral Foley catheters within the nasal cavities. The endotracheal tube was filled with clotted blood. Upon removal of the calvarium and brain, the dura covering the base of the skull was intact and the intracranial portions of the internal carotid arteries were unremarkable. There was focal fresh hemorrhage around the pituitary gland. The external surface of the brain was unremarkable.

Removal and examination of the surgical site was then undertaken. The cavernous sinuses were incised with a scalpel to expose the cavernous portions of the internal carotid arteries. Using an oscillating saw, the intraosseous portions of the arteries were exposed by making a saggital cut into the petrous ridge, approximately halfway along its length. Two axial cuts into the ridge allowed a chunk of bone to be removed, revealing the arteries, which were then transected prior to entering the foramen lacerum. A coronal cut was made through the body of the sphenoid bone, rostral to the anterior clinoid processes (the anterior clinoid processes may be removed at this point to release the clinoid segments of the arteries). A second coronal cut was made through the middle of the clivus. Saggital cuts were then made into the greater wings of the sphenoid bones, angled slightly medially so as to undermine the sella turcica. The entire block was removed, fixed in formalin and decalcified prior to sectioning. The surgical site could then be examined by simply flipping the block over.

The surgical site showed the presence of a bone graft at the posterior wall of the sphenoid sinus and the sinus cavity was occluded by blood clot. There was no evidence of a carotid-cavernous fistula. There was acute hemorrhage within the tissues adjacent to the clinoid/cavernous segment of the right internal carotid artery (Fig. 1), and this

area of hemorrhage was in continuity with the operative site in the sphenoid sinus. The supraclinoid portion of the left internal carotid artery showed an incidental unruptured saccular aneurysm, 0.8 cm in diameter, with associated atheroma (Fig. 2a).

Additional gross findings included the presence of clotted blood within the tracheobronchial tree (Fig. 2b) and evidence of hemoaspiration within all lobes of both lungs. There was blood in various stages of digestion present within the gastrointestinal tract, from the stomach to the sigmoid colon. The remainder of the gross examination was unremarkable.

Histologic investigations included examination of sections obtained from the *en bloc* dissection of the base of skull, including the sella turcica, bilateral cavernous sinuses, and the distal intraosseous segments of both internal carotid arteries. The clinoid/cavernous segments of the internal carotid arteries were sampled by cutting the sections perpendicular to the main axis of the artery. Routine hematoxylin and eosin-stained slides were prepared from all blocks. Sections showed a cellular repair reaction near the pituitary fossa, in keeping with the prior surgery. The cavernous segment of the right internal carotid artery showed a pyogenic arteritis with focal transmural necrosis and a rupture site immediately adjacent to the superior clinoid process (Fig. 3). Bacteria were identified in this area and were seen to infiltrate the artery wall; a Gram stain confirmed the presence of weakly Gram-positive cocci and coccobacilli. Special stains for fungal organisms and acid-fast bacilli were negative. Within the sphenoid bone adjacent to the area of maximal arteritis was a marked chronic inflammatory infiltrate that extended into the bony trabeculae with foci of supparative inflammation and acute bone lysis. A dense fibrinopurulent exudate was also identified at one end of the sphenoid sinus bone graft. There was no evidence of a pre-existing aneurysm within the wall of the right internal carotid artery, nor were there any findings to suggest the presence of a traumatic pseudoaneurysm resulting from the surgery. A Masson's pentachrome stain demonstrated the presence of a circumferential internal elastic layer, even within the areas of mural necrosis. Residual pituitary adenoma was present and invaded the medial dural wall of the cavernous sinus, partially encased the right internal carotid artery and infiltrated around the oculomotor nerve cluster in the lateral compartment of the cavernous sinus with extension into the fibrous connective tissue outside the sinus. The surgical specimen consisted of numerous fragments of sinus mucosa, bone (submitted as "ethmoid" and "sphenoid sinus"), pituitary gland and tumour. Retrospective review of the specimens revealed no evidence of an underlying sinusitis or osteomyelitis at the time of surgery.

The cause of death was certified as "*Airway obstruction by blood clot and hemoaspiration due to hemorrhage into*
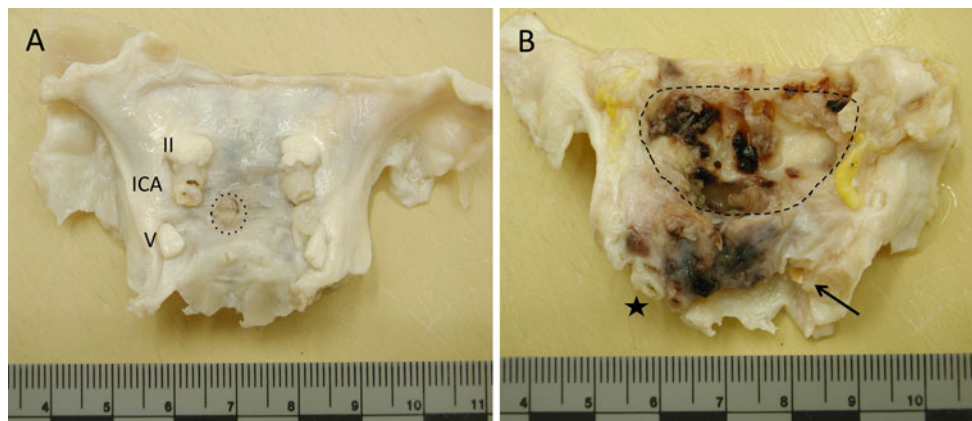
Fig. 1 The *en bloc* resection of the sella turcica, bilateral cavernous sinuses and intraosseous segments of the internal carotid arteries. **a** superior [intracranial] aspect of the tissue block. The pituitary stalk is highlighted with the *dotted line*. **b** Inferior view. The surgical site within the sphenoid sinus is outlined with the dashed line. An area of hemorrhage is seen medial and rostral to the right internal carotid artery, which is indicated by the star. The *arrow* indicates the left internal carotid artery. **II**, left optic nerve; **ICA**, left internal carotid artery; **V**, left trigeminal nerve
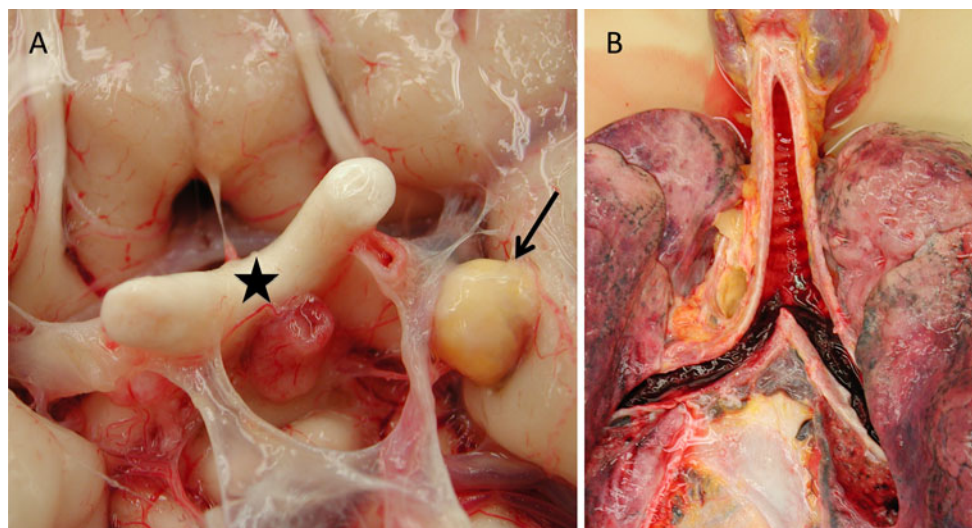

Fig. 2 Additional gross findings. **a** An unruptured berry aneurysm of the left internal carotid artery with associated atheroma. The *star* marks the optic chiasm. **b** Clotted blood within the tracheobronchial tree indicating massive hemoaspiration

the sphenoid sinus from rupture of a necrotic segment of the right internal carotid artery due to pyogenic (bacterial) arteritis associated with osteomyelitis of the sphenoid bone and recent trans-sphenoidal resection of a pituitary adenoma invading the right cavernous sinus".

Discussion

The most common complications following trans-sphenoidal resection of pituitary tumours are non-fatal and biochemical in nature, namely diabetes insipidus and hypopituitarism [1–5]. Post-operative infectious complications are also relatively frequent, with rates of meningitis ranging from 1.5 to 5.5% in the studies reviewed [1, 4, 5]

and a rate of sinusitis of 8.5% in one large American retrospective review based on self-report surveys from neurosurgeons [1]. Although uncommon, hemorrhagic complications carry the greatest risk of short-term mortality, and there are reports in the literature of fatal bleeds from damaged carotid arteries [1, 6, 7]. The internal carotid artery is the vessel most frequently affected, although branches of the external carotid are also vulnerable with trauma to these vessels leading to massive delayed epistaxis, often more than a week post-surgery [8]. In most cases where the internal carotid artery is directly damaged during surgery, the result is the formation of either false aneurysms or carotid-cavernous fistulas, both of which can be readily managed surgically or via endovascular techniques [1, 6, 7, 9].
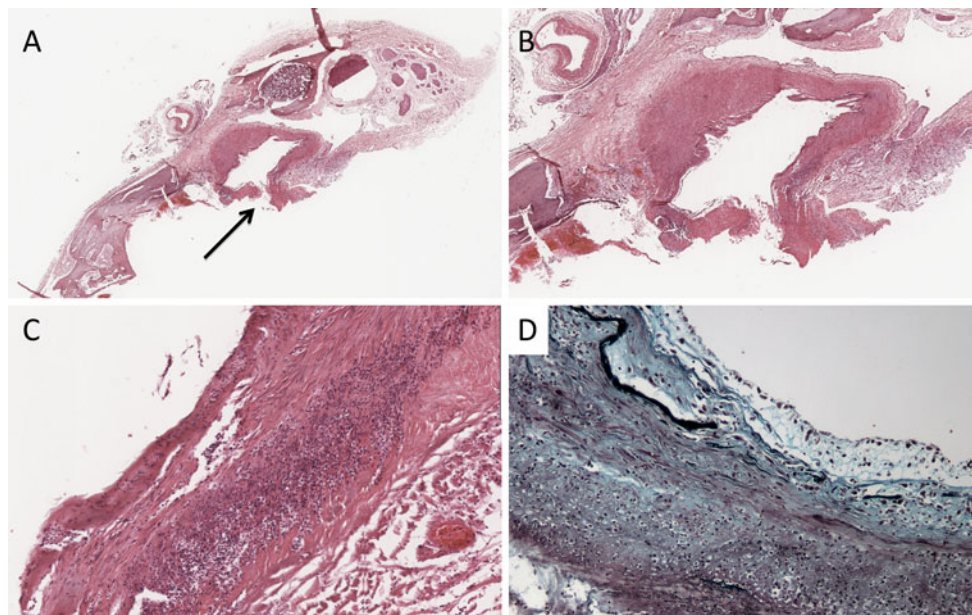
Fig. 3 Photomicrographs of a coronal section through the cavernous segment of the right internal carotid artery. **a** Whole mount H&E at 3× magnification. The *arrow* indicates the rupture site in the internal carotid artery. **b** Internal carotid artery at 8× magnification. **c** Wall of the internal carotid artery showing a dense neutrophilic infiltrate and mural necrosis, H&E at 20× magnification. **d** Movat stain of the arterial wall demonstrating destruction of the elastic lamina, 100× magnification

Hemorrhagic complications may also result from intra-operative damage to pre-existing aneurysms, and although intrasellar aneurysms are infrequent, they are well-recognized mimics of pituitary adenomas [10]. A somewhat more common phenomenon is that of variant arterial anatomy, including persistent trigeminal arteries (PTA). PTA represents the most frequent anomaly of the internal carotid-basilar artery anastomosis, and consists of an arterial branch originating from the cavernous segment of the internal carotid artery and running along the trigeminal nerve, through the posterior fossa to directly supply the cerebellum [11]. PTA has an angiographic incidence of 0.2–0.6% in adults, and may be associated with intracranial aneurysms in up to 26% of patients [11]. Pre-operative angiography will define such anomalous vessels and enable the neurosurgeon to appropriately plan the surgical approach.

Infectious ('mycotic') aneurysms have been reported as post-operative complications, however, they are exceedingly rare [1, 12, 13]. The patient described by Onishi et al. [12] developed a high fever, nuchal rigidity and leucocytosis on POD #5. Angiography disclosed an aneurysm of the supraclinoid portion of the internal carotid artery and subsequent surgical exploration revealed a suprasellar abscess. The patient had a known history of poorly-controlled diabetes mellitus and chronic maxillary sinusitis and development of the aneurysm was attributed to bacterial invasion of the sella, suprasellar arachnoid and optic nerves by organisms from the sinusitis that then spread to the supraclinoid portion of the internal carotid artery. In the report by Mielke et al. [13], the patient died following rupture of a fungal aneurysm of the basilar artery that developed approximately 10 months after trans-sphenoidal resection of a GH-secreting adenoma. Similar to our case, the patient in that report was not immunocompromised and there was no history of sinusitis prior to surgery or any evidence of infection or inflammation in the surgical specimen. At autopsy, hyphae of *Candida albicans* and *Aspergillus fumigatus* with an associated inflammatory response were identified on the surface of the brain, within the left optic nerve and retrobulbar soft tissue, and within the cavernous and sphenoidal sinuses. There was vasculitis involving the circle of Willis, and an unruptured mycotic aneurysm of the intracavernous segment of the left internal carotid artery. The source of this infection was not clearly identified, although it was felt to be secondary to the prior surgery [13].

Although the source of the infection in our case remains unconfirmed, the presence at autopsy of chronic osteomyelitis involving the sphenoid bone suggests that the vasculitis was a result of a post-operative infection of the sphenoid sinus in the setting of a CSF leak. A pre-existing chronic sinusitis or osteomyelitis of the sphenoid bone was also considered as an etiologic possibility; however, the lack of inflammation in the bone and mucosal fragments from the surgical specimen makes this alternative less likely. Furthermore, there was no suggestion of sinusitis on the pre-operative imaging scans. As previously stated, post-

operative sinusitis is a well-recognized complication of this procedure, with published rates ranging from 1 to 15% [1], and the presence of a CSF leak in our patient indicates there was a potential route for organisms to access the surgical site. Post-operative CSF rhinorrhea is one of the more common complications of this surgical approach [1, 10], and CSF leaks are a well-known risk factor for subsequent meningitis. It is possible that the bone autograft was contaminated prior to reconstruction of the sellar floor, however, this is highly unlikely. To the best of our knowledge, there are no reports in the neurosurgical literature describing such a complication.

Of further interest in this case was the presence of an undisrupted saccular aneurysm of the supraclinoid portion of the internal carotid artery on the contralateral side. There is a well-documented but rarely appreciated association between GH-secreting pituitary adenomas and aneurysms of the intracranial arteries [14–16], and it is theorized that high levels of GH and insulin-like growth factor 1 [IGF-1] lead to aneurysm formation through induction of arterial dilation and degenerative changes in the arterial wall [14, 16]. Intrasellar aneurysms represent a small subset of intracranial aneurysms seen in patients with functional adenomas, however, the consequences of their presence can be devastating if they are not adequately documented prior to surgery. There was no such aneurysm in this case. Knowledge of this association is obviously critical to neuroradiologists and neurosurgeons, however, pathologists should also be cognizant when performing autopsies on patients who die following trans-sphenoidal surgery. If hemorrhagic complications are suspected to be the cause of death, special dissection of the sellar, parasellar and suprasellar area and/or special stains of blood vessels may be required to document the presence of a pre-existing carotid artery aneurysm.

In addition to describing an unusual complication of a relatively common surgical procedure, this report also highlights the utility of specialized dissections in forensic pathology. Although challenging and time consuming, the dissection and histologic examination of the cavernous sinus area was essential in this case to determining the source of bleeding, and an accurate determination of the cause of death.

Key points

1. Fatal complications of trans-sphenoidal resection of intra-cranial tumours are rare, but well documented in the literature. In addition to complications common to all surgeries such as pulmonary thromboembolism, fatalities following trans-phenoidal surgery may occur due to hemorrhage from intraoperative damage to the internal carotid artery or its branches, meningitis, or direct injury to the central nervous system.

2. Post-operative hemorrhage may be secondary to direct vascular injury, to infectious processes involving branches of the internal or external carotid arteries, or to pre-existing aneurysms of the internal carotid artery.

3. In cases involving suspected complications following trans-sphenoidal surgery, special dissections of the sella turcica and cavernous sinuses at autopsy are essential for accurate determination of the cause of death.

4. Clinicians and forensic pathologists should be aware of the possible coexistence of GH-secreting pituitary adenomas and saccular aneurysms of intracranial arteries. Prolonged secretion of growth hormone is thought to induce atherosclerotic and/or degenerative changes in the walls of the arteries in the circle of Willis, thus leading to aneurysm formation. Acromegalic patients who come to autopsy should therefore be assessed for the presence of intracranial aneurysms.

References

1. Ciric I, Ragin A, Baumgartner C, Pierce D. Complications of transsphenoidal surgery: results of a national survey, review of the literature and personal experience. Neurosurgery. 1997;40:225–37.

2. Patal CG, Lad SP, Harsh GR, Laws ER, Boakye M. National trends, complications and outcomes following transsphenoidal sugery for Cushing's disease from 1993 to 2002. Neurosurg Focus. 2007;23:E7.

3. Barker FG, Klibanski A, Swearingen B. Transsphenoidal surgery for pituitary adenomas in the United States, 1996–2000: mortality, morbidity, and the effects of hospital and surgeon volume. J Clin Endocrinol Metab. 2003;88:4709–19.

4. Sudhakar N, Ray A, Vafidis JA. Complications after trans-sphenoidal surgery: our experience and a review of the literature. Br J Neurosurg. 2004;18:507–12.

5. Nomikos P, Buchfelder M, Fahlbusch R. The outcome of surgery in 668 patients with acromaegaly using current criteria of biochemical "cure". Eur J Endocrinol. 2005;152:379–87.

6. Ahuja A, Guterman LR, Hopkins LN. Carotid cavernous fistula and false aneurysm of the cavernous carotid artery: complications of transsphenoidal surgery. Neurosurg. 1992;31:774–9.

7. Reddy K, Lesiuk H, West M, Fewer D. False aneurysm of the cavernous carotid artery: a complication of transsphenoidal surgery. Surg Neurol. 1990;33:142–5.

8. Nishioka H, Ohno S, Ikeda Y, Ohashi T, Haraoka J. Delayed massive epistaxis following endonasal transsphenoidal surgery. Acta Neurochir [Wien]. 2007;149:523–7.

9. Kachhara R, Menon G, Bhattacharya RN, Nair S, Gupta AK, Gadhinglajkar S, et al. False aneurysm of cavernous carotid artery and carotid cavernous fistula: complications following transsphenoidal surgery. Neurol India. 2003;51:81–3.

10. Onesti ST, Post KD. Complications of transsphenoidal microsurgery. In: Post KD, Friedman E, McCormick P, editors. Post operative complications in intracranial neurosurgery. New York: Thieme Medical Publishers; 1993. p. 61–73.

11. Rhee SJ, Kim MS, Lee CH, Lee GJ. Persistent trigeminal artery variant detected by conventional angiography and magnetic resonance angiography- incidence and clinical significance. J Korean Neurosurg Soc. 2007;42:446–9.

12. Onishi H, Ito H, Kuroda E, Yamamoto S, Kubota T. Intracranial mycotic aneurysm associated with transsphenoidal surgery to the pituitary adenoma. Surg Neurol. 1989;31:149–54.

13. Mielke B, Weir B, Oldring D, von Westarp C. Fungal aneurysm: case report and review of the literature. Neurosurg. 1981;9:578–82.

14. Seda L, Cukiert A, Nogueira KC, Huayllas MKP, Liberman B. Intrasellar internal carotid aneurysm coexisting with GH-secreting pituitary adenoma in an acromagalic patient. Arq Neuropsiquiatr. 2008;66:99–100.

15. Weir B. Pituitary tumors and aneurysms: case report and review of the literature. Neurosurgery. 1992;30:585–90.

16. Sade B, Mohr G, Tampieri D, Rizzo A. Intrasellar aneurysm and a growth hormone-secreting pituitary macroadenoma. J Neurosurg. 2004;100:557–9.

CASE REPORT

The elusive slug: bullet intestinal "embolism"

**Alon Krispin · Konstantin Zaitsev ·
Jehuda Hiss**

Abstract Bullet retrieval from the body of a gunshot victim is one of many tasks in post-mortem forensic examination. Rarely, it is complicated by the migration of the missile away from the entry point by vessel embolism. Abdominal firearm injuries, in which the bullet enters the intestines and moves inside the lumen away from the point of penetration, are even less common. We present a case of postmortem recovery of a bullet from the intestines of a gunshot victim who died 18 days after being shot in the trunk by three low velocity bullets. A missile had moved within the colon during hospitalization and postmortem handling of the body and was recovered from the sigmoid colon. This case demonstrates an extremely rare type of bullet "embolism" and emphasizes the usefulness of CT scanning in the location of projectiles.

Keywords Bullet "Embolism" · Penetrating trauma · Postmortem examination · X-ray radiography · CT scanning

Introduction

Trauma to the human body caused by shooting is divided into perforating and penetrating. In cases of penetrating trauma, the bullet loses its kinetic energy during movement

A. Krispin (✉) · K. Zaitsev · J. Hiss
The National Center of Forensic Medicine, Assaf Harofeh
Medical Center, Affiliated to the Sackler Faculty of Medicine,
Tel Aviv University, 67 Ben-Zvi Road, POB 49015,
61490 Tel Aviv, Israel
e-mail: alon.krispin@forensic.health.gov.il

along its trajectory and remains within the body. Bullet embolism is a phenomenon in which a bullet that penetrates the body and halts is carried away from its initial site of lodgment to a distant location.

We describe a case of an unusual trajectory of a low velocity bullet that penetrated the peritoneal cavity, and the perplexing obstacles of its retrieval.

Case report

A 27 year old male was admitted to a medical center after being shot by low-velocity bullets in the trunk and upper limbs. The bullets entry wounds of the trunk were located in the right and left chest and in the abdominal wall above the right iliac crest. The victim underwent an emergency explorative laparotomy, where massive venous bleeding was controlled with local packing. After surgery, an abdominal computed tomographic (CT) scan was performed and three middle sized caliber bullets were identified: one in the inter-vertebral disc between the eleventh and twelfth thoracic vertebra, and another between the spinous processes of the first and second lumbar vertebra. A third bullet was visualized near the thickened wall of the descending colon, some 18 cm from the splenic flexure. The exact location of the projectile could not be assessed, owing to imaging interference caused by reflecion of X rays (Fig. 1).

Despite right hepatic lobectomy being performed the next day, and attempts to surgically control the intrapleural and intraperitoneal re-bleeding events, the victim died 18 days later due to septic shock and multi-system organ failure.

Although a complete autopsy is generally required in cases of homicidal shooting [1], in this case, according to
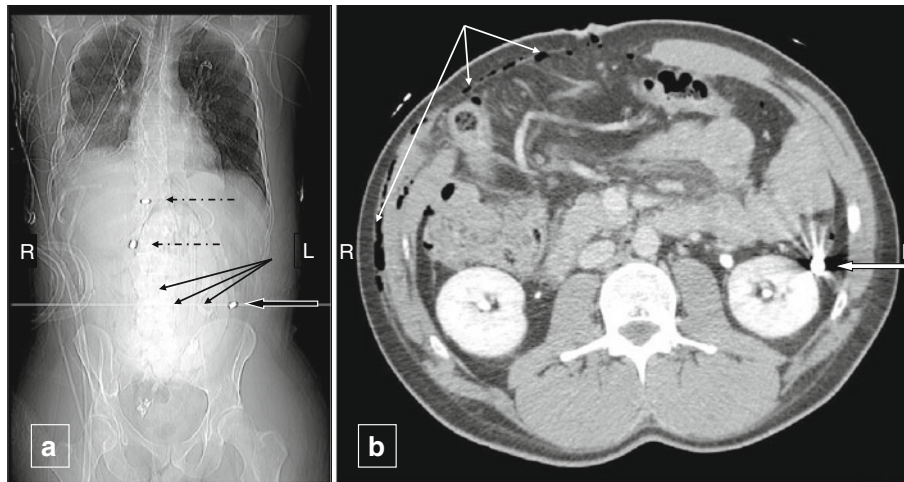
Fig. 1 Antemortem abdominal computerized-tomography scan after first surgery. **a** A low-resolution coronal view ("localizer") of a computerized-tomographic scan performed after the first laparotomy. Three bullets are present: one in the inter-vertebral disc between the eleventh and twelfth thoracic vertebra (*upper dashed arrow*), another between the spinous processes of the first and second lumbar (*lower dashed arrow*), and a third bullet adjacent to the descending colon of second lumbar vertebra (*bolded arrow*). The horizontal line at the level of second lumbar vertebra marks the level of the axial image shown in **b**. Multiple packing surgical pads are present within the abdomen (*successive thin arrows*). *R* = right, *L* = left. **b** Axial section at the level of second lumbar vertebra. A bullet (*bolded arrow*) is located in the descending colon. Note the free air bubbles in the abdominal cavity (*thin arrows*), as well as an incongruence of the anterior abdominal wall. *R* = right, *L* = left

police instructions following a request of the deceased's family, only an external examination and partial autopsy aimed at removal of the bullets were performed.

Two of the three abdominal bullets were easily localized and recovered from the vertebral column. A third bullet appeared on post-mortem antero-posterior (AP) radiography near the left iliac crest, with its long axis oriented medio-laterally (Fig. 2a). Despite thorough exploration, the missing bullet was not detected either throughout the whole thickness of the left abdominal wall, or in the peritoneal cavity. Interpretation of lateral radiographs, added to complement the non-invasive examination, did not contribute much to the understanding of the spatial localization of the bullet.

The mystery was solved when the orientation of the bullet in an additional AP radiograph taken after repeated mobilization of the body was changed to rostro-caudal (Fig. 2b), and the suggestion that the bullet may be found within the intestines was raised. Although external palpation of the large bowel was unproductive, the projectile was found in the sigmoid colon on internal exploration (Fig. 3). Only then was a small, semi-lunar, sutured laceration of the colonic wall just distal to the splenic flexure, which was not mentioned in the summary report issued by the treating medical centre, discovered. Later, a complete medical file was delivered to the medical examiner in charge of the examination. Scrutiny of all the emergency surgical procedures revealed that on the first laparotomy a tiny laceration of the colon wall was sutured. In the antemortem abdominal CT submitted with the medical file the bullet was seen within the lumen of the descending colon (Fig. 1b).

Discussion

Recovery of bullets from the body of a shooting victim is a crucial task in forensic medicine. Their presence is essential for ballistic tests carried out in order to identify the weapon from which the bullets were fired. When a missile is not found in the expected location calculated by the site of entry and its trajectory, it is safe to assume that it could have either been deflected from its previous course by hard tissues, exited through the natural body orifices, or been carried away to a distant location [2].

Embolism refers to the migration of a solid particle, such as a missile, thrombus or a medical device, liquid such as amniotic fluid, or gaseous bubble such as nitrogen, from its point of origin to a distant site [3]. Emboli are carried through a vessel, or propelled by blood flow, air pressure, or active or passive body movement, and therefore can occur even after death [4].

Numerous reports describe bullet embolism in larger blood vessels, followed by complications due to obstruction of systemic blood vessels [5–11] and pulmonary [6, 7, 9, 10, 12] or paradoxical emboli [13]. In a smaller number of reports, bullet "embolism" through the urinary system is described, followed by urinary retention [14–16]. There are
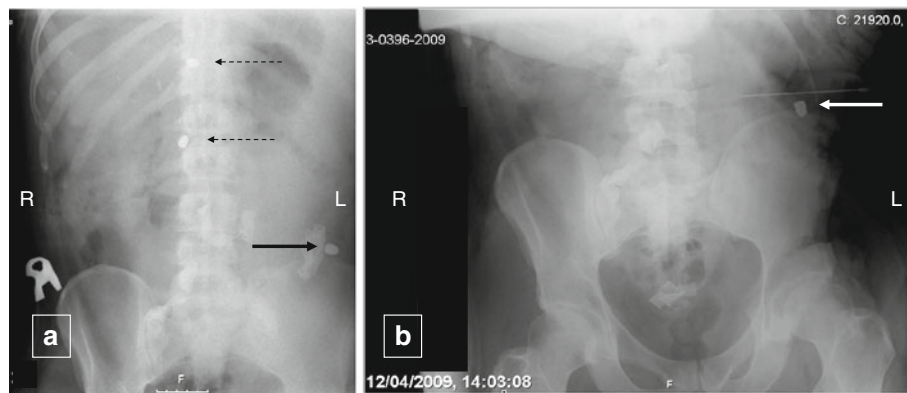
Fig. 2 Postmortem abdominal X-ray antero-posterior views taken during internal examination of the body. **a** Postmortem antero-posterior X-ray view of the victim's abdomen. Prior to the recovery of the bullets, two bullets are lodged in or near the vertebral column (*dashed arrows*). A third bullet is seen above the iliac crest with its long axis oriented medio-laterally (*bolded arrow*). R = right, L = left. **b** Repeated postmortem antero-posterior X-ray view after recovery of the bullets lodged in the spine. The long axis of the third bullet seen in Fig. 2a (*bolded arrow*) has changed to rostro-caudal. R = right, L = left
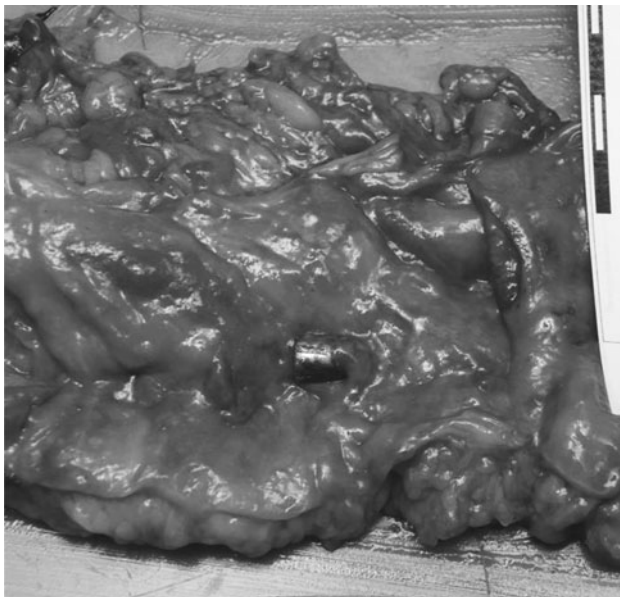

Fig. 3 The sigmoid colon of the victim where the bullet was found. One of the three abdominal bullets (Figs. 1, 2) visualized within the sigmoid colon

also case reports of esophageal injury and subsequent finding of the bullet in the stomach [17] and migration of a bullet from the stomach into the intestines [18].

DiMaio described two cases of bullets expelled through the mouth: in one case a spent bullet from an entry wound in the back was found in the oral cavity; in the other, a projectile from a wound in the chest halted within the lung and was coughed or vomited by the victim [19].

Shooting is the leading cause of violent death in the United States [20]. Bullet injuries constitute the vast majority of abdominal perforating trauma, and the greater part of penetrating trauma [21–23]. A penetrating bullet that punctures the abdominal cavity generally has enough kinetic energy to be able to perforate the intestines, and then halt upon striking the vertebral column, abdominal wall muscles, or just beneath the skin. Nevertheless, there may be cases of low-velocity ammunition in which the bullet course ends within a hollow viscus. These cases seem to be infrequent, and are seldom reported in the literature.

The post-mortem detection and recovery of a bullet in cases of penetrating trauma is generally carried out using X-ray radiography, and in most instances an AP view is sufficient. The recommended additional lateral view is seldom performed in routine forensic practice [24], mainly because of technical limitations. The images are analyzed and compared to the body during internal examination, after deducing the general course of the trajectory from the entrance wound. In most cases, the bullet is easily found using marks such as subcutaneous and deeper hemorrhage, palpation of soft tissue against the skeleton, or using no more than superficial dissection.

However, in the case of a bullet halted within the intestines, lack of awareness of the spatial location may result in the futile seeking of the missile in the abdominal wall. This could be due to the possibility that the two-dimensional X-ray image may be interpreted as if the roentgenic shadow of the bullet on the abdominal wall indicates its real location. The recommended two radio-graphic positions (AP and lateral) might be insufficient, as in the present case.

Lodging of a bullet in the intestine is a very rare event, and although it is rarely reported in the literature, should be taken into consideration when searching for a missile in the abdomen. When enough time has passed between the shooting event and death, changes in the injured tissues and the lack of local hemorrhage that usually indicate the

possible course of the bullet, tend to disappear, depriving the prosector of crucial indication for the location of the foreign object. In such cases, post-mortem CT or MRI scans, if available, in addition to the routine AP and lateral radiographic may facilitate bullet detection [25].

In the present case, the bullet had penetrated the colon through a tiny laceration and moved, after the initial surgical procedure, from its initial reported location near the splenic flexure to the level of the second lumbar vertebra during hospitalization. This migration may be attributed to peristalsis, although contribution of external palpation or manipulation of the bowel during surgical procedures cannot be excluded. The bullet was not expelled from the body by defecation probably due to decreased bowel movement as part of a state of ileus and peritonitis following perforation of the colon. Finally, the projectile was located at the sigmoid colon, probably due to mobilization of the body.

Preforming an autopsy in Israel requires next-of-kin consent or a court order. Partial autopsy in forensic investigation of death is a rare, albeit established policy in our legal system, and is usually performed in special circumstances. When the family is reluctant to consent to a complete autopsy, the investigative leads are straightforward, and the partial autopsy is designated to achieve a particular goal, such as bullet retrieval; thus the police may accede to the family's wish in order to avoid lengthy court procedures.

We advise that, before the post mortem internal exploration of surgically treated shooting victims is carried out, the forensic expert be presented with the complete medical file of the deceased along with a set of the original imaging tests, and not with the "discharge summary" only. Such a policy will expedite and facilitate the retrieval of bullets and avoid the confusion raised by possible bullet "embolism".

Key points

1. Bullets that hit the trunk generally stop at the abdominal or chest wall, and are usually found within a vertebra or a rib, or just underneath the skin. It is a rare event when a bullet halts within the intestines.

2. A bullet that rests within the intestines might migrate within the intestines if the victim survives and undergoes surgery, as it does within blood vessels and the urinary tract. Furthermore, its location and orientation may change while handling the cadaver. In such cases locating the bullet based on imaging produced when the shooting victim was alive, might be difficult.

3. Recovery of a bullet from the body using a two-dimensional plain X-ray film or electronic image may be complicated. A 3D computerized tomography may facilitate the bullet's retrieval.

4. A full medical history of a surgically treated shooting victim is essential for the understanding of such cases before the performance of the autopsy.

References

1. Adelson L. The medico legal autopsy. In: The pathology of homicide—a vade mecum for pathologist, prosecutor and defense counsel. Springfield: Charles C. Thomas; 1974. p. 11. http://catalogue.nla.gov.au/Record/1876474; http://www.amazon.com/Pathology-Homicide-Lester-Adelson/dp/0398030006

2. Adelson L. Homicide by firearms. In: The pathology of homicide—a vade mecum for pathologist, prosecutor and defense counsel. Springfield: Charles C Thomas; 1974. p. 262–3. http://catalogue.nla.gov.au/Record/1876474; http://www.amazon.com/Pathology-Homicide-Lester-Adelson/dp/0398030006

3. Kumar V, Abbas KA, Nelson F. Robbins and cotran pathologic basis of disease. Cortan RS, editor. Philadelphia: Elsevier Saunders; 2005. p. 135–6.

4. Brogdon BG. Forensic radiology. Boca Raton: CRC Press; 1998. p. 229–30.

5. Shen P, et al. Gunshot wound to the thoracic aorta with peripheral arterial bullet embolization: case report and literature review. J Trauma. 1998;44(2):394–7.

6. Khalifeh M, et al. Penetrating missile embolisation. Eur J Vasc Surg. 1993;7(4):467–9.

7. Symbas PN, Harlaftis N. Bullet emboli in the pulmonary and systemic arteries. Ann Surg. 1977;185(3):318–20.

8. McQuaide JR, September ED. Systemic bullet embolism. S Afr J Surg. 1981;19(2):145–9.

9. Michelassi F, et al. Bullet emboli to the systemic and venous circulation. Surgery. 1990;107(3):239–45.

10. Bining HJ, et al. Venous bullet embolism to the right ventricle. Br J Radiol. 2007;80(960):e296–8.

11. Wallace KL, Slovis CM. Hepatic vein bullet embolus as a complication of left thoracic gunshot injury. Ann Emerg Med. 1987;16(1):102–4.

12. Agarwal SK, et al. Wandering bullet embolizing to the pulmonary artery: a case report. Asian Cardiovasc Thorac Ann. 2007;15(2):154–6.

13. Schurr M, McCord S, Croce M. Paradoxical bullet embolism: case report and literature review. J Trauma. 1996;40(6):1034–6.

14. Shiver SA, Reynolds BZ. Urethral obstruction due to the passage of a retained projectile into the genitourrinary system. Am J Emerg Med. 2008;26(7):842 e1–2.

15. Raz O, et al. Late migration of a retained bullet into the urinary bladder presenting with acute urinary retention. Isr Med Assoc J. 2007;9(6):484–5.

16. Bozeman WP, Mesri J. Acute urinary retention from urethral migration of a retained bullet. J Trauma. 2002;53(4):790–2.

17. Smalls NM, Siram SM. The wandering bullet. J Natl Med Assoc 1988;80(6):678–9, 682.

18. Spitz WU, Spitz DJ. Medicolegal investigation of death: guidelines for the application of pathology to crime investigation. Springfield: Charles C Thomas; 2006. p. 702.

19. VJM D. Bullet emboli, in gunshot wounds practical aspects of firearms, ballistics, and forensic techniques. Boca Raton: CRC Press; 1999. p. 279.

20. Karch DL, et al. Surveillance for violent deaths—national violent death reporting system, 16 States, 2006. MMWR Surveill Summ. 2009;58(1):1–44.

21. Asensio JA, et al. Penetrating thoracoabdominal injuries: ongoing dilemma-which cavity and when? World J Surg. 2002;26(5):539–43.

22. Schmelzer TM, et al. Evaluation of selective treatment of penetrating abdominal trauma. J Surg Educ. 2008;65(5):340–5.

23. Demetriades D, et al. Selective nonoperative management of penetrating abdominal solid organ injuries. Ann Surg. 2006; 244(4):620–8.

24. Shkrum MJ, Ramsay DA. Forensic pathology of trauma—common problems for the pathologist. Thau A, editor. Totowa: Humana Press Inc; 2007. p. 321–325.

25. Thali MJ, et al. Image-guided virtual autopsy findings of gunshot victims performed with multi-slice computed tomography and magnetic resonance imaging and subsequent correlation between radiology and autopsy findings. Forensic Sci Int. 2003;138(1–3): 8–16.

CASE REPORT

Postmortem CT findings of "gastromalacia": a trap for the radiologist with forensic interest

Christopher J. O'Donnell · Melissa A. Baker

Abstract Autolytic rupture of the stomach, so called gastromalacia, is a well recognized artifact at autopsy. A 50 year old Asian woman with a past history of alcoholism, head injury and posttraumatic epilepsy was found deceased at home following a 12 h period of feeling unwell, seizures and vomiting. Postmortem CT images of the abdomen showed free gas in the peritoneal cavity adjacent to the stomach and no other abnormality. There were no external or radiological features of putrefaction. Appearances were stated by a radiologist to be strongly suggestive of gastro-intestinal tract perforation. Autopsy revealed typical findings of autolytic gastric rupture without features of peritonitis. Cause of death was determined by the pathologist to be "complication of status epilepticus (posttraumatic)". This case demonstrates that gastromalacia may occur rapidly after death and can be detected on postmortem CT, even in the absence of external putrefactive features or CT findings of putrefaction such as gas within the anterior abdominal wall, cardiac chambers or hepatic vasculature. The radiologist with forensic interest must be aware of this postmortem CT artifact in order to avoid ascribing the presence of free intra-peritoneal gas to antemortem perforation of the bowel.

Keywords CT scan · Gastromalacia · Intestinal perforation · Free gas

C. J. O'Donnell (✉) · M. A. Baker
Victorian Institute of Forensic Medicine and Department of Forensic Medicine, Monash University, 57–83 Kavanagh St, Southbank, Melbourne, VIC 3006, Australia
e-mail: chriso@vifm.org

Introduction

Postmortem artifacts are described as "any change caused or feature introduced in a body after death that is likely to lead to misinterpretation of medico-legally significant antemortem findings" [1]. Forensic pathologists performing autopsy are mindful of these artifacts including hypostasis, decomposition, resuscitation effects, heat-related fracturing of bone, agonal changes such as regurgitation and aspiration, and trauma to the body occurring as a result of postmortem handling. Radiologists interested in interpreting postmortem CT or MRI must also be aware of the artifacts and their imaging equivalents.

Organ autolysis is one such artifact commonly seen at autopsy occurring primarily in the pancreas that can be misinterpreted by the pathologist as hemorrhagic pancreatitis [2]. Autolytic rupture of the stomach, or so called gastromalacia, is another well recognized artifact originally described by John Hunter in the eighteenth century [3]. It is less commonly encountered but occurs usually in the region of the gastro-esophageal junction and fundus. It results in thinning and softening of the gastric wall and eventual slimy, brownish/black mural disintegration producing local perforation. Similar appearances may be visible in the distal esophagus (esophagomalacia). For a pathologist, the key autopsy feature of this normal postmortem finding is the absence of peritonitis on visual inspection and lack of an acute inflammatory or vital reaction on histological examination [2].

Case report

A 50 year old Asian woman with past history of alcoholism, head injury and posttraumatic epilepsy was found

deceased by her friend. The previous evening she had returned from an Alcoholics Anonymous meeting and complained of feeling unwell. She retired to bed at 10.30 pm but awoke later that night with vomiting. She had further vomiting and was incontinent of feces, with seizures that were witnessed by her friend. He described that on one occasion (~3.30 am) during one such seizure; she appeared to hit the left side of her face against a wall but remained conscious. Some 7 h after that incident (~10.30 am) the deceased was found by her partner on the floor of the bedroom with no sign of life and he called an ambulance. Resuscitation was not attempted. Due to the unexpected nature of her death and the presence of external injuries to her face, arm and leg, police were informed and the deceased admitted to the principal investigative facility of the State Coroner.

Radiological findings

A postmortem computed tomography (CT) scan was performed about 11 h after the deceased was found by her friend and ~18 h after she was last seen alive. An Aquilion16® multi-detector CT scanner (Toshiba Medical Systems, Minato-ku, Tokyo, Japan) was used. The head and body were scanned separately with 0.5 mm collimation and images reconstructed into overlapping 1 and 2 mm slices respectively. Images were sent to the Institute's PACS server (IMPAX®, Agfa HealthCare NV, Mortsel, Belgium) and analyzed on a Vitrea® 2 workstation (Vital Images, Inc. Minnetonka, Minnesota, USA).

Prior to autopsy, multi-planar and 3 dimensional CT images were reviewed and demonstrated free intra-peritoneal gas around the body and fundus of the stomach (Fig. 1). There were no radiological features of putrefaction i.e. no gas within the anterior abdominal wall overlying the cecum and sigmoid colon, and no gas in the hepatic vasculature (Fig. 2). No definitive site of bowel wall rupture was identified on CT or fluid collections detected but given the presence of this free gas and its location around the stomach, pathological (antemortem) perforation of the stomach or duodenum was suspected by the reporting radiologist.

Autopsy findings

A full postmortem examination was performed ~23 h after the deceased was found by her friend and ~30 h since she was last seen alive. At autopsy, rupture of the gastric fundus was noted over a length of approximately 9 cm, with leakage of gastric contents into the left upper quadrant of the abdominal cavity (Fig. 3). There was no
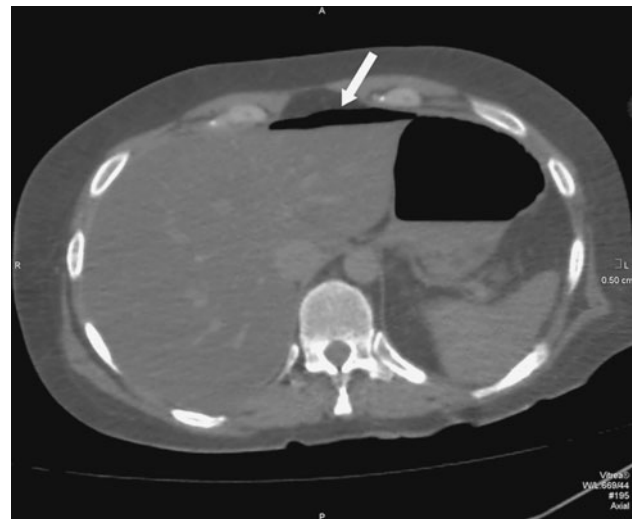
Fig. 1 Axial postmortem CT scan through the upper abdomen of the deceased demonstrating free gas within the peritoneal cavity (*arrow*) anterior to the left hepatic lobe and adjacent to the gastric body. Note the absence of gas in the hepatic vasculature as is often detected on postmortem CT as a result of putrefaction
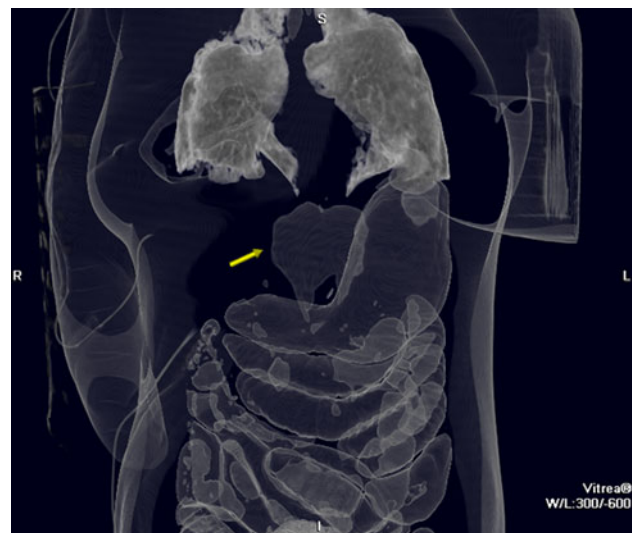
Fig. 2 Postmortem 3D minimal intensity projection (MinIP) CT reconstruction of the deceased's chest and abdomen highlighting normal gas-containing structures. Note the abnormal collection of extra-luminal gas (*arrow*) adjacent to the lesser curve of stomach

macroscopic evidence of peritonitis and the stomach wall adjacent to the rupture site was markedly thinned. The macroscopic appearance was typical of gastromalacia. Histological examination of a section of gastric wall from this area showed advanced autolysis without evidence of an inflammatory reaction (Fig. 4). Postmortem examination also revealed previous left sided craniotomy and chronic posttraumatic changes to the left parieto-temporal and right inferior temporal lobes, consistent with the deceased's past
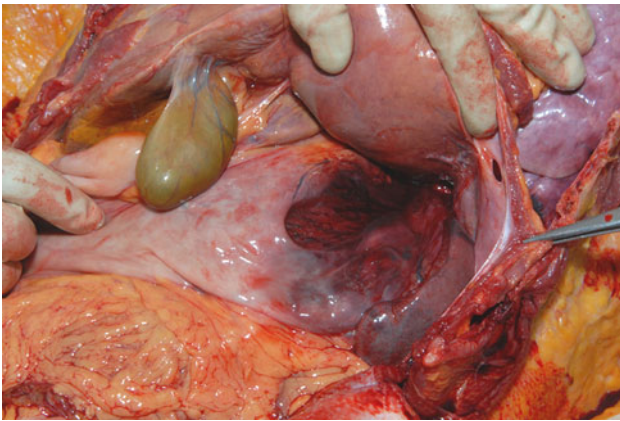
Fig. 3 Photograph of the upper abdominal contents at autopsy showing a large defect in the gastric fundus without signs of surrounding peritonitis consistent with autolytic gastromalacia
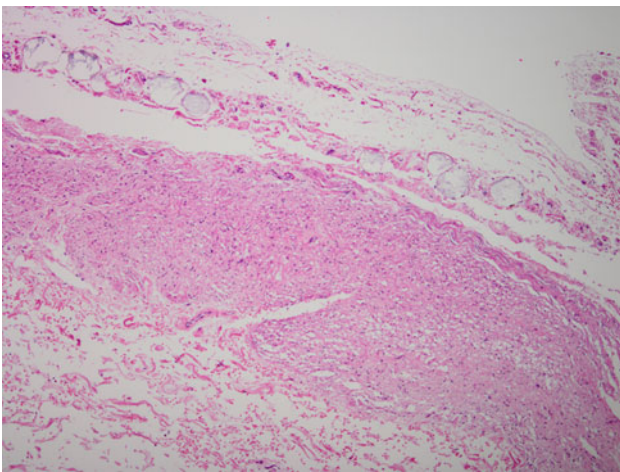
Fig. 4 Photomicrographic section of the gastric wall stained with H & E and magnified 100 times adjacent to the site of perforation, demonstrating autolysis in the absence of acute inflammation

history of head injury and subsequent epilepsy. Neither acute cerebral hemorrhage nor changes of recent cranial trauma were identified. No other significant natural disease was identified. In the absence of natural disease or signs of acute traumatic injury, cause of death was determined by the pathologist to be "complication of status epilepticus (posttraumatic)".

Toxicology findings

Toxological analysis of 10 ml postmortem femoral venous blood using GC-A (gas chromatography packed column with liquid dilution and direct injection) and GC-B/MS/DAD (capillary gas chromatography with nitrogen phosphorus and mass spectrometry detection, and photo-diode

array gradient high performance liquid chromatography) revealed no ethanol, poisons or common drugs. Importantly, levetiracetam, an anti-epileptic prescribed to the deceased to control her seizures, was not detected.

Discussion

CT scanning of the deceased, even when autopsy is to be performed, is valuable for the pathologist as it provides an overview of the deceased's anatomy and in many cases an indication of likely pathology allowing the pathologist to tailor autopsy technique [4]. Postmortem CT is clearly not the same as clinical CT thus interpretation must take into account changes that occur normally in the body after death. The reporting radiologist also needs to be aware of the many postmortem artifacts that are well recognized by forensic pathologists including decomposition.

Decomposition is the normal disintegration of body tissues occurring after death and consists of 2 processes occurring in parallel. The first is autolysis or self dissolution of organs by endogenous body enzymes released from disintegrating cells. The second is putrefaction due to the effects of microorganisms, most commonly bacteria that are characteristically gas forming [5].

Autolytic features are common autopsy and histological findings for the forensic pathologist. Organs rich in enzymes such as the pancreas, gastric wall and liver are most susceptible to the process, especially the pancreas. If occurring in the stomach it is termed gastromalacia due to the appearance of gastric wall thinning and can lead to local perforation causing gastric content to spill into the peritoneal cavity. It should not be confused with pathological perforation [6]. It has a typical autopsy appearance and shows no surrounding inflammatory (vital) reaction in the peritoneum on either visual inspection or histological analysis. It tends to occur towards the gastric fundus but may also involve the distal esophagus leading to perforation into the left chest cavity. It is seen more commonly in patients with closed head injury possibly due to loss of central temperature regulation leading to a terminal surge in body temperature, promoting the autolytic process [5].

In the absence of contrast administration into the gastric lumen, detection of gastric wall thinning is very difficult on postmortem CT. Indeed even in the clinical setting, meticulous CT technique using various intra-luminal contrast agents and dynamic intra-venous contrast enhancement is required to accurately display the gastric wall, allowing detection and staging of conditions such as gastric malignancy [7]. Gastromalacia therefore may only be suspected on routine postmortem CT if there is actual perforation of the gastric wall with release of intra-luminal gas and fluid into the peritoneal cavity.

Gas is readily identified on CT as regions of very low density (blackness) reflected in negative Hounsfield numbers. A Hounsfield number or unit is a normalized value of the calculated X-ray absorption coefficient of a pixel (picture element), expressed in units or numbers, where that unit for air is defined as −1000 and that of water is zero. It is not possible to differentiate between CO_2 and other gases such as room air based on these Hounsfield numbers.

CT in the clinical setting is very sensitive for the detection of even small volumes of free gas in the abdominal cavity and is certainly more sensitive than plain abdominal radiographs [8, 9]. Any free gas detected on clinical CT is considered abnormal and in the absence of penetrating injury it is likely to be due to bowel perforation, although not all bowel perforations are associated with release of gas into the peritoneal cavity. Interestingly only 60% of cases of perforated bowel in the clinical study by Pinto had any free intra-peritoneal gas present even though the vast majority (92.5%) did have evidence of fluid in the peritoneal cavity either in the supra or infra-mesocolic spaces or both [10].

Postmortem CT is also sensitive for the detection of extra-intestinal gas in the abdominal cavity. In a series of deceased persons having CT following blunt trauma, free intraperitoneal gas was detected with a sensitivity of 100% [11]. Interpretation is clearly more difficult as free intra-peritoneal gas can be due to multiple factors apart from injury. Gas is a prominent feature in putrefaction and can be detected on postmortem CT scanning in multiple sites including the abdominal cavity as well as the hepatic vasculature and cardiac chambers [12]. Abnormal collections of gas on postmortem CT have also been described in the heart due to cardiopulmonary resuscitation [13] and liver due to gastrointestinal distension, sepsis, necrotic bowel and blunt force trauma [14–17]. This case had none of the external features of putrefaction notably lack of skin discoloration or marbling on the anterior abdominal wall, skin blistering and slippage or bloating [18]. No gas was identified in the liver or heart on CT and the bowel was not distended at autopsy. No resuscitation attempts were undertaken and there was no evidence of trauma to the chest or abdomen. The only apparent explanation for free intraperitoneal gas on the postmortem CT therefore was bowel perforation.

Postmortem CT findings in gastromalacia have not previously been reported but in a small series of pathological (traumatic) small bowel perforations with autopsy correlation, free intra-peritoneal gas was detected in 2 of 3 cases and "ascites" in 3 of 3 cases on the postmortem CT. Perforation was confirmed at autopsy in all 3 cases but the paper did not comment on the ability of postmortem CT to detect associated inflammatory features in the mesenteric fat, determine the exact site of bowel perforation or state if gas was localized to the site of bowel perforation [19].

In clinical practice, determining the exact site of bowel perforation on CT is important for surgical management of the patient. This can be problematic and relies on the accumulation of gas around the site of bowel rupture and detection of defects in the integrity of the bowel wall. One author has indicated that gas centered on the falciform ligament is more suggestive of an upper gastro-intestinal origin of leak as compared to scattered pockets of gas being more likely in distal perforation [9]. In another large clinical series of 85 perforation cases, CT was able to localize the site of perforation in 73 cases (86%) due in most part to the localization of gas at the site of rupture as well as detection of bowel wall thickening (58%) and defects in the bowel wall (40%) [20]. In a case report of blunt traumatic gastric perforation, CT scan prior to surgery did demonstrate the site of gastric wall rupture and this was confirmed at surgery [21]. This ability to detect bowel wall disruption was not reproduced in another clinical series of 40 surgically proven gastro-intestinal perforations using optimal CT technique, in which no site of bowel wall discontinuity was detected [10]. In a retrospective clinical series by Chen et al. [22], CT showed free air in 100% of 14 patients with perforated peptic ulceration but the site of perforation in only 5 (36%).

Given that detection of free gas and bowel wall discontinuity is not always possible in pathological (antemortem) gastro-intestinal tract perforation, authors have indicated that on clinical CT there are other findings that may be associated with bowel perforation notably bowel wall thickening, focal or generalized fluid collections, and intra-abdominal fat stranding although these are not as reliably detected [9, 20]. These later features are likely to be of benefit in the interpretation of postmortem CT for deceased persons with bowel rupture occurring before death as they are indicative of bowel content leak and reactive peritoneal inflammation.

Conclusion

Free gas in the peritoneal cavity on postmortem CT must be interpreted with caution. In the absence of penetrating injury or resuscitative measures, gas could be due to putrefaction, gastromalacia or pathological (antemortem) bowel perforation. If putrefaction is responsible then gas may also be detected in the abdominal wall, cardiac chambers or hepatic vasculature on CT and features of putrefaction may be evident on external examination of the deceased. If there are no visible or other radiological features of putrefaction and gas is isolated to the peritoneal cavity then bowel perforation is likely.

The differentiation between perforation due to autolysis from pathological gastro-intestinal tract perforation on CT is difficult. Postmortem artifact (gastromalacia) must be suspected if free gas is accumulated around the gastric body and fundus or lower esophagus, however, based on clinical CT studies the actual site of perforation may not always be evident. A short postmortem interval to CT scan does not exclude gastromalacia as in this case the time to scan was less than 24 h after death. In the same way that the pathologist must look for secondary inflammatory changes in the peritoneum so too must the radiologist look for the other reported CT features of bowel perforation notably free or loculated fluid collections in the peritoneal cavity, as well as bowel wall thickening and abdominal fat standing. It is only when such additional changes are detected that a confident postmortem CT diagnosis of pathological (antemortem) bowel perforation with reactive peritonitis can be entertained rather than artifactual gastromalacia with perforation.

Key points

1. Gastromalacia or autolytic gastric wall thinning and rupture is a common postmortem artifact at autopsy
2. CT is very sensitive at detecting free gas in the peritoneal cavity
3. Causes of such free intra-peritoneal gas on postmortem CT include penetrating injury, putrefaction, cardiopulmonary resuscitation, antemortem bowel perforation and gastromalacia
4. Postmortem CT findings of gastromalacia are free gas around the stomach in the absence of features associated with peritonitis
5. Gastromalacia on postmortem CT can occur within hours of death and may not be associated with external or CT findings of putrefaction

References

1. Fatteh A, editor. Handbook of forensic pathology. Philadelphia: Lippincott Williams & Wilkins; 1973. p. 49.
2. Saukko P, Knight B, editors. Knight's forensic pathology. 3rd ed. London: Edward Arnold; 2004. p. 36.
3. Hunter J. On the digestion of the stomach after death. Philos Trans R Soc London. 1772;62:447–52.
4. O'Donnell C, Rotman A, Collett S, Woodford N. Current status of routine post-mortem CT in Melbourne, Australia. Forensic Sci Med Path. 2007;3:226–32.
5. Spitz WU, editor. Medico-legal investigation of death: guidelines for the application of pathology to crime investigation. 4th ed. Springfield, IL: Charles C Thomas; 2006. p. 107.
6. Moritz AR. Classical mistakes in forensic pathology. Am J Clin Pathol. 1956;26:1383–97.
7. Chen CY, Hsu JS, Wu DC, Kang WY, Hsieh JS, Jaw TS, Wu MT, Liu GC. Gastric cancer: preoperative local staging with 3D multi-detector row CT—correlation with surgical and histopathologic results. Radiology. 2007;242:472–82.
8. Furukawa A, Samoa M, Yamasaki M, Kino N, Tanaka T, Nitta N, Kawasaki S, Imoto K, Takahashi M, Murata K, Sakamoto T, Tani T. Gastrointestinal tract perforation: CT diagnosis of presence, site, and cause. Abdom Imaging. 2005;30:524–34.
9. Yeung KW, Chang MS, Hsiao CP, Huang JF. CT evaluation of gastrointestinal tract perforation. Clin Imaging. 2004;28:329–33.
10. Pinto A, Scaglione M, Giovine S, Romano S, Lassandro F, Grassi R, Romano L. Comparison between the site of multislice CT signs of gastrointestinal perforation and the site of perforation detected at surgery in forty perforated patients. Radiol Med. 2004;108:208–17.
11. Christe A, Ross S, Oesterhelweg L, Spendlove D, Bolliger S, Vock P, Thali MJ. Abdominal trauma—sensitivity and specificity of postmortem non-contrast imaging findings compared with autopsy findings. J Trauma. 2009;66:1302–7.
12. Thali M, Yen K, Schweitzer W, Vock P, Ozdoba C, Dirnhofer R. Into the decomposed body—forensic digital autopsy using multislice—computed tomography. Forensic Sci Int. 2003;134:109–14.
13. Shiotani S, Kohno M, Ohashi N, Atake S, Yamazaki K, Nakayama H. Cardiovascular gas on nontraumatic postmortem computed tomography (PMCT): the influence of cardiopulmonary resuscitation. Radiat Med. 2005;23:225–9.
14. Shiotani S, Kohno M, Ohashi N, Yamazaki K, Nakayama H, Watanabe K. Postmortem computed tomography (PMCT) demonstration of the relation between gastrointestinal (GI) distension and hepatic portal venous gas (HPVG). Radiat Med. 2004;22:25–9.
15. Asamura H, Ito M, Takayanagi K, Kobayashi K, Ota M, Fukushima H. Hepatic portal venous gas on postmortem CT scan. Legal Med. 2005;7:326–30.
16. Yamazaki K, Shiotani S, Ohashi N, Doi M, Honda K. Hepatic portal venous gas and hyper—dense aortic wall as post-mortem computed tomography finding. Legal Med. 2003;5:S338–41.
17. Jackowski C, Sonnenschein M, Thali M, Aghayev E, Yen K, Dirnhofer R, et al. Intrahepatic gas at postmortem computed tomography: forensic experience as a potential guide for in vivo trauma imaging. J Trauma. 2007;62:979–88.
18. Saukko P, Knight B, editors. Knight's forensic pathology. 3rd ed. London: Edward Arnold; 2004. p. 64–7.
19. Yamazaki K, Shiotani S, Ohashi N, Doi M, Kikuchi K, Nagata C, Honda K. Comparison between computed tomography (CT) and autopsy findings in cases of abdominal injury and disease. Forensic Sci Int. 2006;162:163–6.
20. Hainaux B, Agneessens E, Bertinotti R, De Maertelaer V, Rubesova E, Capelluto E, Moschopoulos C. Accuracy of MDCT in predicting site of gastrointestinal tract perforation. Am J Roentgenol. 2006;187:1179–83.
21. Takabe K, Ohtani T, Muto I, Takano Y, Miyauchi T, Kato H, Sekido H, Ohki S, Hatakeyama K, Shimada H. Computed tomography (CT) findings of gastric rupture after blunt trauma. Hepatogastroenterology. 2000;47:901–3.
22. Chen CH, Huang HS, Yang CC, Yeh YH. Features of perforated peptic ulcers in conventional computed tomography. Hepatogastroenterology. 2001;48:1393–6.

CASE REPORT

Death by black powder revolver: a case report

**Joseph J. Pavelites · David Kintzele ·
Paul Fotia · Joseph A. Prahlow**

Abstract Deaths resulting from the use of black powder handguns are relatively uncommon compared to other firearms. We report the case of a 48 year-old woman who sustained a lethal gunshot wound to the face from a black powder revolver. Autopsy revealed extensive soot and powder deposition around the entrance wound between the right eye and nose with perforation of the skull and brain. The exit wound also contained evidence of soot. Discussion of this characteristic pattern of discharge deposition from black powder weapons is presented.

Keywords Black powder · Hand gun · Ballistics · Wound

Introduction

Black powder is a propellant once used in ammunition and as the bursting charge in artillery projectiles. It is made of charcoal, sulfur, and potassium nitrate and is commonly referred to as "gunpowder." Black powder is no longer commonly used except in replicas of antique firearms. "Black powder firearm" is a term that describes a weapon that traditionally uses the aforementioned propellant or the closely related, modern substitute powder formulations. The use of black powder firearms in homicides is a rare event even with less stringent government oversight compared to cartridge loaded weapons. Though less government regulation has led to ease of availability, it has been suggested that the complexity of loading and lack of reliability of black powder weapons limits their choice as a weapon [1]. The uncommon use of black powder weapons in homicide cases may lead to a lack of familiarity by clinical and forensic physicians with the characteristics and wounding effects of these firearms. In this paper, a homicide with a black powder revolver is presented as an unusual cause of death that also serves as an example of typical wound features for these types of weapons. A discussion of the special issues involved with firearms examination of black powder weapons is also provided.

J. J. Pavelites (✉)
Transitional Year Program, GME Office, Dwight D. Eisenhower
Army Medical Center, Building 300, Hospital Road, Ft. Gordon,
GA 30905, USA
e-mail: joseph.pavelites@us.army.mil

D. Kintzele · P. Fotia
Indiana State Police Laboratory, Lowell, IN 46356, USA

J. A. Prahlow
South Bend Medical Foundation, 530 North Lafayette
Boulevard, South Bend, IN 46601, USA

J. A. Prahlow
Indiana University School of Medicine-South Bend
at the University of Notre Dame, Raclin-Carmichel Hall,
1234 Notre Dame Avenue, South Bend, IN 46617, USA

Case report

Police were notified of the shooting death of a 48 year-old white female. Allegedly, her husband shot her in the face at close range with a Ruger black powder revolver in their home. The husband testified that he asked his wife to retrieve the loaded weapon that was stored behind their couch. According to the husband, she grasped the weapon by the barrel placing it butt first in his open hand with the barrel pointed towards her right eye. Furthermore, the husband stated that the placement of the weapon in his hand caused the hammer to strike the base of his thumb

Fig. 1 Soot found on the clothing of the right shoulder of the victim as seen from above the victim's seated position on the couch

Fig. 2 Hole in the window made by exit of lead ball projectile. The markings visible on the couch just right of the victim's head are caused by blood spatter

Fig. 3 a Photograph illustrating the extent of soot on the victims face. **b** *White*, *dotted outline* added to distinguish areas covered by soot as opposed to blood. Area enclosed within outline signifies soot

Fig. 4 Photograph illustrating powder tattooing. Note the entrance wound inferior and medial to right orbit

resulting in the accidental discharge of the weapon. At this time the wife sustained a fatal wound and the husband received a small abrasion to his thumb.

The victim was found inside her trailer where her body was seated and slumped over in a small couch. She had been shot in the area of her right eye. There was gunpowder on her face and on the right shoulder of her shirt (Fig. 1) and the exit of the projectile from the home through the nearby window (Fig. 2) was noted. A large pool of blood had formed on the floor behind the couch. Subsequent police investigation revealed that the victim had been shot at a range within 12–18 inches.

Autopsy findings

At autopsy, extensive soot and powder deposition was noted around a gunshot entrance wound between the right eye and nose (Figs. 3a, b, 4). The entrance wound was a .75 by .5 inch, roughly oval-shaped aperture of the medial aspect of the right eye/nasal bridge. It was 3.5 inches below

the top of the head and 1.0 inch to the right of midline. Surrounding the entrance wound was an ill-defined, circumferential marginal abrasion. In addition, within a 6.0 inch by 4.5 inch area surrounding the wound, there was extensive black soot/powder deposition, intermixed with blood. This was most dense within a 3.0 by 3.0 inch area. Multiple stipple marks were associated with the black deposits and were best appreciated after washing the soot from the skin (Fig. 4).

Fig. 5 Photograph illustrating path of projectile through the cranium. The exit wound (*arrow*) of the left occipital bone is seen in the *upper right hand corner* of the picture. The frontal bone is at the *bottom* of the photograph

The pathway of projectile was front-to-back, right-to-left and slightly downward.

After perforating the skin and subcutaneous tissues of the medial aspect of the right eye/nasal bridge area, the bullet sequentially perforated the medial aspect of the right globe, the right zygomatic bone, the medial aspect of the nasal bone, the basilar skull and anterior cranial fossa and the sella turcica (Fig. 5). The projectile continued through the medial aspect of the right temporal lobe of the brain, the pons (with complete transection), the medial aspects of the left parietal lobe and occipital lobe of the brain, and the left occipital skull (with external beveling). The subcutaneous tissues and skin of the left occipital scalp were perforated, where there was a 1.5 by .75 inch stellate gunshot exit wound, 4.5 inches below the top of the head and .5 inches to the left of midline. Associated injuries included extensive basilar skull fractures, subarachnoid hemorrhage, subdural hemorrhage, and hemorrhage along the wound track. In addition, there was blood within the lungs bilaterally, and blood exuding from the ears bilaterally. There was evidence of soot on the external beveling of the exit wound through the skull. However, the soot was not discernable on available photographs. Multiple small fragments of lead were recovered from along the wound path; however, a majority of the projectile exited the head. X-rays of the decedent were non-contributory.

Fig. 6 Photograph of Ruger Old Army Cap and Ball black powder percussion revolver used in presented case

The cause of death was a gunshot wound of the face/head. The manner of death was ruled as a homicide; utilizing the medical definition of "homicide" as "death at the hands of another individual" and not necessarily equating the term to any legal definition. The weapon used was a Ruger Old Army Cap & Ball black powder percussion revolver (Fig. 6) utilizing a .457 pure lead ball round.

The weapon in this case was sent for testing to the Indiana State Police Testing Laboratory. It was received loaded with one fired and five unfired size 11 percussion caps manufactured by CCI as well as five chambers loaded with propellant and .457 caliber ball rounds. The firearm was examined for functional defects and test fired for functionality only. Additional test firing for patterns and range would have been beneficial for educational and experiential purposes. However, they were deemed superfluous by the police and prosecutor's office and would have also exposed the firearms examiner to a potentially more dangerous test-firing compared to a "routine" test-firing, given the weapon/ammunition type. A functional defect was discovered consisting of the inability of the weapon's cylinder to rotate freely in the cylinder frame when the hammer is in the half-cocked position. The cylinder latch did not pivot sufficiently downward into its cutout in the frame to disengage the cylinder stop notches and allow the cylinder to rotate freely for loading. However, pulling the hammer slightly more to the rear of the half-cocked position allowed the latch to be lowered into its cutout, permitting free cylinder rotation. In addition, the trigger was able to be depressed in the half-cocked position causing the hammer to fall. However, in this laboratory test, this action failed to discharge the weapon. Trigger pull was approximately 16.3–17.0 lb with the hammer in the half-cocked position and 4.0–4.8 lb in single action. This is within the expected range for this weapon and comparable to the trigger pull of modern double- and single-action revolvers, respectively.

Test firing revealed that the weapon would only discharge by one of two means: (1) firing as designed in single

action by manually cocking the hammer fully to the rear until it stopped and the trigger being depressed and (2) with the hammer at rest on a loaded and capped chamber and the hammer struck by a hard object or dropped with the hammer impacting on a hard object; a known characteristic of this weapon [2].

Discussion

Though the sale of black powder weapons are often subject to less government regulation and monitoring, the relative ease of procuring these firearms has not contributed significantly to the homicide rates of countries such as the United States and Germany [1]. In fact, a review of the literature finds relatively few entries concerning deaths or injuries, accidental or intentional, from black powder weapons [1, 3–6]. Thus, the homicide case presented here is of interest to the forensic community for its rarity. However, it should also be noted that the autopsy findings of this case are also illustrative of characteristic wounds produced by black powder revolvers and rifles.

Black powder weapons, both antique and reproduction, are used for target shooting, hunting, historical research and reenactment. They are mostly manufactured outside of the United States and are available as rifles, shotguns, flintlock and percussion muskets, as well as the percussion revolver. Ammunition used in these weapons is quite varied, with calibers spanning .31–.75 and types ranging from round ball to Minie bullets [7]. In general, these weapons are muzzle loaders. That is, the projectile and usually the propellant charge are loaded from the forward, open end of the gun's barrel (i.e. the muzzle). The term "muzzle loading" is often used synonymously in the United States with the practice of hunting with modern, high performance black powder rifles.

The weapon used in this homicide was a Ruger Old Army Cap-and-Ball (or alternatively

"Cap-n-Ball" or "Cap-&-Ball") black powder revolver produced in the United States. This revolver is a muzzle loading, percussion revolver that does not fire conventional cartridges. Rather it is loaded from the front of the cylinder and is intended for use with black powder, percussion caps, and soft lead projectiles. Specifically, this revolver is designed to use a .457" diameter round ball or .454" conical bullet of pure lead [3]. Its operation is single-action. That is, the hammer must be cocked manually before firing the revolver. Having been manufactured from 1972 to 2008, this weapon is no longer in production [8].

The manufacturer stipulates that newer smokeless powder may not be used with this weapon. The operator's manual warns that harm to the weapon, user and bystanders may result. The manufacturer recommends a black powder with grain size of "FFFg." However, any size granulation from the largest "Fg" to smallest "FFFFg" may be used with replica black powder such as Pyrodex being an acceptable alternative [2]. Pyrodex is a firearm propellant produced by Hodgdon Powder Company, Inc. It is purported by the manufacturer to produce less smoke than traditional black powders as well as possessing less corrosive properties. It comes in granular and pellet forms and is a proprietary formulation containing charcoal, graphite, sulfur, potassium nitrate, sodium benzoate, dextrine, potassium perchlorate, wax and dicyandiamide [9, 10]. Interestingly, uncombusted dicyandiamide (DCDA) is a characteristic combustion product of Pyrodex that can be detected by TLC, HPLC, FTIR and colorimetric tests [10].

The manufacturer states that it is safe to use as much propellant as the chamber will hold providing there is room left for the bullet. However, accuracy will suffer at maximum loads. Therefore, it is recommended that with the use of a pure lead .457" diameter ball rounds, 20 grains of FFFg and filler (corn meal is suggested) the ball will seat approximately 1/16" below the chamber mouth and provide a good starting accuracy load [2]. Cap and Ball revolver data from Hodgdon Powder Company indicates the Ruger Old Army 45 caliber, loaded with a .457 round ball and 40 grains of Pyrodex P powder, has a velocity of 980 feet per second (fps). The lead round balls removed from the five loaded chambers of the cylinder from the Ruger Old Army submitted for laboratory examination exhibited an average weight of 143 grains [11].

As a comparison, the 357 Magnum introduced by Smith & Wesson in 1935 had a standard loading of a 158 grains bullet with a muzzle velocity of 1,235 fps. Newer semijacketed loadings are generally 110, 128 and 158 grains with a muzzle velocity of 1,090–1,500 fps. Note that powder types and amounts used in magnum cartridges are extremely variable and do not lend themselves to a direct comparison with loads used in the Ruger Old Army 45 caliber [12].

Powder tattoos (stipple marks) are generated by undetonated gunpowder grains penetrating and/or abrading the skin during the firing of a weapon. They are punctate abrasions with or without associated burns. Injuries to the dermis produced from black powder weapons generally result in more extensive tattooing and deposition of soot than wounds produced by smokeless powders [6]. In the paper by Labowitz et al., the authors describe the characteristics and wounding effects of the Ruger Old Army Cap and Ball black powder percussion revolver in swine models. They noted that the main difference between the

wounds made by the black powder weapon and the modern cartridge-firing weapon, used as a control, was in the quantity, character and distribution of the powder marks on the skin. Specifically, there was a markedly increased density of powder marks from the black powder revolver compared to the control. Also, the authors found in their tests that the marks were coarser and larger than those from the modern weapon at firing ranges of 12 and 26 inches [13]. In keeping with these observations, extensive soot and powder stippling in a 6.0 inch by 4.5 inch distribution were noted at autopsy for the decedent in this case (Figs. 3a, b, 4). This is comparable to the reported distributions ranging from 3.9 inches to 7.3 inches at a firing range of 12 and 26 inches respectively [13]. Note that the cartridge-firing weapon produced powder distributions of 1.6 and .3 inches in diameter. However, the fine and relatively uniform appearance of the tattooing in this case (Fig. 4) has more in common with the appearance of true ball powder found in modern cartridge rounds than the coarse and uneven distribution described by Labowitz, et al., where 40 grains of FFFg powder was used or that of the large grain Fg powder commonly used in black powder cannons [6, 7, 10, 13].

In view of the initial police reports that the weapon had been loaded with black powder, the autopsy findings of fine, uniform tatooing raised the question of whether the suspect had loaded the weapon with a smaller FFFFg grain (generally reserved for musket rifles) and/or a larger powder load. However, evidence collected at the scene and results of the police laboratory testing revealed the use of Pyrodex P Powder in the suspect's weapon. The police laboratory report makes no mention of the amount of powder loaded in the remaining five unfired cylinders. Note that P (for "pistol") compares roughly to FFFg black-powder on a particle size basis. However, the particles are more spherical and uniform in size and than those of the jagged and oblong shaped black powder [10]. Considering the shape of Pyrodex P, the uniformity of tattooing in this case is not surprising.

The size, intensity and appearance of the soot pattern of any firearm, as well as the maximum range from which it will occur, depends on numerous factors. These factors include the angle of muzzle to the target, barrel length, weapon caliber, target material and state of the material. Also, and most significantly to this report, the type of weapon and propellant play a significant role [7]. Thus, the black powder weapon's larger amount of expelled soot and powder that can be deposited at a further distance are such that the range of fire estimates that forensic pathologists typically employ with cartridge firing handguns are not applicable. It is best that a test firing be performed to obtain a better estimate. Unfortunately in this case, a test firing was deemed unnecessary by investigating agencies.

For scene investigators and firearms examiners, particular care should be taken when confronted with a black powder firearm, especially when the firearm remains loaded, as in the case presented. The highly unstable nature of black powder, coupled with cartridge-less weapon designs that do not fully enclose the powder, lead to an inherent risk of accidental ignition or explosion that can include synchronous discharge. In addition to copious amounts of soot and unburned powder, significant amounts of flame and sparks are produced during discharge of a black powder weapon. This can ignite the powder in adjacent chambers causing a projectile to emerge from the cylinder. Note that no rifling will be present for this projectile coming off the side, however, shearing may occur and markings from the rammer may be present on the projectile that can be used in ballistics comparisons [7].

In the case presented here, the initial information at the scene suggested that true black powder was present in the loaded weapon, making it particularly dangerous. However, further investigation revealed the presence of Pyrodex, as previously described. Although safer than black powder, a certain amount of risk of accidental ignition remains with this black powder substitute. Handling of the weapon at the scene, transport of the weapon, and subsequent evaluation and unloading at the crime lab required great care. The inherent danger and complexity of unloading the Old Army Ball and Cap revolver has prompted the manufacturer to advise handlers of the weapon to fire all rounds rather than attempt unloading [2].

Manufacturer suggested unloading includes (1) Pointing the weapon in a safe direction. (2) Carefully lowering the hammer into a notch in the cylinder and then pulling the hammer back to the half-cock loading notch while keeping fingers away from the trigger. (3) Removal of percussion caps from all nipples. (4) Unscrewing the nipple from the chamber aligned with the cut-out on the right side of the frame. (5) Taking extra care to elevate the muzzle and pour all the powder from the rear of the cylinder into a storage container. (6) This is repeated for all remaining cylinders. (7) When all chambers are empty of powder, the cylinder may be removed. (8) The projectile is removed by placing some lubricating oil into each chamber and inserting a rod into the rear of the chamber. The rear of the rod is gently tapped until the projectile comes out of the front of the cylinder. This is repeated for the remaining cylinders. An alternative method involves removing the cylinder after the percussion caps have been removed and proceeding to nipple removal, powder dumping, etc. while working on the free cylinder [2].

Extensive damage caused by the projectile is seen in Fig. 4 including fractures to the anterior cranial fossa, basilar skull and left posterior occiput. Soot was found throughout the track of the projectile from the entrance

wound through the exit wound in the occiput. This belies not only the particulate nature of the black powder discharge but the close range at which this weapon was shot. Equivalent patterns of soot deposition found along projectile paths were reported in the three cases involving black powder percussion handguns described by Karger and Teige [3].

There is little information from the literature regarding the kinetics or "stopping power" of percussion revolvers. The stopping power of any handgun bullet is a function of its ability to disrupt bodily functions, not the diameter or weight or initial shape of the bullet. For example, the difference in the size of an entrance hole made by a .451-inches bullet compared to that made by a .355-inches bullet in elastic material like skin turns out to be largely irrelevant to stopping power. Therefore, it would be difficult to ascertain the stopping power of the weapon used in this case based upon its static physical qualities, prompting further investigation into this and other characteristics of these unique weapons.

In conclusion, the case presented is an example of a relatively uncommon homicide by black powder revolver utilizing Pyrodex propellant that is also illustrative of the extensive tattooing and soot deposition of the dermis typically seen in wounds produced by black powder weapons. In addition, the close proximity of the weapon during firing distributed soot and unburned black powder along the path of the projectile including powder within the exit wound. Such deposits are more extensive and are produced at much greater distances than are typically seen with conventional firearms. Understanding of these findings will aid the clinician as well as the forensic specialist in identifying the weapon responsible for these types of injuries. Parties interested in the testing of black powder weapons are cautioned to handle the weapons with extreme care. This is due to the unstable nature of the propellants used and the design of these weapons making unintended exposure of the propellant to muzzle flash and other ignition possible.

Key points

1. Deaths resulting from the use of black powder handguns are relatively uncommon compared to other firearms.
2. The size, intensity and appearance of the soot pattern of any firearm, as well as the maximum range from which it will occur, depends on numerous factors including the angle of muzzle to the target, barrel length, weapon caliber, target material and state of the material.

3. In order to estimate the range of fire in a given case, it is best to test fire the weapon at various ranges, using a similar ammunition configuration as utilized during the event.
4. Black powder weapons produce wounds with extensive tattooing and soot deposition.
5. The range of fire estimates that forensic pathologists typically employ with cartridge firing handguns are not applicable to black powder weapons due to the larger amounts of expelled soot and powder that can be deposited at further distances
6. The highly unstable nature of black powder, coupled with cartridge-less weapon designs, leads to an inherent risk of accidental ignition or explosion that can include synchronous discharge.

References

1. Hartwig S, Tsokos M, Byard R. Black powder handgun deaths remain an uncommon event. Am J Forensic Med Pathol. 2009;30:350–3.
2. Instruction Manual for Ruger Old Army "Cap & Ball" Black Powder Percussion Revolver. Sturm, Ruger & Co., Inc.; 2009:9–20.
3. Karger B, Teige K. Fatalities from black-powder percussion handguns. Forensic Sci Int. 1998;98:143–9.
4. Vila RI, Martin JV, Wetli CV, et al. Accidental death from a black-powder rifle breech plug. Am J Forensic Med Pathol. 1990;11:241–3.
5. Dehaan JD. Homicide with a black powder handgun. J Forensic Sci. 1983;28:486–91.
6. Hanke CW, Conner AC, Probst EL, et al. Blast tattoos resulting from black powder firearms. J Am Acad Dermatol. 1987;17:819–25.
7. Di Maio VJM. Gunshot wounds: practical aspects of firearms, ballistics and forensic techniques, 2nd ed. Boca Raton: CRC Press; 1999:30, 45–7, 74, 142–3.
8. Revolver instruction manuals and history webpage. Sturm, Ruger and Co., Inc. http://www.ruger.com/service/productHistory.html#. Accessed 12 December 2009.
9. Pyrodex Propellant Material Safety Data Sheet. http://www.pyrodex.com. Accessed 16 December 2009.
10. Haag CL. Black powder substitutes: their physical and chemical properties and performance. AFTE J. 2001;33:313–25.
11. Reloading Data Center. http://data.hodgdon.com/main_menu.asp. Accessed 05 June 2010.
12. Barnes FC. Cartridges of the World, 10th Ed. Iola, WI: Krause Publications; 2003, 276.
13. Labowitz DI, Menzies RC, Scroggie RJ. Characteristics and wounding effects of a blackpowder handgun. J Forensic Sci. 1981;26:288–301.

CASE REPORT

Erosive gastritis, Armanni-Ebstein phenomenon and diabetic ketoacidosis

Roger W. Byard · Chong Zhou

Abstract The Armanni-Ebstein phenomenon, which is found in the kidneys in diabetic ketoacidosis, has also been proposed as an independent diagnostic postmortem marker for hypothermia. A case is reported to demonstrate the possibility of a more complex inter-related etiology in certain instances. A 44-year-old man with a past history of hospital admission for hypothermia, alcoholism and insulin dependent diabetes mellitus was found dead at his home address. At autopsy there were prominent superficial erosive gastritis (Wischnewsky spots) in keeping with terminal hypothermia. In addition there was also marked cortical pallor of the kidneys due to subnuclear renal tubular epithelial vacuolization (Armanni-Ebstein phenomenon). Thus there was evidence for both hypothermia and Armanni-Ebstein phenomenon, suggesting a relationship. Subsequent biochemical testing of vitreous humor, however, demonstrated markedly elevated levels of glucose (36.5 mmol/l; $N = 3.6–6.0$ mmol/l), β-hydroxybutyrate (23.2 mmol/l; $N < 0.3$ mmol/l), and lactate (29.4 mmol/l; $N = 0.2–2.0$ mmol/l). Death was, therefore, due to diabetic ketoacidosis complicated by hypothermia. Diabetes mellitus has a known association with both hypothermia and Armanni-Ebstein phenomenon, thus, before renal tubular vacuolization can be taken as a marker of hypothermia in isolation, it is important to consider the possibility that in certain cases underlying diabetic ketoacidosis may be present.

R. W. Byard (✉) · C. Zhou
Discipline of Anatomy and Pathology, Level 3 Medical School
North Building, The University of Adelaide & Forensic Science,
Frome Road, Adelaide, SA 5005, Australia
e-mail: roger.byard@sa.gov.au

Introduction

Subnuclear vacuolization of renal tubular epithelium (Armanni-Ebstein phenonemon) is a microscopic marker of diabetic ketoacidosis that has been referred to as glycogen nephropathy, based on the belief that the accumulated intracellular material was glycogen due to increased amounts of filtered glucose [1]. There is now, however, evidence that the material may contain lipid [2]. Another association that has been reported with Armanni-Ebstein vacuolization is hypothermia, with assertions that it may be used as a diagnostic postmortem marker in individuals who have endured significantly low antemortem core temperatures [3, 4]. The following case is reported to demonstrate that the link between hypothermia and Armanni-Ebstein phenonemon may in some cases be through diabetic ketoacidosis.

Case report

A 44-year-old man was found dead at his home address sitting in a lounge chair. He had a past history of alcohol abuse with chronic pancreatitis and unstable insulin dependent diabetes mellitus necessitating numerous hospital admissions that were often precipitated by collapse from diabetic ketoacidosis. He had also been admitted to hospital 2 years before with hypothermia. There was no police record of the heating arrangements at his home

address and the minimum overnight temperature on the night of death was 16.7°.

At autopsy the major findings were of superficial erosive gastritis (Wischnewsky ulcers) (Fig. 1) and prominent cortical pallor of the kidneys (Fig. 2) which was shown on histology to be due to subnuclear renal tubular epithelial vacuolization, Armanni-Ebstein phenomenon (Fig. 3). There was also pancreatic fibrosis and calcification in keeping with the history of chronic pancreatitis. There was no extensor surface pigmentation. There were no other significant underlying organic diseases present that could have caused or contributed to death and there was no evidence of trauma. Biochemical testing of vitreous humor demonstrated markedly elevated levels of glucose (36.5 mmol/l; $N = 3.6–6.0$ mmol/l), β-hydroxybutyrate (23.2 mmol/l; $N < 0.3$ mmol/l), and lactate (29.4 mmol/l; $N = 0.2–2.0$ mmol/l). The vitreous sodium level was within the normal range (137 mmol/l). Toxicology revealed no alcohol or common prescription or non-prescription drugs. Death was, therefore, due to diabetic ketoacidosis complicated by hypothermia.

Discussion

The diagnosis of hypothermia is made when a body temperature falls below 35°C. It may be associated with aberrant behaviour such as paradoxical undressing due to thermoregulatory imbalance, or seeking out secretive locations in the so-called 'hide and die' syndrome [5, 6]. A common situation encountered in forensic practice involves an elderly reclusive individual who is incapacitated by organic illness or trauma and who is then exposed for some time to low environmental temperatures. Death

Fig. 2 A sectioned kidney opened to demonstrate marked cortical pallor with prominent corticomedullary demarcation due to Armanni-Ebstein phenomenon
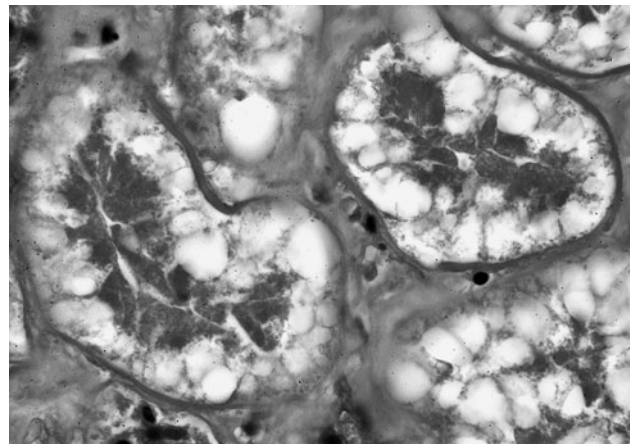
Fig. 3 Histologic section of the kidney revealing subnuclear vacuoles within renal tubular epithelial cells (Armanni-Ebstein phenomenon), discernable despite autolytic changes. (Hematoxyllin & eosin × 100)

occurs when electrolyte abnormalities, elevated catecholamine levels and myocardial ischemia cause lethal cardiac arrhythmias [3].

The pathological diagnosis of hypothermia is often difficult as antemortem core temperatures are usually not available and autopsy findings are relatively nonspecific. Features suggestive of hypothermia include reddish-brown discolouration of the skin over the elbows and knees, bright red lividity, pancreatic inflammation and hemorrhage, and erosive gastritis or Wischnewsky spots. While superficial erosive gastritis may result from terminal stress, the literature cites this finding as the most specific feature of hypothermia that can be seen histologically as superficial erosions with mucosal necrosis and acid hematin deposition [7].
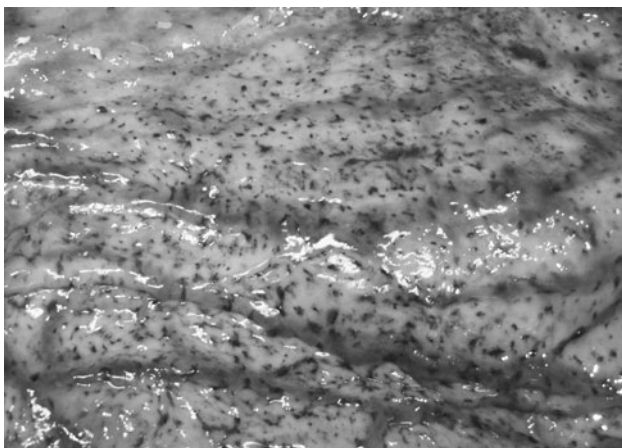

Fig. 1 A portion of stomach mucosa showing prominent superficial erosive gastritis (Wischnewsky spots) in a 44-year-old man indicating terminal hypothermia

While Armanni-Ebstein phenomenon has usually been taken as a feature of diabetic ketoacidosis, it has recently been suggested that it may also be a useful marker of hypothermia [4]. However, it is important to recognize that hypothermia itself may have a very close relationship with the metabolic derangements associated with diabetes mellitus. For example, in one series of patients admitted to hospital with severe hypothermia, close to 12% had underlying diabetic ketoacidosis [8]. Hypothermia may not only be caused by diabetes mellitus due to impaired thermoregulation, reduced endogenous heat production and peripheral vasodilation [9, 10], but it may also exacerbate diabetic ketoacidosis. For example, increased steroid and adrenalin secretion, reduced insulin release and diminished insulin activity have all been reported on exposure to low temperatures [11, 12]. These factors demonstrate that hypothermia and diabetic ketoacidosis may be quite intimately related and may reinforce the adverse effects of each other.

In the reported case significant tubular vacuolization was present, to such an extent that it was first identified macroscopically [13], and this was associated with Wischnewsky spots indicating hypothermia. Diabetic ketoacidosis was, however, subsequently identified biochemically by testing of vitreous humor for glucose, lactate and β-hydroxybutyrate. Thus, before renal tubular vacuolization can be taken as a marker of hypothermia in isolation, it is important to consider the possibility of underlying diabetic ketoacidosis, as in some cases these conditions may be inextricably linked.

Key points

1. Armanni-Ebstein phenomenon has been reported in the kidneys of individuals dying of hypothermia.
2. It is also known to occur with diabetic ketoacidosis.
3. Given that diabetic ketoacidosis may also lead to hypothermia, it is possible that renal tubular vacuolization in certain cases of hypothermia may be more involved with metabolic derangements associated with diabetes, rather than from the fall in body core temperature.

References

1. Kock KF, Vestergaard V. Armanni-Ebstein lesions of the kidney: diagnostic of death in diabetic coma? Forensic Sci Int. 1994;67: 169–74.
2. Thomsen JL, Kristensen IB, Ottosen PD. The histological demonstration of lipids in the proximal renal tubules of patients with diabetic coma. Forensic Sci Med Pathol. 2006;2:249–52.
3. Turk EE. Hypothermia. Forensic Sci Med Pathol 2010; [Epub ahead of print].
4. Preuß J, Dettmeyer R, Lignitz E, Madea B. Fatty degeneration in renal tubule epithelium in accidental hypothermia victims. Forensic Sci Int. 2004;141:131–5.
5. Rothschild MA. Lethal hypothermia: paradoxical undressing and hide and die syndrome can produce very obscure death scenes. In: Tsokos M, editor. Forensic pathology reviews, vol. 1. Totowa: Humana Press; 2004. p. 263–72.
6. Byard RW, Gilbert JD, Tsokos M. Forensic issues in cases of Diogenes syndrome. Am J Forensic Med Pathol. 2007;28: 177–81.
7. Madea B, Tsokos M, Preuß J. Death due to hypothermia: morphological findings, their pathogenesis and diagnostic value. In: Tsokos M, editor. Forensic pathology reviews, vol. 5. Totowa: Humana Press; 2008. p. 3–21.
8. Gale EAM, Tattersall RB. Hypothermia: a complication of diabetic ketoacidosis. Br Med J. 1978;2:1387–9.
9. Scott AR, MacDonald IA, Bennett T, Tattersall RB. Abnormal thermoregulation in diabetic autonomic neuropathy. Diabetes. 1988;37:961–8.
10. Ozawa Y, Maruyama H, Nakano S, Saruta T. An unconscious diabetic patient. Postgrad Med J. 1998;74:549–50.
11. Guerin JM, Meyer P, Segrestaa JM. Hypothermia in diabetic ketoacidosis. Diabetes Care. 1987;10:801–2.
12. Ritchie S, Waugh D. The pathology of Armanni-Ebstein diabetic nephropathy. Am J Pathol. 1957;33:1035–57.
13. Zhou C, Gilbert JD, Byard RW. Early diagnosis of Armanni-Ebstein phenomenon at autopsy. Forensic Sci Med Pathol. 2010; 6:133–4.

TECHNICAL REPORT

A survey of warning colours of pesticides

**Annette Thierauf · Wolfgang Weinmann ·
Volker Auwärter · Benedikt Vennemann ·
Michael Bohnert**

Abstract Pesticides are used to protect plants all over the world. Their increasing specificity has been due to utilization of differences in biochemical processes, and has been accompanied by lower human toxicity. Nevertheless cases of poisoning are still observed. While certain toxic substances are provided with characteristic dyes or pigments to facilitate easy identification, no overview of pesticide colors exists. The lack of available product information prompted us to explore the colors and dyes of pesticides registered in Germany, most of which are commercially available worldwide. A compilation of the colors and odors of 207 pesticide products is presented. While some of the substances can be identified by their physical characteristics, in other cases, the range of possibilities can be narrowed by their nature and color.

Keywords Forensic science · Pesticides ·
Warning colors · Dyes · Odor · Poisoning

Introduction

Pesticides are used all over the world, in large agricultural centers as well as in private households. They are easily available and procurable. Plant protecting products are defined by the US Environmental Protection Agency as agents that protect plants and plant products against animals, plants and micro-organisms (http://www.epa.gov/ pesticides). In a broader sense, substances that kill plants, regulate growth or inhibit germination are also counted among plant protecting agents.

The risk of human toxicity and the resulting forensic interest in these substances is especially related to agents used against animals. Agents used against other pests make use of the differences in metabolic pathways between humans and non-mammals resulting in a lower human toxicity [1].

Schmoldt divided insecticides into three groups: halogenated hydrocarbons, pyrethroids and inhibitors of acetylcholinesterase [2]. The former have been prohibited to a large extent and play only a minor role at the present time. The most known substance in this group is DDT (Dichloro-diphenyl-trichloroethane). The pyrethroids decelerate the closing of voltage-gated sodium channels of the nervous system of insects and are highly selective for this class [3]. In humans, toxic effects are seen only after intravenous injection and long-lasting and intensive inhalation [4]. There are mainly two classes of acetylcholinesterase inhibitors: organophosphates and carbamates. Whereas inhibition by organophosphates is of an irreversible nature, carbamates cause a reversible enzyme inhibition [2]. Due to their lipophilic character the inhibitors are well absorbed enterally, and percutaneous absorption is moderate [5]. The inhibition of acetylcholinesterase by phosphorylation of serine in the active centre of the enzyme in the synaptic gap inhibits the inactivation of acetylcholine [2]. Therefore, parasympathomimetic effects determine the clinical response, and poisoning is frequently fatal. Symptoms depend on the degree of intoxication: First miosis, lacrimation, hypersecretion of the mucous membranes, hypersalivation, nausea, emesis and diarrhoea occur; critical stages are accompanied by dyspnea, agitation, convulsions, muscular disorders, unconsciousness and respiratory

A. Thierauf (✉) · W. Weinmann · V. Auwärter ·
B. Vennemann · M. Bohnert
Institute of Forensic Medicine, Freiburg University Medical
Centre, Albertstrasse 9, 79104 Freiburg, Germany
e-mail: Annette.Thierauf@uniklinik-freiburg.de

Table 1 Form, colors and odors of products of solid consistency

Form	Color	Trade name	Active ingredient	Odor
Granulate	White/whitish	Dantop	Clothianidin	
	Beige	Provado 5 WG	Imidacloprid	
		Provado 5 WG Universalspritzmittel	Imidacloprid	
	Yellow to brownish	Nemathorin 10G	Fosthiazate	
		Plenum 50 WG	Pymetrozine	
	Brown	Confidor WG 70	Imidacloprid	
		Asulfa Jet	Sulphur	
		Steward	Indoxacarb	Wood-like
		Sufran Jet	Sulphur	
		Thiovit Jet	Sulphur	
	Dun	Kumulus WG	Sulphur	
		Insegar	Fenoxycarb	
		Compo-Mehltau-frei Kumulus WG	Sulphur	
		Netzschwefel WG	Sulphur	
	Grey	Schädlingsfrei Careo Combi-Granulat	Acetamiprid	Sharp
		Lizetan Combigranulat	Imidacloprid	
	Green–blue	Pirimor Granulat	Pirimicarb	
	Blue	COMPO Schneckenkorn	Metaldehyde	Aromatic
		Glanzit Schneckenkorn	Metaldehyde	Aromatic
		FCS Schneckenkorn	Metaldehyde	Aromatic
		Delu Schneckenkorn	Metaldehyde	Aromatic
		Detia Schneckenkorn	Metaldehyde	Aromatic
		Ferramol Schneckenkorn	Fe-III-phosphate	
		Metarex	Metaldehyde	
		Schneckenkorn Spiess-Urania	Metaldehyde	
		Clartex blau	Metaldehyde	
		Pro Limax	Metaldehyde	Aromatic
Crystalline	Red	Garten-Loxiran	Chlorpyrifos	
Lentil-like	Blue	Delicia Schnecken-Linsen	Metaldehyde	
		Etisso Schnecken-Linsen Power-Packs	Metaldehyde	
Pressed	Grey	Detia Pflanzenschutz-Stäbchen	Dimethoate	
		Gabi-Combi-Pflanzenschutz-Düngestäbchen	Dimethoate	
	Grey-green	Detia-Gas-Ex B	Aluminiumphosphide	Garlic-like
		Detia-Gas-Ex P	Aluminiumphosphide	Garlic-like
		Detia-Gas-Ex T	Aluminiumphosphide	Garlic-like
		Detia-Magphos	Magnesiumphosphide	Garlic-like
		Phostoxin Pellets	Aluminiumphosphide	Garlic-like
		Phostoxin Tabletten	Aluminiumphosphide	Garlic-like
		Delicia-Gastoxin-Pellets	Aluminiumphosphide	Garlic-like
		Delicia-Gastoxin-Tabletten	Aluminiumphosphide	Garlic-like
Powder	Whitish	Ordoval	Hexythiazox	
	Beige	Masai	Tebufenpyrade	
		Insekten-Streumittel Nexion Neu	Chlorpyrifos	
	Yellow	Netz-Schwefelit WG	Sulphur	Sharp
	Brown	Cruiser 70 WS	Thiamethoxam	
	Blue	Mospilan	Acetamiprid	
	Grey	Degesch-Magtoxin Granular	Magnesiumphosphide	Garlic-like

Table 1 continued

Form	Color	Trade name	Active ingredient	Odor
Sticks	White	Etisso Blattlaus-Sticks	Dimethoate	
		Etisso Combi-Sticks	Dimethoate	
		Combi-Sticks Insektan	Dimethoate	
		Schädlings-Sticks Insektan	Dimethoate	
	Yellow	Compo Axoris Insekten-frei Quick-Granulat	Thiamethoxam	
		Compo Axoris Insekten-frei Quick-Sticks	Thiamethoxam	
	Grey	Lizetan Combistäbchen	Imidacloprid	
		Combi-Stäbchen Hortex-D	Dimethoate	
		Schädlingsfrei Careo Combi-Stäbchen	Acetamiprid	Sharp
	Grey-brown	Bi 58 Combi-Stäbchen	Dimethoate	
		Compo Bi 58 Combi-Stäbchen	Dimethoate	
	Brown	Pflanzenschutz-Zäpfchen	Dimethoate	
Unspecific	Whitish	Dimilin 80 WG	Diflubenzuron	
	Grey-green	Degesch-Magtoxin Tabletten	Magnesiumphosphide	Garlic-like
	Blue	Mesurol Schneckenkorn	Methiocarb	
		Karate WG forst	Lambda-Cyhalothrin	
		Trafo WG	Lambda-Cyhalothrin	
	Brown	Dr. Stähler Tandem-Stäbchen plus	Dimethoate	

Missing indication of odor stands for uncharacteristic

paralysis [2]. Recently developed insecticides like imidacloprid or tebufenozide show a high specificity for insects and are barely toxic for humans; nevertheless, fatal cases have, however, been reported for imidacloprid [6, 7].

It is well recognized that toxic substances are frequently provided with characteristic dyes or pigments, such as blue colored paraquat and parathion. The use of warning colors is not a recent new occurrence, even at the end of the 19th century, leach that was used as a detergent was supplemented with ultramarine [8]. However, our enquiry into pesticides in the scientific literature, safety data sheets, and manufacturers' and other internet sites did not reveal an overview of commercial substances and their colors and this has prompted us to explore the colors and dyes of pesticides that are registered and in use in Germany.

For descriptions of colors (dyes, pigments) standardized tables or normalized color systems can be used. Color tables are based on different standardized systems, for example. BS381C, BS5252, RAL840 h and Pantone 1000 can easily be found on the internet. It must be recognized that variations of visible color depend on the quality of the monitor TFT (thin film transistor) display. However, these standardized systems can be used for the description of colors. Another method is to use standardized systems such as the CIEL*a*b* color system, which has already been applied for forensic purposes [9–12]. The CIEL*a*b*

system is an objective method to determine the brightness, the hue and the saturation of a color.

Materials and methods

The safety data sheets of the substances that are registered in Germany were collected and the active ingredients, the color, the form and the odor were compiled. This survey includes insecticides, molluscicides, nematicides and miticides. Rodenticides and avidicides were not dealt with. In Germany, according to the Federal Office of Consumer Protection and Food Safety, the number of registered substances in these categories was 299 in September 2007 (www.bvl.bund.de). Mainly due to multiple citations and because of the non-availability of some safety data sheets our compilation includes 207 trade products.

In five pesticide preparations color measurements were performed with a diode array spectrophotometer MCS 400 (Carl-Zeiss-Jena GmbH, Jena, Germany) with a halogen bulb as the light source (standard illuminant D65). The measuring head allowed recording of the directed surface reflection of a 5 mm wide measuring spot (measuring geometry 45°/45°). Compressed barium sulphate was used as a white standard according to DIN 5033. The measurements were controlled and evaluated with the help of a personal computer. The software (MCSCol 2.11,

Table 2 Colors and odors of liquid products

Color	Trade name	Active ingredient	Odor
White	Pflanzenspray Hortex Neu	Pyrethrin	
	Schädlingsfrei Spray	Pyrethrin	
	Substral Pflanzenspray	Pyrethrin	
	Bayer Garten Gießmittel gegen Schädlinge	Thiaclopride	
	Bayer Garten Kombi-Schädlingsfrei	Thiaclopride	
	Alverde	Metaflumizone	Aromatic
	Fastac Forst	Alpha-Cypermethrin	
	Compo Austrieb-Spritzmittel	Mineral oil	
	Nomolt	Teflubenzuron	
	Mimic	Tebufenozide	Mouldy
	Promanal AF Neu Schild- und Wolllausfrei	Mineral oil	
	Promanal Neu	Mineral oil	
	Promanal Neu Schild- und Wolllausfrei	Mineral oil	
	Austrieb-Spritzmittel Weißöl	Mineral oil	
	CEL 265 43 AE	Acetamiprid	
	Celaflor Austriebs-Spritzmittel	Rape oil	
	Celaflor Blattlausfrei	Rape oil	
	Celaflor Schildlausfrei	Rape oil	
	Schädlingsfrei Careo Konzentrat	Acetamiprid	
	Schädlingsfrei Careo	Acetamiprid	
	Schädlingsfrei Careo Rosenspray	Acetamiprid	
	Schädlingsfrei Careo Spray	Acetamiprid	
	Schädlingsfrei Hortex	Rape oil	
	Chrysal Pflanzenspray	Pyrethrin	
	Micula	Rape oil	
	Austrieb-Spritzmittel Eftol-Öl	Mineral oil	
	Para Sommer	Mineral oil	
	Para Sommer S	Mineral oil	
	Applaud	Buprofezine	
	Force 20 CS	Tefluthrin	
	Biscaya	Thiaclopride	
	Chinook	Beta-Cyfluthrin + Imidacloprid	
	Elado	Beta-Cyfluthrin + Clothianidine	
	Janus	Beta-Cyfluthrin + Clothianidine	
	Poncho Beta	Beta-Cyfluthrin + Clothianidine	
	Kiron	Fenpyroximate	
	Fastac SC Super Contact	Alpha-Cypermethrin	
	Bayer Garten Oliocin Austriebsspritzmittel	Mineral oil	
Whitish	Envidor	Spirodiclofen	
	Raptol AF Rosen-Schädlingsfrei	Pyrethrin + Rape oil	
	Pflanzenspray Hortex N	Pyrethrin + Rape oil	
	Spruzit AF Schädlingsfrei	Pyrethrin + Rape oil	
Beige	Calypso	Thiaclopride	
	Karate mit Zeon Technologie	Lambda-Cyhalothrine	Aromatic
	Contur plus	Beta-Cyfluthrin	
	Magister 200 SC	Fenazaquine	
	Cruiser 600 FS	Thiamethoxam	
	Magister 200 SC	Fenazaquine	

Table 2 continued

Color	Trade name	Active ingredient	Odor
Yellow	Aco.sol PY-Z	Pyrethrin	
	Sumicidin Alpha EC	Esfenvalerate	
	Decis flüssig	Deltamethrine	Aromatic
	Bayer Garten Obst- und Gemüse-Schädlingsfrei	Pyrethrin + Rape oil	
	Compo Schädlings-frei plus	Pyrethrin + Rape oil	
	Bulldock	Beta-Cyfluthrin + Imidacloprid	Aromatic
	Neudosan Neu	Potassic placer	Alcoholic
	Neudosan Neu Blattlausfrei	Potassic placer	Alcoholic
	Promanal Neu Austriebspritzmittel	Mineral oil	
	Spruzit Neu	Pyrethrin + Rape oil	
	Spruzit Käfer-&Raupenfrei	Pyrethrin + Rape oil	
	Spruzit Käferfrei	Pyrethrin + Rape oil	
	Spruzit Schädlingsfrei	Pyrethrin + Rape oil	
	Schädlingsfrei Parexan Plus	Pyrethrin + Rape oil	
	Milbeknock	Milbemectine	Aromatic
	Rogor 40 L	Dimethoat	Mercaptane-like
	Rogor 40 LC	Dimethoat	
	Schädlingsfrei Eftol	Pyrethrin + Rape oil	
	Kanemite SC	Acequinocyl	
	Pyreth Natur-Insektizid	Pyrethrin + Rape oil	
	Promanal Austriebsspritzmittel	Rape oil	
	Kanemite SC	Acequinocyl	
Yellowish	Neudosan AF Neu Blattlausfrei	Potassic placer	
	Raptol Schädlingsspray	Pyrethrin + Rape oil	Aromatic
	Vertimec	Abamectin	Aromatic
	Celaflor Schädlingsfrei	Rape oil	
	Schädlingsfrei Naturen	Rape oil	
	Substral Schädlingsfrei	Rape oil	
	Micula	Rape oil	
	Appeal	Cyfluthrin	
Apricot-coloured	Danadim Progress	Dimethoat	
Pink	Apollo	Clofentezine	
Red	Monceren G	Pencycuron + Imidacloprid	
	Poncho	Clothianidine	
	Cruiser 350 FS	Thiamethoxam	
	Gaucho 600 FS	Imidacloprid	
	Manta Plus	Fuberidazole + Imazalil + Triadimenol + Imidacloprid	
	Mesurol flüssig	Methiocarb	
	Smaragd	Clothianidine	
Blue	Perfekthion Insektenvernichter	Dimethoat	Malodorous
	Bi 58	Dimethoat	Malodorous
	Perfekthion	Dimethoat	Malodorous
	Tamaron	Methamidophos	
	Insekten Spritzmittel Roxion D	Dimethoat	Malodorous
	Insekten-Spritzmittel Roxion	Dimethoat	Malodorous
	Cruiser osr	Fludixonil + Metalaxyl-M + Thiamethoxam	

Table 2 continued

Color	Trade name	Active ingredient	Odor
Brown	Naturen Schädlingsfrei Neem	Azadirachtin (Neem)	
	NeemAzal-T/S	Azadirachtin (Neem)	
	Actellic 50	Pirimiphos-methyl	Aromatic
	Fury 10 EW	Zeta-Cypermethrin	Sharp
Brownish	SpinTor	Spinosad	
	Conserve	Spinosad	
	Runner	Methoxyfenozide	
	Schädlingsfrei Neem	Azadirachtin (Neem)	
Colourless	Bayer Garten Spinnmilbenfrei	Acequinocyl	
	Bayer Garten Spinnmilbenspray	Methiocarb + Imidacloprid	
	Lizetan Plus Zierpflanzenspray	Methiocarb + Imidacloprid	
	Provado Gartenspray	Methiocarb + Imidacloprid	
	Bi 58 Spray	Dimethoat	Acetone-like
	Compo Zierpflanzen-Spray Bi 58	Dimethoat	Acetone-like
	Etisso Blattlaus-Spray	Pyrethrin	
	Spruzit Zimmerpflanzenspray	Pyrethrin	
	Spruzit Gartenspray	Pyrethrin	
	Gartenspray Hortex	Pyrethrin	
	Bio-Insektenfrei Gartenspray	Pyrethrin	
	Blattlaus-frei Spiess-Urania	Dimethoat	Acetone-like
	Blattlaus-Spray Dimeton	Dimethoat	Acetone-like
	Zierpflanzenspray Pyreth	Pyrethrin	

Missing indication of odor stands for uncharacteristic

Carl-Zeiss-Jena GmbH, Germany) automatically calculated the color measures CIE-L*a*b* from the spectral reflectance curves in the visible light spectrum.

Results

With the aid of the safety data sheets available, the colors and odors of the substances were sorted. These products contain 55 different active ingredients. As a result of multiple combinations, lack of human toxicity of single active ingredients did not lead to their exclusion from the compilation. The preparations had 17 different colors.

According to German and European regulations, admixed additives have to be specified under certain circumstances only, therefore, detailed chemical information could not be gained from the safety data sheets, neither for the dyes nor for the odors. Furthermore, the description of the perceptible characteristics has little detail, so that the subdivision in shades of colors is limited (Tables 1, 2).

The information on the odor of a pesticide preparation given in the respective safety data sheet of most substances is "nonspecific", and in our compilation of products (Tables 1, 2) information about the odor is only provided

Table 3 Calculated CIEL*a*b color measures

	L	a	b
Pirimor granulat	4.28	−3.38	−1.3
Technoate	1.53	6.93	−16.03
Hostaquide	0.98	0.19	0.61
Confirm	88.26	0.54	9.29
Mesurol	37.98	34.23	12.78

when it was characteristic. Individual differences in the perception of odors also has to be taken into account.

The results of the color measurements are shown in Table 3.

Discussion

Accidental and suicidal intoxications are a frequent occurrence, and due to their ready availability pesticides are still among the most often ingested toxic substances. In many cases of intoxication, the symptoms are nonspecific and reflect underlying pathophysiological mechanisms, e.g. inhibition of acetylcholinesterase. On the basis

of the clinical symptoms, the specific toxic agent can hardly be identified. Therefore, deductions based on the perceptible characteristics of a toxic agent are of particular interest and possible benefit. The rapid identification of an ingested substance by its color and odor could significantly reduce the effort put into diagnostic testing and thereby save time not only in post-mortem toxicology, but also in the acute poisoning of living patients.

Our survey is limited to products that are available on the German market, but an internet search revealed that to a great extent these products are traded internationally—mostly under the same or a similar product designation.

Products are of liquid and solid consistency. Preparations of solid consistency can be identified more easily than liquids, although reliable identification of a specific product on the basis of its characteristic is often only partly successful. The range of possible products can clearly be narrowed by their nature and color. For liquid preparations the type of the product can only to some extent be deduced from the color and the odor.

For accurate color identification we suggest the use of remission spectrometry as well as the use of standardized color models and color tables that are available on the internet.

Key points

1. Even modern pesticides carry an inherent risk of human toxicity.
2. Toxic substances are frequently provided with characteristic warning colors.
3. A register of the colors of commercial pesticides could not be found.
4. The safety data sheets of insecticides, molluscicides, nematicides and miticides were assembled and the active ingredients, colors, forms and odors were compiled.
5. Some of the substances can be identified by their physical characteristics, for other products the number of possible preparations can be reduced by examining their color and odor.

References

1. Narahashi T, Zhao X, Ikeda T, Nagata K, Yeh JZ. Differential actions of insecticides on target sites: basis for selective toxicity. Hum Exp Toxicol. 2007;26(4):361–6.
2. Schmoldt A. Schädlingsbekämpfungsmittel gegen tierische Schädlinge. In: Madea B, Brinkmann B, editors. Handbuch gerichtliche Medizin 2. Berlin, Heidelberg: Springer-Verlag; 2003. p. 357–68.
3. Bradberry SM, Cage SA, Proudfoot AT, Vale JA. Poisoning due to pyrethroids. Toxicol Rev. 2005;24(2):93–106.
4. Wax PM, Hoffman RS, Goldfrank LR. Fatality associated with inhalation of a pyrethrin inseciticide. Vet Hum Toxicol. 1991;33:363.
5. Garfitt SJ, Jones K, Mason HJ, Cocker J. Oral and dermal exposure to propetamphos: a human volunteer study. Toxicol Lett. 2002;134(1–3):115–8.
6. Proenca P, Teixeira H, Castanheira F, Pinheiro J, Monsanto PV, Marques EP, et al. Two fatal intoxication cases with imidacloprid: LC/MS analysis. Forensic Sci Int. 2005;153(1):75–80.
7. Shadnia S, Moghaddam HH. Fatal intoxication with imidacloprid insecticide. Am J Emerg Med. 2008;26(5):634.e1–4.
8. Ritter von Hofmann E. Atlas der Gerichtlichen Medizin. München: J.F. Lehmann; 1898.
9. Bohnert M, Vogt S, Weinmann W. Farbmetrische Untersuchungen der menschlichen Kopfhaare. Rechtsmedizin. 1998;8:207–11.
10. Bohnert M, Weinmann W, Pollak S. Spectrophotometric evaluation of postmortem lividity. Forensic Sci Int. 1999;99(2):149–58.
11. Bohnert M, Werp J. Die Anwendung farbmetrischer Meßmethoden zur optischen Beurteilung von weißlichen Pulver-Proben. Rechtsmedizin. 1999;9:218–21.
12. Bohnert M, Baumgartner R, Pollak S. Spectrophotometric evaluation of the color of intra- und subcutaneous bruises. Int J Legal Med. 2000;113(6):343–8.

CONTINUING MEDICAL EDUCATION REVIEW

Postmortem toxicology

Gisela Skopp

Abstract Results from toxicological analyses in death investigations are used to determine whether foreign substances were a cause of death, whether they contributed to death, or whether they caused impairment. Drug concentrations are likely to change during pre-terminal stages due to altered pharmacokinetics, to treatment during resuscitation or in the intensive care unit, to concomitant illness or to the presence of drug tolerance. The potential for postmortem changes must be considered in all but a few drugs. Formation of new entities as well as degradation of drugs may occur, especially in putrefied corpses; in addition, body fluids and tissues may be severely affected by autolysis and putrefaction. Specimens should be selected based on individual case history and on their availability. Analytical procedures should be performed in accordance with a proper quality assurance program for toxicological investigations. Problems are most likely to occur during the isolation and identification of a drug. Interpretation of analytical results is often limited by the inadequate information provided in a particular case.

Keywords Antemortem factors · Changes during the postmortem interval · Putrefaction · Autolysis · Drug redistribution · Selection of samples · Specimen collection · Analysis

Introduction

In many unnatural, sudden, violent or unexpected deaths the investigator often needs evidence as to whether alcohol, or illegal or prescription drugs may have caused, or are a contributing factor in the death [1, 2]. The forensic toxicologist will usually employ a 2-stage testing following selection and collection of appropriate specimens at autopsy. First, a screening test will be performed to establish whether there are any components within the sample that are not normally present. After confirmatory testing, the quantity of a foreign substance and/or its major metabolite(s) is determined, preferably from femoral venous blood and a further specimen. Quantitation of a drug is necessary to state whether its amount is sufficient to cause, prevent or be directly involved in the death [3]. Guidelines and a quality assurance program can assist in the selection and collection of specimens—as far as available—as well as in storage, transport, processing and analysis. However, the interpretation of analytical results remains the most challenging task in forensic toxicology. It is unique and fundamentally different from the situations encountered in clinical toxicology. There is evidence that substantial changes can occur in blood drug concentrations during the interval between the agonal phases of death and autopsy, mainly due to drug degradation, neo-formation or artefactual formation and postmortem redistribution [2, 4]. Interpretation may become still more difficult in decomposed or embalmed cases. It is essential to be aware that many of these changes will not be identifiable by postmortem sampling and toxicological analysis.

Antemortem factors

Basic pharmacokinetic concepts provide an estimate on the quantitative relationship between administered doses of a drug and the observed plasma or blood concentrations in a living individual. The field of pharmacokinetics is

G. Skopp (✉)
Institute of Legal Medicine, University Hospital,
Voss-Str. 2, 69115 Heidelberg, Germany
e-mail: gisela.skopp@med.uni-heidelberg.de

concerned with the liberation of a drug from its dosage form, absorption, distribution, metabolism and excretion (LADME processes). These processes, in addition to the dose, determine the concentration of drug at its active site. Pharmacokinetics assumes that a relationship exists between the concentration of a drug in an accessible site such as blood and the pharmacological or toxic response. Factors which affect the concentration-time profile of a drug are summarized in Table 1 [3, 5].

While arterio-venous differences following alcohol consumption are well documented, studies on arterio-venous differences in drug concentrations during lifetime are rare. For example, during the absorption and distribution phase, arterial plasma concentrations of amitriptyline are up to four times higher than venous concentrations. Up to 10 fold higher concentrations in arterial blood compared to venous blood were observed for diacetylmorphine and 6-acetylmorphine, whereas morphine glucuronides did not exhibit such arterio-venous differences [2].

Ethanol is commonly detected in medicolegal investigations. Many drugs interact with ethanol, commonly present in postmortem specimens, thereby altering the mechanism or effect of the alcohol and the drug involved. Ethanol is a central nervous system depressant and a similar effect is found with other hypnotic or narcotic drugs [3, 6]. Interaction may also occur through the induction of CYP2E1—a member of the cytochrome P450 family with high catalytic activity towards ethanol.

There are 2 types of drug-drug-interactions: pharmacodynamic and pharmacokinetic. Pharmacodynamic interactions take place at receptor sites and occur between drugs with similar or opposing therapeutic or adverse effects. Pharmacokinetic interactions consist of changes in the absorption, distribution or excretion, or in the quantity of drug that reaches its site of action. Most pharmacokinetic interactions occur at the metabolic level and generally result from enzyme inhibition or induction. An overview of drug-drug-interactions is available from the Drug Interaction Database [7].

Table 1 Factors affecting the concentration–time profile of xenobiotics

Dosage form, clandestine manufacturing process

Dose, route and frequency of drug administration, development of tolerance

Non-linear pharmacokinetics, e.g. acetylsalicylic acid, methylenedioxymethamphetamine

Time interval between drug administration and death and between death and collection of samples for analysis

Age, sex, ethnicity, genetic disposition

Weight, physical activity, nutritional state, general condition, disease

Nutritional ingredients, smoking, concurrent use of other drugs or alcohol

Far less is known about drug-nutrient interactions or interactions where active herbal constituents are involved. For example, grape fruit juice can inhibit the activity of CYP3A4 in the liver and the intestine and may elevate blood concentrations of drugs that are substrates of CYP3A4. A number of clinically significant interactions of St. John's wort have been identified with prescription drugs, resulting in a decrease in the concentration or effect, most probably due to induction of cytochrome P450 enzymes and the drug transporter *P*-glycoprotein [2, 3].

Pharmacokinetics during the pre-terminal phase are likely to be very different from that in study subjects or patients, due to a decrease in cardiac output and blood supply, low blood pressure, impaired ventilation, acidosis, dehydration, acute overdose and disease effects. Disease affects various organ systems and also the way drugs are absorbed, distributed, metabolized and excreted. Cardiovascular disease can substantially affect drug transportation to eliminating organs such as the kidneys and the liver. Renal diseases directly affect drug excretion, and hepatic diseases affect drug metabolism. For example, sepsis may induce a decrease in hepatic metabolism. Trauma and burns not only reduce the clearance of morphine, but also its volume of distribution. Also, volume distribution of drugs may be significantly reduced in patients with congestive heart failure [6, 8].

Disappearance of the drug may occur during lifetime in some cases. For example, paracetamol causes delayed hepatic toxicity that can be fatal, but by the time death occurs, the drug may not be detectable in the blood. Paraquat causes pulmonary fibrosis, and sometimes a slow death several weeks after ingestion [9].

Information on treatment and therapy during resuscitation or hospitalization should be provided. For example, even without restoration of the heart action during resuscitation, high concentrations of lidocaine may be present in the left side of the heart as intubation-related lidocaine may be absorbed by the trachea during cardiac massage. Interpretative problems involving alcohol and drug findings may also arise from lengthy treatment with intravenous fluids, from devices which automatically deliver medication by the parenteral route, or from transdermal patches that have been left on the body [10]. All these factors may affect drug concentrations in the body after death. However, further unique aspects of postmortem changes will be discussed below.

Changes occurring after death

Postmortem redistribution

In 1960, Curry and Sunshine reported on large differences in the amounts of barbiturates in blood obtained from

different sampling sites. Differences in drug concentrations in postmortem samples collected from different anatomical sites have been observed for numerous drugs including imipramine, diphenhydramine, codeine, methadone, doxepin, clomipramine, amitriptyline, cimetidine, cocaine, digoxin, zopiclone and methylendioxymethamphetamine. From a few studies comparing ante- and postmortem drug levels in blood it is also evident, that postmortem drug concentrations do not necessarily reflect concentrations at the time of death. For example, a 3.9 and 2.6-fold increase has been noted for amitriptyline and methadone, respectively, in postmortem blood [11, 12]. Generally, drugs with wide concentration ratios in ante- and postmortem blood also tend to have wide central/peripheral concentration ratios in postmortem specimens. Nevertheless, attempts to estimate antemortem concentrations from postmortem measurements are prone to considerable error [13].

All mechanisms and processes causing artefactual increases or decreases in drug concentration during the postmortem period can be included under the generic term of postmortem redistribution. Postmortem changes are site and time dependent. Potential factors that govern postmortem redistribution are summarized in Table 2 [2, 5, 13].

It appears that lipophilic drugs that have an apparent volume of distribution >3 L/kg and exhibit a central/peripheral blood concentration ratios >1 are candidates for postmortem redistribution (Table 3) [2, 11, 13].

Site dependent differences can arise from incomplete distribution of a drug at the time of death, release from major binding sites and/or passive diffusion through blood vessels or from the lumen of a body cavity into surrounding organs. Vascular pathways may depend on the blood remaining fluid after death. Organs such as the intestines, stomach, liver, lungs and myocardium are major sources of postmortem redistribution. Pleural and peritoneal fluids are also regarded as a route for drug exchanges between the lungs and the liver.

Redistribution from the lungs is more likely than from the stomach contents due to the large surface of the alveoli, the thin cell membranes and high vascularisation. Diffusion of ethanol from the stomach into femoral venous blood does not pose a problem. However, an investigation on postmortem diffusion from gastric residues in a human cadaver model using amitriptyline, paracetamol and lithium carbonate revealed high concentrations in the lungs as well as in the liver, whereas diffusion into gallbladder bile, cardiac and aortic blood was less pronounced. Redistribution from drug molecules sequestered in the liver may occur via hepatic vessels, or directly to adjacent organs such as the gall bladder or the stomach. Liver lobes may contain variable drug concentrations, and the left liver lobe being in close contact with the stomach will be more involved in postmortem redistribution. If a drug is also heavily concentrated in gastric contents it may be difficult to correctly determine the source of hepatic concentrations postmortem [5, 14].

Often, drug levels are higher in heart blood than in femoral venous blood. Substantial differences may be

Table 2 Major factors influencing postmortem redistribution of drugs

Physico-chemical and pharmaco-kinetic properties of the drug	Size, shape, charge, pKa-value, partition coefficient, apparent volume of distribution, binding to proteins, blood cells and/or tissues, residual enzyme activity during the early postmortem time period
Environmental conditions	Initial concentration, pH-value, orientation of solute flux, temperature, time, blood coagulation and hypostasis, blood movement due to fluidity changes and pressure, position of the corpse, lysosomal enzyme activities, bacterial invasion

Table 3 Drugs that are liable to postmortem redistribution

Drug	Octanol/water partition coefficient	Apparent volume of distribution (L/kg)	Concentration ratio heart/peripheral blood
Amitriptyline	4.94	ca. 15	3.1
Amphetamine	1.80	3–4	2.0
Clozapine	3.23	2–7	2.8
Cocaine	2.30	1–3	1.5–2.3
Diphenhydramine	3.30	4.5–8.0	2.3
Doxepin	2.40	20–24	5.5
Fluoxetine	4.05	ca. 27	2.9
Haloperidol	3.23	10–30	3.6
Midazolam	4.30	0.5–2.0	4.0
Trimipramine	5.43	20–50	1.6

noted for drugs such as calcium channel blockers or cardiac glycosides which are strongly bound to cardiac tissue. The lungs, the liver or gastric contents may serve as further drug sources [2, 11].

Temporal changes of drug concentrations have been studied in animal models showing that the most important quantitative changes occur very rapidly during the first 24 h [2]. A few case reports have determined that there is little evidence of time dependent variability, which may be due to delayed sampling [14].

Postmortem changes of blood

Decomposition of a corpse involves the processes of autolysis and putrefaction, which also effect the composition and integrity of tissues and fluids, and thus drug analysis. As blood is the specimen of choice for detecting, quantifying and interpreting drug concentrations, a more detailed review of postmortem changes in blood will be given.

In postmortem drug analyses whole blood is used, as separation of red blood cells from serum is usually not possible. Drug concentrations provided in literature are determined from serum or plasma which is traditionally used in clinical settings. Tables of drug levels determined from plasma or serum previously reported in therapeutic or toxic conditions can serve as a reference point. But only after weighing all possible influences and—if available—referring to postmortem values established from femoral blood samples can postmortem results be reliably interpreted [5, 8, 10]. Many drugs also do not evenly distribute between the cellular and fluid constituents of blood. For example, the concentration ratio between blood and plasma varies from 0.5 for phenytoin to 2.0 for maprotiline. Blood/plasma ratios may not only vary among drugs, but may also differ between a drug and its metabolite (Table 4).

Distribution ratios are generally derived from in vitro partition experiments where plasma water, plasma proteins and red blood cells are pooled. Some caution is advisable in using these data. When spiked blood is diluted with autologous plasma, erythrocytes discharge compounds more than plasma proteins. Also, non-linear, concentration dependent variations of the blood/plasma distribution have been observed, for example for topiramate. Ratios may also differ depending on whether the sample has been collected from a living person or a corpse. Distribution ratios of cannabinoids, for example, were essentially constant over the concentration ranges in samples collected from living individuals, but scattered over a wider range of values in postmortem specimens. The mean ratio between the initial postmortem blood specimens and corresponding supernatants was 0.42, but was 0.63 in samples obtained from living subjects. It seems that the distribution ratio that

Table 4 Blood/plasma concentration ratios for drugs of forensic interest

Drug	Blood/plasma ratio
Amitriptyline	1.0–1.1
Nortriptyline	1.5–1.7
Cocaine	1.00
Diazepam	0.70
Oxazepam	1.00
Ethanol	0.74–0.90
Methadone	0.75/1.00[a]
Morphine	1.02
Morphine-3- and -6-glucuronide	Dependent on the hematocrit value
Δ^9-Tetrahydrocannabinol	0.55/0.66[a]
11-Hydroxy-Δ^9-tetrahydrocannabinol	0.57/0.58[a]
11-Nor-9-carboxy-Δ^9-tetrahydrocannabinol	0.62

[a] Depending on the particular source

exists during life due to active processes decays after death. Generally, the concentration differences observed between blood or plasma might be less important compared to other effects acting on the drug concentration prior to sampling [2, 10, 11].

Drug concentrations may also change during agonal phases. Hypoxia reduces intracellular pH thus inducing an accumulation of basic drugs into cells, whereas neutral or acidic drugs are less affected. After death had occurred, acidification up to a pH-value of 5.5 and changes in ionic strength cause damage to lysosomal membranes, and subsequently enzymatic digestion of the cell membrane and components. As the permeability of membranes increases, drugs are redistributed into the extra cellular space, and hemolysis occurs. There is a rapid progress in postmortem redistribution processes due to disintegration of physiological and anatomical barriers.

A postmortem blood specimen may differ substantially from a sample of whole blood collected from a living person. In addition to hemolysis and a fall in the pH, blood coagulates postmortem, and then becomes fluid again. The extent of these two processes will determine whether postmortem blood is clotted, fluid or partially clotted and partially fluid. Sedimentation of cellular blood components to the lower parts of the body under gravity, a phenomenon called hypostasis, is a visible manifestation of postmortem changes. There is also a wide variation in the water content of postmortem blood, ranging from 59 to 89%. All these changes may effect the original blood drug levels.

Invasion of intestinal flora into tissues and body fluids occurs after death, especially at ambient or elevated temperatures but not within a specified time frame.

Postmortem blood samples taken 6 h after death from patients who had died of causes other than infectious diseases tested positive for bacteria whereas in a study on heart blood samples collected 85 h postmortem, bacteriologic cultures gave negative results [15]. Microbial enzymes degrade lipids, carbohydrates and proteins resulting in a slow increase in the pH during the postmortem interval. Both endogenous and exogenous substrates may be utilized as nutrients or energy sources (see also section "Degradation and formation of drugs during the postmortem interval").

Degradation and formation of drugs during the postmortem interval

Degradation and formation of drugs or new entities during the postmortem interval are processes that compete with postmortem redistribution. Potential mechanisms operating on drugs postmortem are summarized in Table 5 [2, 3, 16].

A most prominent example of postmortem metabolic formation is ethanol. It appears that ethanol is not produced postmortem except by microbial action, the amount generated depending on the species of microorganisms present, the availability of substrates, the antemortem condition of the deceased and the storage conditions of the corpse prior to collection of samples for analysis. The majority of the cases attributed to neo-formation do not have significant alcohol levels (≤0.07%). A few case reports, however, demonstrate that levels of up to 0.22% may be produced under the most favorable conditions. If the body is refrigerated within a few hours of death and kept in a cool place, alcohol formation could not be detected within 24 h despite positive blood cultures. Also, alcohol is not always detectable in the advanced stages of putrefaction, possibly due to its utilization by microorganisms after an initial increase in levels.

As postmortem synthesis or loss of ethanol is difficult to accurately assess, determination of further putrefactive products or markers of recent alcohol ingestion have been suggested as indicators to differentiate ethanol formed postmortem from that due to antemortem consumption. The following volatiles can be produced along with ethanol: acetaldehyde, acetone, 1- and 2-propanol, 1-butanol, isobutanol, isoamyl alcohol, acetic, propionic, butyric and isobutyric acids, and ethyl esters. Co-detection of "abnormally high concentrations" of volatiles with ethanol during ethanol analysis has been suggested as suspicious for microbial contamination. However, minimum volatile levels indicating microbial contamination, as well as the correlation of these levels with the amount of ethanol produced, have still to be established. Also, all volatiles that could be microbial products are minor ingredients of alcoholic beverages, except 1-butanol. Methanol is not likely to be formed postmortem, and levels >10 mg/L blood may be the result of heavy antemortem exposure. Aminobutyric and aminovaleric acids have been used to verify postmortem ethanol formation but are also produced at variable rates. Measurement of ethyl glucuronide is a helpful tool to determine in vivo ingestion of ethanol. If ethyl glucuronide is not detectable along with ethanol, ethanol formation might have occurred postmortem; however, alcohol synthesis can not be excluded with certainty if both ethanol and its glucuronide conjugate are present, and ethyl glucuronide may also disappear from blood due to marked putrefaction [6, 16, 17].

Although time- and temperature-dependent decreases in cyanide concentration are the usual findings from studies, increases have also been reported in certain situations, again possibly due to microbial action in poorly preserved samples.

Gamma hydroxybutyrate (GHB) is increasingly abused as a recreational drug. It is also an endogenous metabolite formed during biosynthesis and degradation of the inhibitory neurotransmitter gamma-aminobutyric acid. There is significant postmortem formation of GHB in blood and tissues and also during storage of specimens, where levels may increase up to 100 mg GHB/L blood. Further, microbial degradation of GHB has been observed [18]. A compilation of toxicological findings in deaths involving GHB has recently been published [19].

The possible role of enteric bacteria in the bioconversion of nitro benzodiazepines has been studied in detail. It is well known that higher concentrations of the 7-amino-metabolite are present in the blood in deaths involving

Table 5 Potential mechanisms operating on drugs postmortem

Mechanism	Example(s)
Chemical instability	
Hydrolysis	Diacetylmorphine, cocaine, O-acyl- and N-glucuronides
Oxidation	Sulphur containing drugs, morphine
Metabolic instability	
Esterases	Hydrolysis of ester type drugs, phase-II-metabolites such as e.g. glucuronides
	Reduction, e.g. nitro benzodiazepines
Metabolic formation	Oxidation, e.g. thioridazine
	Ethanol, volatile compounds, gamma-hydroxybutyrate, carbon monoxide, cyanide

flunitrazepam. Postmortem degradation also involves acid-labile conjugates such as the ester glucuronides of propofol or diflunisal, and to a lesser extent, ether glucuronides such as 3- and 6-morphine glucuronide [2].

Specimens stored in formaldehyde or collected after embalming

Occasionally it is necessary to perform analysis on pathologic specimens stored in formaldehyde or on samples that were collected from an embalmed body. With modern techniques of embalming, blood is drained from the veins and replaced by a fluid, usually based on formaldehyde, that is injected into one of the main arteries; cavity fluid is removed with a trocar and replaced with preservative fluid, composed of formalin mixed with alcohols and emulsifiers. The embalming procedure may therefore have diluted blood and may have partially or completely removed drugs or poisons present at the time of death from major vessels. Analysis of pathological specimens should also cover determination of the drug in fixing and storing solutions as leaching of drugs from solid specimens occurs.

Formaldehyde present in both embalming and fixing fluids is a highly reactive chemical. Most likely reaction pathways are through hydrolysis, degradation or methylation via the Eschweiler-Clarke reaction. Conversion of nortriptyline to amitriptyline may occur during formalin fixation and storage; and N-methylation has also been reported for amphetamine, methamphetamine, and fenfluramine. Alternatively, embalming fluid may maintain acidic conditions and contribute to a drug's stability such as e.g. succinylcholine, which will be rapidly hydrolyzed.

However, some compounds such as alprazolam or midazolam decompose more rapidly under acidic conditions [2].

Autopsy findings indicating intoxication or poisoning

Clinical symptoms may provide valuable information in a case of suspected poisoning or intoxication facilitating the selection of appropriate and correct samples at autopsy. It should, however, be considered, that these symptoms may be subtle, hidden by diseases or misleading, especially in children and the elderly [20]. As the majority of drugs and chemical agents do not produce characteristic pathological findings, most drug related deaths do not leave obvious or specific signs. Often, the only finding at autopsy is pulmonary congestion and edema. In occasional cases, however, clues indicating poisoning may be observed, and in some of these specific signs may be present (Table 6) [1].

Acquisition of specimens for toxicological investigations

General considerations

The purpose of sampling is to provide a representative part of the whole that is suitable to target the analysis for likely poisons, but also to help in the interpretation of any analytical result. The term "sample" covers the fluid and tissue and its primary container, and the sampling procedure starts with the selection of appropriate samples and ends with the correct disposal of the materials (Table 7) [5, 12, 21]. It is one of the principal roles of the forensic

Table 6 Autopsy findings indicative of intoxication or poisoning

Odor	Indicative of:
Bitter almond	Cyanide, hydrogen cyanide, nitrobenzene
Fruity, aromatic	Ethanol, solvents
Like leek or garlic	Organophosphorous compounds, arsenic, phosphorous
Sweet	Chloroform or other halogenated hydrocarbons
Orifices of the body, e.g. mouth or gastrointestinal tract	
Residues of powder or colored material	Tablet or capsule remains (e.g. flunitrazepam - blue-stained gastric contents), herbicides or pesticides, intranasal drug use (e.g. cocaine)
White, corrosive staining	Hydrochloric or acetic acid
Black-brown, corrosive staining	Sulphuric acid
Glass-like, reddish necrosis	Alkaline agents, e.g. sodium hydroxide
Lividity	
Cherry red to light red	Carbon monoxide
Bright pink	Cyanide
Greyish to brownish	Nitrate, nitrite, aniline
Atrophic scarring, abscess and ulceration of the skin, puncture marks	Intravenous drug use, e.g. opiates
Perforated nasal septum	Intranasal cocaine misuse

Table 7 To maximise the reliability of toxicology results it is recommended that

The interval between death and collection of specimens at the postmortem examination is minimised
Appropriate specimens with regard to case history, legal aspects and availability are selected
Sufficient sample volumes or amounts are taken
The possibility of cross-contamination during collection is minimised
All samples should be placed in separate and clean containers capable to maintain evidential quality
Specimens are individually labelled, stored refrigerated or frozen as appropriate, and securely packaged if transported
Samples ideally be submitted in person to the laboratory
The identity and integrity of the samples is guaranteed from collection through reporting results
All information available is provided with the samples to help the laboratory in planning the analysis
The history of the sample is documented from submission through analysis, reporting results and disposal (chain of custody procedures)

pathologist to select and collect appropriate specimens. There are regulations on the minimum storage time of toxicological specimens after the toxicology report has been issued, which may be considerably longer than that for clinical samples [22, 23].

Specimens

To date, a coordinated protocol for sampling suspected poisoning or drug related deaths has not been established. Some recommendations from *Leitlinien der Deutschen*

Gesellschaft für Rechtsmedizin: Rechtsmedizinische Leichenöffnung are summarized in Table 8 [2, 21].

In cases of exsanguination, burns or advanced putrefaction the availability of specimens may be limited, and alternative samples for drug identification such as skeletal muscle, pleural effusions, bone or bone marrow and entomological specimens may be collected. Insect eggs, larvae or pupae can be used not only to analyze for harmful substances and to estimate the postmortem interval, but also to indicate movement of the corpse. Postmortem samples from a patient who has died in hospital several days after a poisoning episode are likely to be negative. In these cases, specimens obtained at or soon after admission to hospital should preferably be investigated. Evidence found at the scene including spoons blackened with soot, syringes, and mugs or glasses containing drug residues, household products, solvents or pesticides, may provide additional information to assist and focus toxicological analyses [1, 3]. In cases where poisoning by volatiles or gas is suspected, a specimen should be collected directly at the scene, for example an aerosol container, or other source [4].

Quantity and use of postmortem specimens

The scope of the sampling procedure has to be case-dependent as the selection and volume or amount of specimens will vary considerably from case to case, depending on requests, legal aspects and availability. Clinical samples may be collected on several occasions, however in a death investigation there is rarely an opportunity to collect further specimens once an autopsy has been concluded. Two blood samples, including at least one

Table 8 Recommendations for sampling postmortem materials

All autopsies	Cases in which the cause of death remains uncertain	Special cases
Materials that should be collected prior to autopsy		
Peripheral blood (femoral or subclavian)	Hair sample of the scalp, alternatively: body hair or nails	Vitreous humour
Urine		Cerebrospinal fluid
Vomitus		Nails
		Skin, subcutaneous fat and control samples
		Swabs from the skin or mucous membranes and control samples
Materials that are collected during autopsy		
Heart blood	Bile bladder fluid	Deep muscle tissue
Gastric contents	Tissue samples of	Subcutaneous fat
	Liver	Hematoma (epidural, subdural)
	Lungs	Contents of the large and small intestine
	Brain	Pericardial fluid
	Kidneys	Pleural fluid
		Bone and bone marrow
		Entomological specimens

Table 9 Type, volume/amount and use of postmortem specimens

Specimen	Volume/amount	Use/comment
Blood from the femoral or subclavian veins	10–20 mL	Quantitative data, acute impairment or poisoning
Heart blood	50 mL or all available	General unknown analysis, concentration may be increased due to postmortem redistribution
Urine	50 mL or all available	Standard sample for drug screening, general unknown analysis, organophosphates, aromatic hydrocarbons (metabolites)
Gastric contents	50 mL or all available	Result should be referred to the total amount; tablets, herbal remains, etc. placed in individual containers
Tissues (brain, liver, lungs, kidneys, muscle, subcutaneous fat)	10–50 g	Body load may help to interpret postmortem blood data
		Lungs, brain: inhalant poisoning
Gall bladder fluid	All available	Drug screening, accumulation of drugs undergoing enterohepatic cycling
Hair sample from the scalp or the body, or nails as an alternative	Pencil-like tuft	Exposure data for weeks or months before death, tolerance
Vitreous humour	All available	Alcohol, cardiac glycosides, diabetes
Cerebrospinal fluid	All available	General unknown analysis, devoid of enzymes and proteins
Skin and subcutaneous fat	Approx $2 \times 2 \times 1$ cm^3	Skin exposure, injection marks (insulin, i.v. drug abuse), anesthetic-related incident
Contents of large and small intestine	All available and fractionated, if applicable	Suspicion of drug exposure by the rectal route, poisoning by plants or mushrooms
Pericardial fluid	50 mL or all available	In putrefied cases
Pleural fluid	50 mL	In putrefied cases
Entomological specimens species	As available	In putrefied cases, should immediately be frozen
Bone, bone marrow	Piece of 3–5 cm, >1 g	Advanced putrefaction, extensively burnt bodies
Swabs (intranasal, rectal, vaginal)	≥2 swabs	Route of administration or exposure

from a peripheral site, and urine and gastric contents should be collected as a minimum set of specimens. Collection of other appropriate fluids and tissues is recommended and even imperative in cases where the autopsy fails to determine a cause of death, or where there is an incomplete investigation. A guide to the collection of specimens is given in Table 9 [4, 5, 8, 12, 24].

Collection of samples

Separate disposable or clean devices or instruments should be used for each sample to avoid contamination. Body fluids can be taken by needle aspiration using a hypodermic syringe or by a pipette, whereas a spoon or ladle is more appropriate for viscous materials. Swabs should be taken using cotton pads, and tissue specimens can be cut out with disposable scalpels, knives or scissors. If inhalants are suspected it is important to promptly collect and seal the tissue specimen in a container as soon as possible after the body has been opened. Gas tight syringes may help to collect volatiles [4]. Collection of scalp hair, urine, femoral blood and gastric contents is shown in Figs. 1, 2, 3, 4.

Specimen preservation is not necessary except for a portion of the blood sample. Ideally, the blood sample should be divided between an unpreserved and a preserved

tube containing sodium fluoride at a final concentration of 1–5%. Preservation of a vitreous humour specimen for alcohol analysis is also recommended. Generally, preservation of specimens with sodium fluoride aids in ethanol, GHB, cocaine and carbon monoxide analyses, whereas fluoride preservation must not be used when organophosphorous chemicals are involved. Instead, early acidification and storage at a temperature below −20°C are recommended to stabilize these compounds. Ascorbic acid is not widely used as an antioxidant, but may reduce losses in olanzapine during storage and also stabilize drugs such as apomorphine [2].

Although tubes containing liquids should be filled to minimize the evaporation of volatiles and oxidative losses of drugs, a small headspace of about 20% should be left if they are likely to be frozen. If analysis of volatiles is to be directly performed on a sealed container, a head space of 90–95% is recommended. Break- and leak-proof disposable tubes or containers should be used during collection and if specimens are to be stored frozen. Most types of plastic containers (polycarbonate, polyethylene or polypropylene copolymers) are suitable for the collection of body fluids and tissues in drug related fatalities. Bags that can be tightly sealed are also appropriate for the sampling of tissue specimens. Glass tubes/containers may break if

Fig. 1 Collection of a hair specimen prior to autopsy by tying with a piece of thread

Fig. 2 Collection of a urine specimen prior to postmortem examination

Fig. 3 Dissection of the femoral vein prior to collection of a blood sample

sent by post or upon freezing. Sampling into a glass container is, however, a must if solvent abuse or an anesthetic death is suspected. Samples should be sealed in such a way that tampering will be evident.

Specimens must be individually labelled and include the following information:

- Postmortem reference number or unique identifier
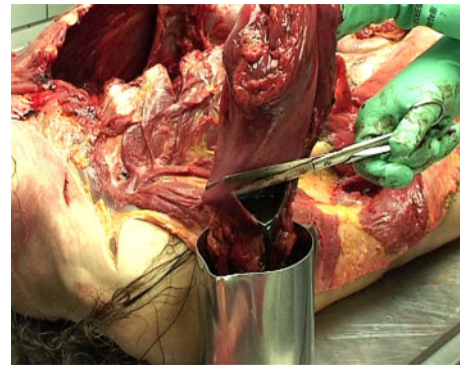- Name or unique identifier of the deceased

Fig. 4 Determining the total volume of gastric concents

- Type/source of specimen
- Date of specimen collection.

All samples except for the hair tuft and the portion of blood to be submitted for alcohol analysis should be combined as a batch. The specimen collection protocol should preferably include the following details (Table 10) [2, 22]:

Storage, transport, receipt and disposal of postmortem specimens

It is important to guarantee the identity and integrity of samples from collection through to the reporting of results. Safe transport within the mortuary and to the laboratory is essential. Whenever specimens are left unattended, they should be secured in a locked container, refrigerator or freezer. Handling and processing of specimens should be restricted to authorized personnel. Freezing of specimens is highly recommended except for hair and a portion of the blood sample, which should be kept at ambient temperatures or refrigerated. Also, if analyses are performed within a few days after collection, freezing may not be necessary.

Upon arrival at the laboratory, specimens should be checked for completeness and integrity. This information is essential when deciding how to approach the request of the police or coroner. Precautions should be taken to preserve the stability of the analytes present in the specimens, which often need to be kept for several months, and to avoid accidental contamination of the specimens in the laboratory, also [8].

To target the analysis to likely poisons and to simplify the interpretation of analytical results, the following information should be available when submitting samples for analysis [10]:

- Request including the name, telephone number and address of the investigating officer or coroner
- Postmortem reference number or unique identifier

Table 10 Specimen collection protocol

Name, address and telephone number of the pathologist and coroner's officer
Postmortem reference number, date of postmortem examination
Surname and first name of the deceased or unique identifier
The date of specimen collection
Type and source of specimens, amount or volume, and addition of preservatives, if applicable
Indication of any biological risk or chemical hazards associated with the specimen(s)
Abnormal appearance of the specimen or degree of autolysis/putrefaction
Specimens should be accompanied by a chain of custody form which should be signed by each individual handling the sample

- Surname/first name of the deceased or unique identifier
- Police involvement, circumstances surrounding death
- Autopsy report, at least a preliminary version
- Emergency report, recent medical history and treatment
- Specimen collection protocol (see Table 10)
- Predefined time periods to complete the toxicology investigation

The documentation of analytical results is mandatory. Once the finished report has been submitted and specimens are not required any longer, or if the predefined time for specimen storage has been reached, samples may be discarded. The date that specimens are discarded must be recorded [2, 22].

Analytical pitfalls

There is little to differentiate analytical procedures used in other branches of forensic toxicology from those used in postmortem investigations. The same quality standards as established for the analysis of specimens derived from living individuals also apply to postmortem specimens [21]. Analytical methods can be broadly classified into three types: screening procedures, confirmation procedures and specific methods. Screening for volatiles by gas chromatography (GC) is recommended, and immunoassays for common drugs of abuse are regularly included in a toxicology investigation. Interaction with putrefactive amines is commonly seen in immunoassays for amphetamine type drugs; and ambroxol was reported to show some cross reactivity in immunoassays for LSD. If death occurs within a very short time after drug administration an insufficient concentration may be present in urine to give a positive result [25].

Additionally, comprehensive chromatographic screens for basic, neutral and acidic drugs using UV- or mass spectrometric (MS) detection are required [8]. Screening methods based on MS data will provide confirmation of a suspected compound. The particular compound should also be detected in at least one other specimen. The second method may use a different detection mode or an entirely different procedure. Although GS/MS is generally accepted as unequivocal identification for many drugs, a few drawbacks have been reported:

- erroneous identification at a low analyte concentration or due to a low extraction efficiency
- misidentification due to interfering substances
- inadequate information due to similar fragmentation behaviour (e.g. barbiturates)
- production of low fragment ions (e.g. tricyclic antidepressant agents).

Several LC/MS procedures for the screening of drugs in blood have been developed in recent years using time-of-flight mass analyzers, ion traps or classical triple quadrupoles that cover a sometimes more limited range of substances compared to GC/MS [8]. At present, there is still a need for studies of matrix effects, selectivity, analyte stability and appropriate internal standards [18].

Numerous procedures exist that quantify specific drugs, especially by GC/MS or LC/MS, with LC/MS becoming a gold standard for detection of very low drug concentrations [18]. Depending on the type and quality of a sample, homogenization and modified or multiple extraction procedures have to be applied. Drug conjugates that have been co-extracted may subsequently be hydrolyzed leading to erroneously high levels of the non conjugated drug proportion. The phenomenon of conjugate instability is most common with labile conjugates such as *N*- or *O*-acyl glucuronides [2].

The extraction efficiency from a postmortem specimen may vary from case to case, or even from site to site within the same body. It may also differ from that of a blank specimen used for calibration. The use of stable isotope internal standards may provide a higher degree of accuracy in the analytical results. However, few deuterated standards are commercially available for drugs or major metabolites. If impurities present in the sample interact with the analyte to change the instrumental response, the method of standard addition may be used as an alternative; i.e. the sample can be measured before and after adding increasing amounts of the analyte. Major drawbacks are the high sample volume, an increase in analytical runs and extrapolation of the curve to "zero" concentration, e.g. beyond the valid calibration range.

It is now recognized that determination of major metabolites and degradation products along with the parent drug is essential to avoid misinterpretation of the data due to artefacts. Such a stability-indicating assay is one that can accurately and selectively differentiate the intact drug from its potential decomposition products.

Implications for practice

A toxicological death investigation is often unique and totally different from investigations in clinical toxicology. The following issues might assist in targeting requests relative to poisoning in a particular case:

- Is there adequate information on the circumstances surrounding death?
- Is there any information available on the drug, and if so, is there adequate scientific information available to define the concentration-toxicity relationship?
- Is the drug either known or suspected to undergo postmortem redistribution? Is there information on the drug stability during autolysis and putrefaction?
- Are special sample collection techniques and/or storage conditions required?
- Are there autopsy findings consistent with drug overdose?
- What kinds of specimens are available?
- When, how and where does a particular specimen have been collected?
- Were blood samples collected from a minimum of two different sites?
- Has the chain of custody be maintained?
- Is there sufficient scientific and practical experience to perform appropriate analyses on the materials provided?
- Has a request form been submitted? Have additional requests emerged from pathological or initial toxicological findings?

Drug concentration measurements cannot be interpreted without a thorough review of all the medicolegal findings and circumstances surrounding death. Success in arriving at the correct conclusion will depend on the combined efforts of all of the investigators, the pathologist and the toxicologist.

Key points

1. Many changes occurring postmortem will not be identifiable by postmortem sampling and toxicological analysis.
2. There are a lot of antemortem factors affecting the concentration-time profile of drugs.
3. All mechanisms causing artefactual changes during the postmortem period can be included under the term postmortem redistribution.
4. Degradation and formation of drugs or new entities compete with postmortem redistribution.

5. Most drug related deaths do not leave obvious or specific signs.
6. The purpose of sampling is to provide a representative part of the whole that is suitable to target the analysis for likely poisons and also help in the interpretation of the analytical results.
7. The scope of the sampling procedure has to be case-dependent.
8. The identity and integrity of the samples must be guaranteed from collection through to the reporting of results.
9. Interpretation of the analytical results may be limited by the inadequate information.

CME questionnaire

1. **No significant influences on the pharmacokinetics of a drug are to be expected from:**
   - ☐ acidosis
   - ☐ perfusion of the liver
   - ☐ cyanosis
   - ☐ dehydratation
   - ☐ hypoxia

2. **Varying drug amounts in blood samples collected from different sampling sites in a corpse are not due to:**
   - ☐ arterio-venous differences
   - ☐ development of tolerance
   - ☐ local drug reservoirs within the corpse
   - ☐ drug release from tissue binding sites
   - ☐ diffusion along a concentration gradient

3. **The phenomenon of postmortem redistribution largely depends on:**
   - ☐ a decrease of the water content of postmortem blood
   - ☐ a partial or nearly total clotting of blood
   - ☐ several processes such as a non-uniform distribution of the drug within the body, a release from its binding sites and/or passive diffusion
   - ☐ hypostasis
   - ☐ hemolysis

4. **During the postmortem interval drugs maybe degraded as a result of chemical decomposition or metabolic processes, and new entities may be formed by microbial actions. There is evidence, however, that the following compound is not likely to be formed postmortem:**
   - ☐ propanol
   - ☐ cyanide
   - ☐ ethanol
   - ☐ gamma hydroxybutyrate
   - ☐ methanol

5. **Conversion of N-desmethyl metabolites to the parent drug through reductive N-methylation has been observed in specimens stored in formaldehyde containing solutions. This reaction is named after:**
   - ☐ Eschweiler-Clarke
   - ☐ Canizzaro
   - ☐ Traub
   - ☐ Mannich
   - ☐ Grignard

6. **The following finding at postmortem examination may indicate intoxication or poisoning by the assigned agent:**
   ☐ Garlic-like odor – arsenic compounds
   ☐ Fruity-like odor - nitrobenzene
   ☐ Cherry red to light red lividity – nitrate or nitrite
   ☐ Sweet, etheral odor - cyanide
   ☐ Glass-like, reddish necrosis – acetic acid

7. **Sampling of specimens for a toxicological investigation does not cover:**
   ☐ Selection of the specimens
   ☐ Packaging and transport of specimens
   ☐ Extraction of specimens for toxicological analysis
   ☐ Storage of samples over a fixed period of time
   ☐ Disposal or destruction of specimens

8. **The following specimen is not suitable for the detection of:**
   ☐ Hair sample – acute overdose
   ☐ Urine – screening for drugs of abuse
   ☐ Vitrous humor – cardiac glycosides
   ☐ Skin and subcutaneous fat - injection of insulin
   ☐ Gastric contents – identification of herbal materials

9. **Acquisition of specimens for a toxicology investigation**
   ☐ will preferably be performed during or after dissection of a corpse.
   ☐ should always be performed on muscle tissue.
   ☐ will reasonably not be performed in cases of severe putrefaction
   ☐ should be performed on skin and subcutaneous fat if solvent abuse or an anesthetic death is suspected.
   ☐ can be done using plastic tubes if solvent abuse or an anesthetic death is suspected.

10. **The following specification is not considered an inherent part of the sample acquisition protocol:**
    ☐ the name of the deceased
    ☐ the name of the pathologist
    ☐ the date of receipt for the postmortem examination of the corpse
    ☐ information on the biological risk or chemical hazard associated with the specimen
    ☐ date of transfer and submission to the laboratory

CME questionnaire answers

1. cyanosis
2. development of tolerance
3. several processes such as a non-uniform distribution of the drug within the body, a release from its binding sites and/or passive diffusion
4. methanol
5. Eschweiler-Clarke
6. Garlic-like—arsenic compounds
7. Extraction of specimens for toxicological analysis
8. Hair sample—acute overdose
9. should be performed on skin and subcutaneous fat if solvent abuse or an anaesthetic death is suspected
10. the date of receipt for the postmortem examination of the corpse

References

1. Madea R, Dettmeyer R, unter Mitarbeit von Mußhoff F. Basiswissen Rechtsmedizin. Berlin, Heidelberg: Springer; 2007. pp. 182–217.
2. Skopp G. Preanalytic aspects in post-mortem toxicology. Forensic Sci Int. 2004;142:75–100.
3. Jones GR. Interpretation of post-mortem drug levels. In: Karch SB, editor. Drug abuse handbook. Boca Raton: CRC Press; 1998. p. 970–85.
4. Tiess D. Asservierung, Exhumierung, Thanatochemie. In: Madea B, Brinkmann B (Hrsg). Handbuch gerichtliche Medizin, Bd. 2. Berlin, Heidelberg, New York: Springer. pp. 70–88.
5. Moffat AC, Osselton MD, Widdop B. Clarke's analysis of drugs and poisons, vol. 1 and 2. 3rd ed. London, Chicago: Pharmaceutical Press; 2004.
6. Kugelberg FC, Holmgren A, Eklund A, Jones AW. Forensic toxicology findings in deaths involving gamma-hydroxybutyrate. Int J Legal Med. 2008. doi:10.1007s00414-008-0299-2.
7. Drug Interaction Database. www.druginteractioninfo.org.
8. Drummer OH. Requirements for bioanalytical procedures in postmortem toxicology. Anal Bioanal Chem. 2007;388:1495–503.
9. Ferner RE. Post-mortem clinical pharmacology. Br J Clin Pharmacol. 2008;66:430–43.
10. Richardson T. Pitfalls in forensic toxicology. Ann Clin Biochem. 2000;37:20–44.
11. Baselt RC. Disposition of toxic drugs and chemicals. In: Man, 7th ed. Foster City: Biomedical Publications; 2004.
12. Flanagan RJ, Connally G, Evans JM. Analytical toxicology. Guidelines for sample collection post-mortem. Toxicol Rev. 2005;24:63–71.
13. Leikin JB, Watson WA. Post-mortem toxicology: what the dead can and cannot tell us. J Toxicol Clin Toxicol. 2003;41:47–56.
14. Pelissier-Alicot AL, Gaulier JM, Champsaur P, Marquet P. Mechanisms underlying postmortem redistribution of drugs: a review. J Anal Toxicol. 2003;27:533–44.
15. Morris JA, Harrison LM, Partridge SM. Postmortem bacteriology: a re-evaluation. J Clin Pathol. 2006;59:1–9.
16. Boumba VA, Ziavrou KS, Vougiousklakis T. Biochemical pathways generating post-mortem volatile compounds co-detected during forensic ethanol analysis. Forensic Sci Int. 2008; 174:133–51.
17. Høiseth G, Karinen R, Johnsen L, Normann PT, Christophersen AS, Mørland J. Disappearance of ethyl glucuronide during heavy putrefaction. Forensic Sci Int. 2008;176:147–51.
18. Maurer HH. Current role of liquid chromatography-mass spectrometry in clinical and forensic toxicology. Anal Bioanal Chem. 2007;388:1315–25.
19. Kugelberg FC, Jones AW. Interpreting results of ethanol analysis in postmortem specimens: a review of the literature. Forensic Sci Int. 2007;165:10–29.
20. Ludewig R. Akute Vergiftungen. Ratgeber zur Erkennung, Verlauf, Behandlung und Verhütung toxikologischer Notfälle. Stuttgart: 9. Aufl., Wissenschaftliche Verlagsgesellschaft mbH; 1999. pp. 31–37.
21. Gesellschaft für Toxikologische und Forensische Chemie. www.GTFCh.org.
22. Skopp G, v. Meyer, L. Empfehlungen der Gesellschaft für Toxikologische und Forensische Chemie (GTFCh) zur Asservierung von Obduktionsmaterial für forensisch-toxikologische Untersuchungen. Toxichem + Krimtech 2004;71:101–7.
23. AWMF Leitlinien-Register Nr. 054/001, Entwicklungsstufe 3 (2007). Leitlinien der Deutschen Gesellschaft für Rechtsmedizin: Die rechtsmedizinische Leichenöffnung. www.awmf.org.
24. McGrath KK, Jenkins AJ. Detection of drugs of forensic importance in postmortem bone. Am J Forensic Med Pathol. 2009;30:40–4.
25. Baker JE, Jenkins AJ. Screening for cocaine metabolite fails to detect an intoxication. Am J Forensic Med Pathol. 2008;29:141–4.

BOOK REVIEW

Jim Fraser: Forensic science: a very short introduction

Oxford University Press 2010, ISBN 978-0-19-955805-6

Claas T. Buschmann

The "Very Short Introductions" book series published by Oxford University Press is designed to give general readers a fascinating and readily understandable account of complex subjects and will ultimately encompass around 300 titles. Professor Jim Fraser, Director of the Centre for Forensic Science at the University of Strathclyde, has a broad background and wide experience in forensic teaching, research and practice. He now provides a clear and exciting glimpse into the world of forensic science as a realm of complex activity at the interface of science and law. The reader is held spellbound by references to famous criminal cases in British legal history as well as to popular movies such as Quentin Tarantino's "Pulp Fiction". The book is enjoyable and delightful to read, and the topics can easily be grasped and appreciated even by non-expert readers. It comprises 130 pages organized into 9 well-written and well-structured chapters (Introduction, Investigating crime, Crime scene management and forensic investigation, Laboratory examination, DNA, Prints and marks, Trace evidence, Drugs, Science and justice) and is enriched with 18 black and white illustrations and 17 tables, some quite comprehensive. The short but up-to-date reference list is a valuable tool for gathering further information.

While some important facets of forensic science such as DNA analysis, fingerprints and bloodstain pattern analysis are presented in great depth, clarity and detail, others such as post-mortem examination, forensic autopsy, reconstruction aspects of violent deaths, and forensic odontology are not included in this edition. As Professor Fraser aptly states, the exclusion of whole areas is due to the necessity for selection. Nevertheless, it may be worthwhile to consider adding a short chapter on the principles and practice of forensic autopsy in future editions. Since mainly American and British forensic practice and methodology are explained, a forthcoming edition could perhaps also contain a chapter on general forensic practice in other European countries.

To sum up, the author gives an account of the techniques used and the challenges faced in forensic science. Answering questions like "How is a crime scene investigated?" or "How does DNA profiling work, and how can it help solve crimes that happened 20 years ago?" not only provides interested non-experts with useful information but is also an excellent way of presenting our complex discipline to the public.

Considering the limitations inherent in a series of small-format books spanning a wide range of topics from history, philosophy, and religion to science, technology and medicine, this small but excellent volume is sure to fan the flames of a growing fascination with our discipline and will give interested readers a deep understanding and broad grasp of the complex and multi-faceted field of forensic science.

C. T. Buschmann (✉)
Institute of Legal Medicine and Forensic Sciences, University Medical Centre Charité, University of Berlin, Turmstr. 21, Building L, 10559 Berlin, Germany
e-mail: claas.buschmann@charite.de
URL: http://remed.charite.de